

Integrated Optics
- Sensors, Sensing Structures and Methods
IOS'2019

PROGRAMME
and
ABSTRACTS

Organizers of IOS 2019

Photonic Society of Poland,

**Upper Silesian Division of
the Polish Acoustical Society**

and

**Committee of Electronics and Telecommunication
at the Polish Academy of Sciences**

**25th February to 1st March 2019,
Hotel "META"
Szczyrk - Beskidy Mountains, POLAND**

<http://ios-conference.pl>

Dear Participants

**of 14th Conference INTEGRATED OPTICS - Sensors, Sensing Structures and
Methods IOS'2019**

Organizers welcome All of You very cordially in Szczyrk, in the beautiful scenery of the Beskidy Mountains.

We wish all Participants of the Conference IOS'2019 plenty of scientific satisfactions and many professional and social impressions.

Organizers

President of the Conference: Prof. Tadeusz Pustelny
Treasurer: Dr eng. Aneta Olszewska
Secretary: Dr eng. Marcin Procek
Members: Dr eng. Kamil Barczak
Dr eng. Przemysław Struk
Dr eng. Sabina Drewniak

**This book includes the Program of IOS'2019 and Abstracts
of presentations and posters sent by their Authors**

Conference Programme

INTEGRATED OPTICS - SENSORS, SENSING STRUCTURES and METHODS

Szczyrk 25.02-01.03.2019

25.02.2019 Monday	
13:00	<i>Dinner</i>
14:30-14:35	OPENING CEREMONY of the Conferences 48th WSW&QA 47th WSEA&V 14th IOS'2019
14:35-15:30	JUBILEE OF PROFESSOR WIESŁAW WOLIŃSKI
15:30-16:30	SESSION DEDICATED TO PROFESSOR WIESŁAW WOLIŃSKI IN JUBILEE'S CELEBRATION
15:30-16:00	<i>Invited lecture</i> Graphene in infrared and terahertz detector family A. ROGALSKI
16:00-16:30	<i>Invited lecture</i> Examination of the bottom of the Gdansk Bay by means of acoustic methods <u>E. KOZACZKA</u> , G. GRELOWSKA
16:30-17:00	<i>Coffee break</i>
17:00-18:00	SESSION DEDICATED TO PROFESSOR WIESŁAW WOLIŃSKI IN JUBILEE'S CELEBRATION

17:00-17:20	<p><i>Invited lecture</i></p> <p>Synthesis and propagation of structured light beams in nematic liquid crystals</p> <p>U. A. LAUDYN, M. KWAŚNY, J. PIŁKA, P. JUNG, <u>M. A. KARPIERZ</u></p>
17:20-17:40	<p><i>Invited lecture</i></p> <p>The problems of the direction finding by air vehicles of the radars working with rotating antenna</p> <p>A. RUTKOWSKI, <u>A. KAWALEC</u></p>
17:40-18:00	<p><i>Invited lecture</i></p> <p>Near-infrared emission in fluoroindate glasses co-doped with rare-earth</p> <p>M. KOCHANOWICZ, J. ŻMOJDA, P. MILUSKI, A. BARANOWSKA, T. RAGIŃ, J. DOROSZ, M. KUWIK, W. A. PISARSKI, J. PISARSKA, M. LEŚNIAK, B. STARZYK, M. FERRARI, <u>D. DOROSZ</u></p>
19:00	<i>Supper</i>
20:00	MUSIC GLANCE – moment with string quartet

26.02.2019 Tuesday

13:00

Dinner

14:30-15:00

Plenary Lecture

Investigation depolarization in variable medium by spatial interferometric system

A. KALBARCZYK, L. R. JAROSZEWICZ, N. BENIS, I. MERTA, M. CHRUSCIEL, P. MARC

15:00-15:30

Plenary Lecture

Sensors characteristics of helically twisted microstructured optical fibers

P. MERGO, M. MAKARA, K. POTURAJ, L. CZYZEWSKA, G. WÓJCIK, A. WALEWSKI, J. KOPEĆ

15:30-15:50

Optimization of silica glass capillary and rods drawing process

G. WÓJCIK, K. POTURAJ, M. MAKARA, P. MERGO

15:50-16:10

The SS-OCT endomicroscopy probe based on MOEMS Mirau

micro-interferometer and MEMS 2-axis electrothermal microscanner for optical coherence tomography imaging

P. STRUK, S. BARGIEL, Q. TANGUY, F. E. GARCIA RAMIREZ, R. CHUTANI, P. LUTZ, O. GAIFFE, L. FROEHLY, N. PASSILLY, H. XIE, CH. GORECKI.

16:30-17:00

Coffee break

17:00-17:30	<p><i>Plenary lecture:</i></p> <p>Coupled Microresonators <u>M. TRIPPENBACH</u>, V. KONOTOP, N. VIET HUNG, A. RAMANIUK, K. ZEGADŁO</p>
17:30-18:00	<p><i>Plenary Lecture:</i></p> <p>Integrated photonics – technologies and applications <u>R. PIRAMIDOWICZ</u>, S. STOPIŃSKI, A. KAŻMIERCZAK, A. PAŚNIKOWSKA, M. SŁOWIKOWSKI, A. JUSZA, K. ANDERS, W. PLESKACZ, P. SZCZEPAŃSKI</p>
18:00-18:20	<p>Distributed optical fiber sensors for high temperature applications <u>A. RAFALAŁ</u>, K. WILCZYŃSKI, T. STAŃCZYK, K. MARKIEWICZ, A. DOMINGUEZ LOPEZ, J. KACZOROWSKI1, Ł. SZOSTKIEWICZ, M. NAPIERAŁA, T. NASIŁOWSKI</p>
18:20-18:40	<p>Bend sensor based on microstructured multicore optical fiber <u>D. BUDNICKI</u>, P. DĘBOWSKI, Z. HOLDYNSKI, L. SZOSTKIEWICZ, K. MARKIEWICZ, K. WILCZYNSKI, M. MURAWSKI, G. WOJCIK, M. MAKARA, K. POTURAJ, P. MERGO, O. KARCZEWSKI, M. NAPIERAŁA, T. NASIŁOWSKI</p>
18:40:19:00	<p>Research of advanced signal detection methods for optical fiber methane sensor <u>S. CHOJNOWSKI</u>, K. WYSOKIŃSKI, Z. HOŁDYŃSKI, J. ZAJIC, K. MARKIEWICZ, O. KARCZEWSKI, T. TENDERENDA, M. NAPIERAŁA, T. NASIŁOWSKI</p>
18:30-19:00	POSTER SESSION -mounting of posters
19:00	<i>Supper</i>

20:00

POSTER SESSION

27.02.2019 Wednesday

13:00

Dinner

14:30-15:00

Plenary Lecture:

Generation of optical vortices in nonlinear photonic crystals

K. SWITKOWSKI, S. LIU, Y. SHENG,
W. KROLIKOWSKI

15:00-15:20

Optimization of optical properties of photonic crystal fibers infiltrated with chloroform for supercontinuum generation

C. V. LANH, V. T. HOANG, V. C. LONG,
K. BORZYCKI, K. D. XUAN, V. T. QUOC,
M. TRIPPENBACH, R. BUCZYŃSKI, J. PNIEWSKI

15:20-15:40

Experimental analysis of the Bragg reflection peaks splitting in gratings fabricated using a multiple order phase mask

G. STATKIEWICZ-BARABACH, K. TARNOWSKI,
D. KOWAL, P. MERGO

15:40-16:00

Integrated ring lasers for optical gyroscope systems

S. STOPIŃSKI, M. SIENNICKI, R. PIRAMIDOWICZ

16:00-16:20

Liquid-crystal diffraction gratings based on azo polymer aligning layers exposed to blue light interference pattern

A. KOZANECKA-SZMIGIEL, K. RUTKOWSKA,
M. NIEBOREK, M. KWAŚNY, D. SZMIGIEL

16:30-17:00

Coffee break

17:00-17:30	<p><i>Plenary Lecture:</i></p> <p>High-resolution optical fiber bundles based on high-contrast soft glasses for fluorescence imaging</p> <p><u>R. BUCZYŃSKI</u>, B. MOROVA, R. KASZTELANIC, N. BAVILI, Ö. YAMAN, A. FILIPKOWSKI, D. PYSZ, B. YIĞIT, M. ZEYBEL, M. AYDIN, B. DOGAN, A. KIRAZ</p>
17:30-17:50	<p>Ellipsometric studies of antibody-functionalized sensors: estimation of surface coverage of diamond and gold electrodes</p> <p><u>B. DEC</u>, M. RYCEWICZ, R. BOGDANOWICZ</p>
17:50-18:10	<p>0.3 mW MIR output power from multimode chalcogenide glass fiber doped with praseodymium</p> <p><u>S. SUJECKI</u>, L. SOJKA, M. SHEN, D. JAYASURIA, Z. TANG, E. BARNEY, D. FURNISS, T. BENSON, A. SEDDON</p>
18:10-18:30	<p>Structural properties and mid-infrared emission of heavy metal oxide glass and optical fibre co-doped with Ho³⁺/Yb³⁺ ions</p> <p><u>T. RAGIŃ</u>, A. BARANOWSKA, M. KOCHANOWICZ, J. ŻMOJDA, P. MILUSKI, D. DOROSZ</p>
18:30: 18:50	<p>Broad-band polymers planar waveguide interferometer</p> <p>K. GUT</p>
19:30	<i>Festive Supper (Banquet)</i>

28.02.2019 Thursday

8:00	<i>Breakfast</i>
13:00	<i>Dinner</i>
14:30-14:50	<i>Plenary Lecture:</i> T2SLs InAs/GaSb and T2SLs InAs/InAsSb higher operating temperature detectors – where is the limit? <u>P. MARTYNIUK</u> , K. HACKIEWICZ
14:50-15:10	<i>Plenary Lecture:</i> Ultrasensitive detection of selected gases by infrared absorption spectroscopy <u>J. WOJTAS</u> , Z. BIELECKI, T. STACEWICZ, J. MIKOŁAJCZYK, M. NOWAKOWSKI, B. PIETRZYK, D. SZABRA, A. PROKOPIUK, K. ACHTENBERG
15:10-15:30	Silk fibroin thin films - biomaterial for optical humidity sensing <u>M. PROCEK</u> , Z. OPILSKI, A. MARQUEZ-MARQEDA, X. MUÑOZ-BERBEL, C. DOMINGUEZ-HORNA
15:30-15:50	<i>Plenary Lecture:</i> Objects tracking in virtual reality applications using SteamVR tracking system - selected issues M. MACIEJEWSKI, M. PISZCZEK, <u>N. PAŁKA</u>
15:50-16:10	Stability of information coding in the phase difference of radiation pulses in a fibre optic pulse interferometer M. ŻYCZKOWSKI
16:10-16:30	Identification of optical signatures for the augmented reality system <u>T. PAŁYS</u> , A. ARCIUCH
16:30-17:00	<i>Coffee break</i>

17:00 – 17:30	<i>Plenary lecture:</i> Vision sensor to measure liquid volume K. MURAWSKI, M. MURAWSKA
17:30-17:50	Determination of gas pressure with use of a camera and neural networks L. GRAD, T. MALINOWSKI, K. MURAWSKI
17:50-18:10	Evaluation of the impact of evolution strategy parameters on the optimization of the markers distribution on the VAD membrane T. MALINOWSKI, L. GRAD, K. MURAWSKI
18:10-18:30	Study on feature detection analysis used for designing hand-held retina vessels detection sensor P. A. BULER, K. MURAWSKI
18:30-18:50	Thrombogenicity assessment of biomaterials – do we need new methods? M. GAWLIKOWSKI
18:50	<i>Closing ceremony</i>
19:00	<i>Supper</i>
01.03.2019 Friday	
8:00	<i>Breakfast</i>

POSTER SESSION

Analysis of optical magnetic field sensor in wide range of wavelengths

Kamil BARCZAK

Ellipsometric studies of antibody-functionalized sensors: estimation of surface coverage of diamond and gold electrodes

Bartłomiej DEC, Michał RYCEWICZ, Robert BOGDANOWICZ

Luminescence properties in SGB glass fibers co-doped with Eu³⁺/Ag ions

Karol CZAJKOWSKI, Jacek ŻMOJDA, Piotr MILUSKI,
Marcin KOCHANOWICZ

Spectral characteristics of anion derivatives of the benzoic acid

Lidia CZYZEWSKA, Małgorzata GIL, Paweł MERGO

Sensitivity of the graphene oxide under the influence of hydrogen

Sabina DREWNIĄK, Marcin PROCEK

Determination the optimal extrusion temperature PMMA optical fibers

Malwina NIEDŹWIEDŹ, Małgorzata GIL, Mateusz GARGOL,
Wiesław PODKOŚCIELNY, Paweł MERGO

Organic Thin Film Transistor based on conductive graft copolymer thin films as a gas sensor

P. KAŁUŻYŃSKI, M. PROCEK, E. MACIAK, A. STOLARCZYK

Light-driven bending of the azo poly(amide imide) cantilevers

Anna KOZANECKA-SZMIGIEL, Dariusz SZMIGIEL,
Jolanta KONIECZKOWSKA, Ewa SCHAB-BALCERZAK

Set of the fiber optic rotational seismographs for mining activity monitoring

Anna KURZYCH, Leszek R. JAROSZEWICZ, Zbigniew KRAJEWSKI,
Jerzy K. KOWALSKI, Michał DUDEK

Growth and preliminary characterization of InAsSb photodiodes for mid-wave infrared range

Kordian LIPSKI, Łukasz KUBISZYN, Krystian MICHALCZEWSKI
Krzysztof MURAWSKI, Piotr MARTYNIUK

Investigation of room temperature optical gas sensing properties of chitosan/AuNPs blend nanostructures

Erwin MACIAK

Singular-value decomposition model for partial polarizing optical fiber elements

Paweł MARC, Karol STASIEWICZ, Joanna KOREC, Leszek R. JAROSZEWICZ

Hybrid connection of functional materials and tapered optical fiber

Joanna E. MOŚ, Karol A. STASIEWICZ, Leszek R. JAROSZEWICZ

Temperature dependence of Raman scattering in nanometric films of GaS and SnS₂

Katarzyna OLKOWSKA, Cezariusz JASTRZEBSKI, Daniel J. JASTRZEBSKI
Sławomir PODSIADLO

Sensor-based perimeter protection of hard-to-reach wetlands and rivers - conception of the system

Norbert PAŁKA*, Jarosław MŁYŃCZAK, Marek ŻYCKOWSKI,
Marek PISZCZEK, Mateusz KAROL, Marcin MACIEJEWSKI,
Wiesław CIURAPIŃSKI, Marcin KOWALSKI, Artur GRUDZIEN, Michał WALCZAKOWSKI, Elżbieta CZERWIŃSKA,
Piotr MARKOWSKI, Konrad BREWCZYŃSKI
and Mieczysław SZUSTAKOWSKI

A simulation tool to check correctness of optical signatures detection

Artur ARCIUCH, Tomasz PAŁYS

Zero- and ultra- low-field nuclear magnetic resonance with atomic magnetometer

Kacper POPIOŁEK, Piotr PUT, Szymon PUSTELNY

Theoretical studies on refractive index profile of nanostructured fibre

Piotr PUCKO, Marcin FRANCZYK, Adam FILIPKOWSKI, Ryszard BUCZYŃSKI

The hypothesis about the electrical non-neutrality of the Universe

Tadeusz PUSTELNY

Light guiding channels in polymer-supported liquid crystalline materials and structures

Katarzyna RUTKOWSKA, Anna KOZANECKA-SZMIGIEL,
Miłosz CHYCHŁOWSKI

Tuning optical properties of fluorescent nanodiamonds: influence of solvent polarity and pH

Mateusz FICEK, Michał RYCEWICZ, Maciek GŁOWACKI,
Marcin MARZEJON, Katarzyna KARPIENKO, Mirosław SAWCZAK
and Robert BOGDANOWICZ

Design of an integrated optics sensor structure for haemoglobin property detection

Przemysław STRUK

An application of thulium doped fiber laser in wood cutting

Sławomir SUJECKI, Monika ANISZEWSKA, Adam MACIAK,
Witold ZYCHOWICZ, Samir LAMRINI, Karsten SCHOLLE, Peter FUHRBERG

Application of Evolutionary Algorithm to Optimization of DWDM networks

Kacper WNUK, Sławomir SUJECKI, Stanisław KOZDROWSKI

Application of Machine Learning Methods in provisioning of DWDM channels

Piotr PAZIEWSKI, Sławomir SUJECKI, Stanisław KOZDROWSKI

Integrated transceiver of free space optics

Janusz MIKOŁAJCZYK, Dariusz SZABRA, Artur PROKOPIUK,
Krzysztof ACHTENBERG, Jacek WOJTAS, Zbigniew BIELECKI

Optical anisotropy of phosphorene flakes

Aleksandra WIELOSZYŃSKA, Łukasz MACEWICZ, Paweł JAKOBCZYK,
Robert BOGDANOWICZ

Laser detection and tracking system for low-flying objects

Marek ŻYCHKOWSKI, Piotr MARKOWSKI, Konrad BREWCZYŃSKI,
Norbert PAŁKA, Jarosław MŁYŃCZAK, Marek PISZCZEK, Mateusz KAROL, Marcin
MACIEJEWSKI, Wiesław CIURAPIŃSKI, Marcin KOWALSKI,
Artur GRUDZIĘ, Michał WALCZAKOWSKI, Elżbieta CZERWIŃSKA
and Mieczysław SZUSTAKOWSKI

ABSTRACTS

OF

ORAL PRESENTATIONS

High-resolution optical fiber bundles based on high-contrast soft glasses for fluorescence imaging

Ryszard BUCZYNSKI^{1,2,*}, Berna MOROVA^{3,,}, Rafal KASZTELANIC^{1,2}, Nima BAVILI³, Ömer YAMAN³,
Adam FILIPKOWSKI¹, Dariusz PYSZ¹, Buket YIĞIT⁴, Mujdat ZEYBEL⁴, Musa AYDIN⁵, Buket DOGAN⁶,
and Alper KIRAZ^{3,7}

¹Department Glass, Institute of Electronic Materials Technology, Wolczynska 133, 01-919 Warsaw, POLAND,

² Faculty of Physics, University of Warsaw, Pasteura 5, 02-093 Warsaw, POLAND

³Department of Physics, Koç University, 34450 Sariyer, Istanbul, TURKEY

⁴School of Medicine, Koç University, 34450 Sariyer, Istanbul, TURKEY

⁵Department of Computer Engineering, Fatih Sultan Mehmet Vakif University, 34445 Beyoglu, Istanbul, TURKEY

⁶Department of Computer Engineering, Marmara University, 34730 Kadikoy, Istanbul, TURKEY

⁷Department of Electrical and Electronics Engineering, Koç University, 34450 Sariyer, Istanbul, TURKEY

ryszard.buczynski@fuw.edu.pl, akiraz@ku.edu.pl

Fluorescence optical imaging is a powerful tool in biology and medical science. It enables labelling targeted structures and distinguishing them unambiguously from the host while collecting functional and spatial information on biological tissues, cells and subcellular structures. However, due to limited penetration of light into a biological tissue, non-invasive in vivo imaging is extremely difficult with conventional, high-resolution fluorescence microscopes. To overcome this limitation, fiber-based fluorescence microscopy systems have been applied [1].

We have developed high resolution flexible optical fiber bundles with in-house synthesized high-index and low-index thermally matched glasses. The fiber bundles are composed of around 12000

single core fibers with pixel sizes between 1.1 - 10 μm (Fig. 1).

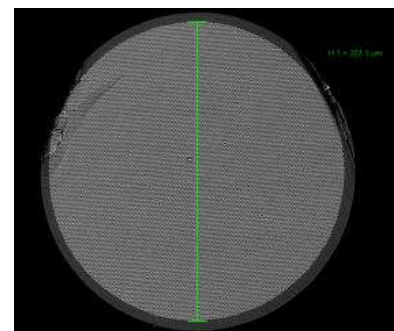


Fig. 1. SEM images of the fiber bundle with the core sizes of 1.1 μm . The fiber bundle contains around 12000 single cores.

They are fabricated using the stack-and-draw technique from sets of thermally matched zirconium-silicate ZR3, borosilicate SK222, sodium-silicate K209,

and lead-silicate F2 glasses (Fig. 2) [2]. With high refractive index contrast pair of glasses ZR3/SK222 and K209/F2 FBs the set of various fiber bundles with very high numerical apertures (NAs) of 0.53 and 0.59 are obtained. Seven different FBs with varying pixel sizes and bundle diameters are characterized. Bright field imaging of a micro-ruler and a *Convallaria majalis* sample, and fluorescence imaging of a dye stained paper tissue and a cirrhotic mice liver tissue are demonstrated using these imaging fiber bundles, demonstrating their good potential for microendoscopic imaging.

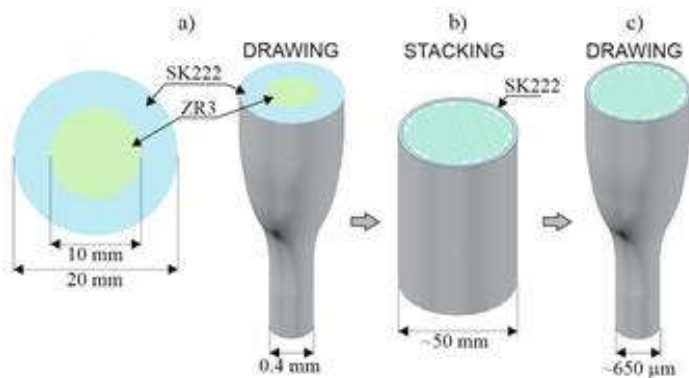


Fig. 2. Schematic of stack-and-draw process for optical fiber bundle fabrication: (a) development of rods made of two types of thermally matched glasses, (b) assembly of perform, (c) drawing final fiber optic bundle.

Brightfield and fluorescence imaging performance of the studied FBs are compared. For both sets of glass compositions, good imaging performance is observed for the fiber bundles with minimum core diameter and core-to-core distance values larger than 1.6 μm and 2.3 μm , respectively. FBs fabricated with K209/F2 glass pair revealed better performance in fluorescence imaging due to their higher NA of 0.59.

Acknowledgements

This work was supported by the project TEAM TECH/2016-1/1 operated within the Foundation for Polish Science Team Programme co-financed by the European Regional Development Fund under Smart Growth Operational Programme (SG OP), Priority Axis IV.

-
- [1]. J. A. N. Fisher, E. F. Civillico, D. Contreras, and A. G. Yodh, *Opt. Lett.* **29**, 71-73 (2004),
- [2]. D. Pysz, I. Kujawa, R. Stępień, M. Klimczak, A. Filipkowski, M. Franczyk, L. Kociszewski, J. Buźniak, K. Haraśny, and R. Buzyński, *Bulletin of the Polish Academy of Sciences Technical Sciences* **62**, 667-682 (2014).

Bend sensor based on microstructured multicore optical fiber

Dawid BUDNICKI¹, Piotr DEBOWSKI¹, Zbigniew HOLDYNSKI¹, Lukasz SZOSTKIEWICZ¹, Krzysztof MARKIEWICZ¹, Krzysztof WILCZYNSKI¹, Michal MURAWSKI², Grzegorz WOJCIK³, Mariusz MAKARA^{1,3}, Krzysztof POTURAJ³, Pawel MERGO³, Oskar KARCZEWSKI¹, Marek NAPIERALA¹, Tomasz NASILOWSKI¹

¹ InPhoTech Sp. z o.o., 15 Dzika Str. 12, 00-172 Warsaw, POLAND

² Polish Centre for Photonics and Fibre Optics, Rogoznica 312, 36-060 Glogow Malopolski, POLAND

³ Department of Optical Fiber Technology, Marie Curie-Sklodowska University, Pl. M. Curie-Sklodowskiej 3, 20-031 Lublin, POLAND

dbudnicki@inphotech.pl

Monitoring the geometry of an element in real time is essential in automating many industrial processes. The robots integrated with an optical fiber bending sensor can be a promising solution for medicine [1], physiotherapy and also for application in computer games or structural health monitoring of construction like e.g.: bridges, pipeline, tunnels, dams [2], [3]. Optical sensors present many advantages resulting from the use of fiber optic technology. They have small size and weight, ability to perform remote measurements up to several kilometers from the sensing point, high safety - no sparks or EM interference and high durability (over 20 years). Fiber optic bend sensors can be divided into three main groups: sensors based on long-period gratings [4], interferometric sensors [5]–[7] and intensity sensors. The most popular bending (deformation) sensor on the market is an electrical sensor which changes resistance under the influence of an external factor such as

temperature or bending. However, such sensors are not able to measure the direction of deformation over the full range of angles. Moreover, the bend sensors based on interferometric method or long-period gratings have high cross-sensitivities to different external factors (temperature, strain and pressure). We present an all-fiber intensity bend sensor, which is based on microstructured multicore optical fiber [8]. Our solution allows to measure the bending orientation as well as the bending radius. This is possible thanks to a special air-hole structure which makes the sensor sensitive only to bending.

The reported solution is an all-fiber intensity bend sensor, which measures power transmitted along the fiber, influenced by the bend. The sensor has seven cores that allows detection of bending orientation over 360°. Each core in the multicore fiber is sensitive to bending in a specific direction. This is realized thanks to different confinement

loss of fundamental mode propagating in each core. Therefore, measurements of optical signal losses in each core enable defining the direction of bending and radius of bending. The independent introduction of light into each core in a multicore fiber and independent detection of these signals is possible by a fan-in/fan-out element.

The setup consists of a light source at 1550nm, detectors and system for the bending sensor. It is presented in Fig. 1.

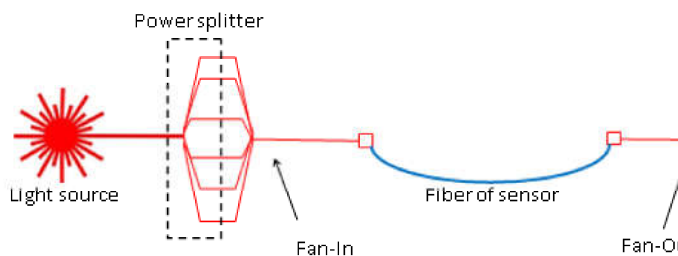


Fig.1 Diagram showing the bend measurement system [5]

In this paper we presented results of the research focused on the possibility of the use of the multicore fibers for bend sensing. Each of the six bend-sensitive cores is possible to detect changes in the orientation of the fiber over 80°. The sensitivity of the proposed solution allows to perform end point detection with millimeter precision.

Acknowledgments:

This research was supported by the Polish National Centre for Research and Development within the research project LIDER/103/L-6/14/NCBR/2015.

- [1] T. Barczak and K. Mianowski, "Project of the assigning/executive manipulator to surgery," *Challenges of Modern Technology*, pp. 20–24, 2011.
- [2] M. DeMerchant, A. Brown, X. Bao, and T. Bremner, "Structural monitoring by use of a Brillouin distributed sensor," *Appl. Opt.*, vol. 38, no. 13, p. 2755, May 1999.
- [3] K. S. C. Kuang, S. T. Quek, C. G. Koh, W. J. Cantwell, and P. J. Scully, "Plastic Optical Fibre Sensors for Structural Health Monitoring: A Review of Recent Progress," *J. Sens.*, vol. 2009, pp. 1–13, 2009.
- [4] D. Zhao *et al.*, "Implementation of vectorial bend sensors using long-period gratings UV-inscribed in special shape fibres," *Meas. Sci. Technol.*, vol. 15, no. 8, pp. 1647–1650, Aug. 2004.
- [5] H. P. Gong, C. C. Chan, P. Zu, L. H. Chen, and X. Y. Dong, "Curvature measurement by using low-birefringence photonic crystal fiber based Sagnac loop," *Opt. Commun.*, vol. 283, no. 16, pp. 3142–3144, Aug. 2010.
- [6] Y. Gong, T. Zhao, Y.-J. Rao, and Y. Wu, "All-Fiber Curvature Sensor Based on Multimode Interference," *IEEE Photonics Technol. Lett.*, vol. 23, no. 11, pp. 679–681, Jun. 2011.
- [7] M. J. Gander *et al.*, "Two-axis bend measurement using multicore optical fibre," *Opt. Commun.*, vol. 182, no. 1–3, pp. 115–121, Aug. 2000.
- [8] D. Budnicki *et al.*, "All-fiber intensity bend sensor based on photonic crystal fiber with asymmetric air-hole structure," 2017, p. 18.

Study on feature detection analysis used for designing hand-held retina vessels detection sensor

Piotr Adam BULER, Krzysztof MURAWSKI

Military University of Technology Urbanowicza Str. 2, 00-908 Warsaw, POLAND

piotr.buler@wat.edu.pl

The aim of this paper is to compare two digital ocular fundus imaging methods, that are primarily used nowadays in ophthalmology clinics and research centres, with a smartphone-based fundus camera system.

Ophthalmic examination of posterior ocular segment - especially imaging of human retina, light-sensitive layer of tissue of the eye, improves early diagnosis of choroidal neovascularization [1] that is the main cause of age related macular degeneration which is considered to be the most common reason of blindness nowadays [2]. The detailed analysis of that eye tissue, especially retina vessels may also help to asses the risk for coronary artery disease (atherosclerosis) as well as hypertension and diabetes [3].

Digital processing of fundus images requires excellent quality of the input data, hence tiny vessels on retina [4] need to be correctly detected and analysed [5].

Retinal images recorded with the traditional fundus cameras are very good quality, i.e. wide view angle, high resolution color images. These advantages as well as an ease of use make that devices popular among ophthalmologists. However, an adaptive optics confocal scanning laser ophthalmoscope is considered as a gold standard in that field, producing high-contrast, detailed images of human eye fundus [6]. Both solutions help to monitor the health status of the human eye but a high price point and heavy design may not allow this devices be available for everyone and everywhere.

This paper is to present a hand-held system that consist of few elements - a smartphone and a powerful convex lens, encased together in 3D-printed adapter, that keep them in place on fixed distance and allow to expand regular back-side mobile camera's capabilities by acquisition of human retina images. The key part of this solution is to determine and present a correct off-line image processing path so the acquired results using this portable

device may be comparable with commercially available table-top systems and be useful in detecting fundus features such as retinal vessels.

[1] K. Murawski, et al., *Measurement of Corneal Neovascularisation with the Use of Image Processing Techniques*, Acta Physica Polonica, 2015,

[2] W. Wong, et al., *Global prevalence of age-related macular degeneration and disease burden projection for 2020 and 2040 : a systematic review and meta-analysis*, The Lancet Global Health, Vol 2 February 2014,

[3] S. Wang, et al., *A spectrum of retinal vasculature measures and coronary artery disease*, Atherosclerosis, 2018,

[4] G. Hildebrand, et al., *Anatomy and Physiology of the Retina*, Pediatric Retina, Springer-Verlag Berlin Heidelberg, 2011,

[5] P. Liskowski, *Segmenting Retinal Blood Vessels with Deep Neural Networks*, IEEE Transactions on Medical Imaging, 2016,

[6] M. Szkulmowski, et al., *Analysis of posterior retinal layers in spectral optical coherence tomography images of the normal retina and retinal pathologies.*, J. Biomed Opt. 12(4), 041207, 2007.

Research of advanced signal detection methods for optical fiber methane sensor

Sylwester CHOJNOWSKI¹, Karol WYSOKIŃSKI¹, Zbigniew HOŁDYŃSKI¹, Jan ZAJIC¹,

Krzysztof MARKIEWICZ¹, Oskar KARCZEWSKI¹, Tadeusz TENDERENDA², Marek NAPIERAŁA¹, Tomasz NASIŁOWSKI¹

¹ InPhoTech Sp. z o.o., 15 Dzika Str. 12, 00-172 Warsaw, POLAND

² IPT PLUS Sp. z o.o., 15 Dzika Str. 12, 00-172 Warsaw, POLAND

schojnowski@inphotech.pl

The development of optoelectronic and photonic technologies give rise to modern optical fiber gas sensors. Currently, there is a growing demand for sensors of various gases that can operate in a wide range of concentrations in a complex gas or high dust environment in real time [1, 2, 3, 4]. The development of such sensors allows for continuous analysis of composition of the atmosphere near sources of hazardous and explosive gas, enabling early hazard detection [4, 5]. One of the commonly used hazardous gases is methane. Methane is also highly explosive under the influence of certain external factors [3, 4]. To be able to detect this gas in a safe way (non-sparking) and to carry out all the above criteria, we have developed optical fiber methane sensor. Advanced methods of detection and processing of optical signals increase sensitivity, reduce response time and reduce measurement uncertainty. The purpose of this research was analysis of the impact of selected advanced signal

detection methods on the methane sensor measurement.

We present a methane sensor operation based on the TDLAS (Tunable Diode Laser Absorption Spectroscopy) method, in optical fiber configuration. In order to an analysis of the methane absorption bands in the NIR range was performed in order to select the absorption line with the minimal cross-sensitivity to other gaseous substances using the HITRAN database. Selected advanced detection methods and signal processing of optical signals e.g. phase-sensitive detection (lock-in), boxcar averaging, will be discussed [6, 7]. An analysis of the effect of the selected detection methods on the parameters of the developed sensor, such as response time and sensitivity, was carried out. The effect of time averaging using Allan variants was also taken into account. Research has been carried out to determine the optimal parameters of

advanced methods for the developed sensor.

The use of the described methods can effectively improve the sensitivity and uncertainty of methane concentration measurement. The sensor is additionally characterized by a wide measuring range and a response time of 2 seconds. The developed an optical fiber methane sensor can be used in:

- the chemical industry, e.g. for monitoring of chemical processes,
- the energy industry, e.g. for monitoring biogas production and leaks in gas transmission installations.

Acknowledgments

The work was supported by European Regional Development Fund within the research project RPMA.01.02.00-14-5656/16 carried out within Regional Operational Programme of Mazovian Voivodeship 2014-2020.

[1] X. Liu, S. Cheng, H. Liu, S. Hu, D. Zhang, H. Ning, *A Survey on Gas Sensing Technology (Review)*, *Sensors*, Vol. 12, 2012, ISSN 1424-8220.

[2] H. Abramczyk, *Wstęp do spektroskopii laserowej*, PWN, Warszawa, 2000, ISBN 83-01-13141-1.A.

[3] Q. He, Ch. Zheng, H. Liua, Y. Wanga, F. K. Tittel, *A near-infrared gas sensor system based on tunable laser absorption spectroscopy and its application to CH₄/C₂H₂ detection*, *Proc. of SPIE*, Vol. 10111 1011135-1, 2017, ISSN: 0277-786X.

[4] O. Vovna, I. Laktionov, A. Zori, R. Akhmedov, *Development and Investigation of Mathematical Model of an Optoelectronic Sensor of Methane Concentration*, *Advances in Electrical and Electronic Engineering*, Vol. 16, 2018, ISSN 1336-1376.

[5] N. P. Sanchez, Ch. Zhengb, W. Yeb, B. Czadera , D. S. Cohana, F. K. Tittel, R. J. Griffin, *Exploratory study of atmospheric methane enhancements derived from natural gas use in the Houston urban area*, *Atmospheric Environment*, Vol. 176, 2018, ISSN 1352-2310.

[6] Z. Bielecki, A. Rogalski, *Detekcja Sygnałów Optycznych*, WNT, Warszawa, 2004, ISBN 8320426545.

[7] J. Mikołajczyk, *Zaawansowane metody detekcji w wybranych technikach laserowej spektroskopii absorpcyjnej*, *Przegląd Elektrotechniczny*, Vol. 9, 2014, ISSN 0033-2097.

Ellipsometric studies of antibody-functionalized sensors: estimation of surface coverage of diamond and gold electrodes

Bartłomiej DEC¹, Michał RYCEWICZ¹, Robert BOGDANOWICZ¹

¹ Faculty of Electronics, Telecommunications and Informatics,
Gdańsk University of Technology, 11/12 Narutowicza Str., 80-233 Gdansk, POLAND

bartlomiej.dec@pg.edu.pl

Ellipsometry one of the most advanced techniques for optical properties estimation such as complex refractive index or transmittance/reflectance. The basis of this technique relies on measuring reflected or transmitted light polarization. One of the most attractive approaches in the novel material analyses take spectroscopic ellipsometry. Thanks to a wide spectrum of measurements enables studies on the refractive index, material composition and its optical band gap.

One of our recent experiments is focused on the detection of influenza virus using doped diamond (BDD) electrodes or gold electrodes with antibody-functionalized surface [1]. The common problem during the fabrication of this type of electrodes is an evaluation of the quality of activated electrodes and rate of surface coverage by a specific antibody. This effect is usually investigated by verifying wetting angle of the electrode but this approach does not deliver information about modified material and is strongly influenced by substrate roughness.

In this work, we propose the evaluation of surface coverage of functionalized surfaces by M1 protein by conducting spectroscopic ellipsometry (SE). Antibody functionalized gold and BDD electrodes were fabricated using electrochemically driven modification and 24 hours incubation. Ellipsometric angles were recorded at bare and freshly prepared electrodes for direct comparison of polarization properties and coverage estimation. The 4-layer optical model (surface roughness / amorphous organic film - antibody / inter-layer / BDD or gold) was assumed to simulate the studied structure and measure optical constants, thickness along with homogeneity of organic antibody over-layer. The organic amorphous model films was applied to estimate optical density and thickness of antibody layer. The surface roughness was defined as the mixture of void and organic film using the effective medium approximation delivering in-direct information about surface coverage. The influence of the electrode surface and fabrication conditions were particularly studied by SE to reveal the most efficient

parameters of functionalization. Optically-driven data was compared with electrochemical and sensing performance of antibody-functionalized sensors.

Acknowledgements

The authors gratefully acknowledge financial support from the Polish National Science Centre (NCN)

under Grant No. 2016/21/B/ST7/01430, 2016/22/E/ST7/00102 and National Centre for Science and Development Grant Techmatstrateg No. 347324.

[1] D. Nidzworski *et al.*, 'A rapid-response ultrasensitive biosensor for influenza virus detection using antibody modified boron-doped diamond', *Sci. Rep.*, vol. 7, no. 1, p. 15707, Nov. (2017).

Near-infrared emission in fluoroindate glasses co-doped with rare-earth

Marcin KOCHANOWICZ^{1*}, Jacek ŻMOJDA¹, Piotr MILUSKI¹, Agata BARANOWSKA¹,

Tomasz RAGIN¹, Jan DOROSZ¹, Marta KUWIK², Wojciech A. PISARSKI², Joanna PISARSKA², Magdalena LEŚNIAK³, Bartłomiej STARZYK³, Maurizio FERRARI^{4,5}, Dominik DOROSZ³

¹Białystok University of Technology, Wiejska 45D Street, 15-351 Białystok, POLAND

²Institute of Chemistry, University of Silesia, Szkolna 9, 40-007 Katowice, POLAND

³AGH University of Science and Technology, 30 Mickiewicza Av., 30-059 Krakow, POLAND

⁴IFN - CNR CSMFO Lab. and FBK, Via alla Cascata 56/C Povo, 38123 Trento, ITALY

⁵Enrico Fermi Centre, Piazza del Viminale 1, 00184 Roma, ITALY

ddorosz@agh.edu.pl

Fluoroindate glasses belong to the low-phonon **Heavy Metal Fluoride Glass (HMFG)** family, which have been extensively studied for their numerous applications [1-5]. The systematic studies indicate that fluoroindate glasses show enhanced thermal stability compared to the known fluorozirconate glasses (ZBLAN), but they are susceptible to crystallization. Moreover, fluoroindate glasses are more transparent in the infrared region than traditional oxide (silica) glasses or ZBLAN, indicating that they have lower phonon energies. The phonon energy of fluoroindate close to 510 cm^{-1} is lower than the value of 580 cm^{-1} obtained for fluorozirconate glass. The lower maximum phonon energy tends to lower rates of non-radiative multiphonon relaxation. Summing-up extended transparency in the infrared region and relatively low phonon energy it makes fluoroindate glasses as an

attractive for active optical fiber applications. It's known that fluoroindate glasses doped with rare-earth ions are promising materials for up-conversion luminescence. However, the near-infrared luminescence studies were limited practically to fluoroindate glasses containing Er^{3+} or $\text{Er}^{3+}/\text{Yb}^{3+}$. The potential applications of extended infrared transmission of fluoroindates justify research on the fiber development. Moreover, there is no information about rare earth co-doped fluoroindate glass fibers and analysis of energy transfer processes. Still, the scientific task is to develop fluoroindate glasses and optical fibers co-doped with lanthanides with mid-infrared luminescence (pumped by high power commercial laser diodes) for application in new optical fiber sources of radiation.

In this work, emission properties of $\text{InF}_3\text{-ZnF}_2\text{-BaF}_2\text{-SrF}_2\text{-GaF}_3\text{-LaF}_3\text{-ErF}_3$

fluoroindate glasses sensitized by TmF₃ have been investigated. Fig. 1 presents the luminescence spectra of glasses in the 1350-1650 nm spectral range under 796 nm laser excitation.

Analyzing the results, we observed that Er³⁺/Tm³⁺ co-doping enables obtaining broadband emission in the 1.5 μm spectral band. It is the result of the partial

Tm³⁺ → Er³⁺ energy transfer and superposition of two emission transitions in the energy structure of rare-earth ions at 1540 nm (Er: ⁴I_{13/2} → ⁴I_{15/2}) and 1450 nm (Tm: ³H₄ → ³F₄). The broad luminescence band at 1.5 μm (Δλ=152 nm) has been observed in glass co-doped with 0.1ErF₃/0.3TmF₃.

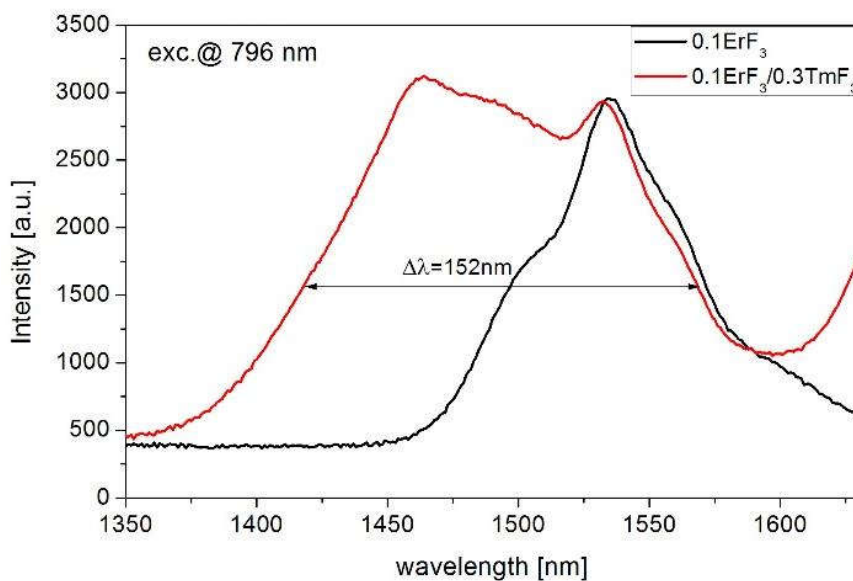


Fig. 1 Luminescence spectra of fluoroindate glasses co-doped with 0.1ErF₃ and 0.1ErF₃/0.3TmF₃ ions, obtained in the range of (1350-1650) nm, excited at 796 nm.

Acknowledgment

The research project was funded by the National Science Centre, Poland granted on the basis of the decision No. 2017/25/B/ST8/02530.

- [1] D. Dong, Z. Bo, J. Zhu, F. Ma, , J. Non-Cryst. Solids **204**, 260 (1996),
 [2] A. Akella, E.A. Downing, L. Hesselink, New fluoroindate glass

- compositions, J. Non-Cryst. Solids **161**, 213-214 (1997) ,
 [3] J. Pisarska, J. Non-Cryst. Solids **382**, 345-346 (2004).
 [4] M.A.S. de Oliveira, C.B. de Araujo, Y. Messaddeq, Opt. Express **19**, 5620 (2011),
 [5] N. Rakov, G.S. Maciel, C.B. de Araujo, Y. Messaddeq, J. Appl. Phys. **91**, 1272 (2002).

Thrombogenicity assessment of biomaterials – do we need new methods?

Maciej GAWLIKOWSKI

Foundation of Cardiac Surgery Development, Artificial Heart Lab. , 345a Wolności Str. 41-800 Zabrze, POLAND
mgawlik@frk.pl

Introduction: Thombogenicity is a feature of biomaterial, which induces or promotes formation of clots. Physiological processes in human body assure endothelial tissue regeneration in case of its damage and avoid serious bleeding. The balance between clot growth (coagulation) and thrombus lysis, which allows to maintain blood liquidity and commonly avoids bleeding, is called hemostasis.

In case of blood contact with artificial materials the coagulation system is activated. In consequence of cascade biochemical reactions the fibrinogen contained in blood undergoes polymerization and fibrin clot is forming (Fig. 1).



Fig. 1. Small clot adhered to the leaflet of artificial valve

This phenomena may has dangerous consequences while blood is flowing through the blood pumps, vascular prostheses, oxygenators, artificial valves

or other medical devices. This kind of thrombus detached from the valve may cause occlusion of small arterial vessel and ischemic stroke.

Contemporary blood-contacting medical devices are made of different biomaterials: metals (mostly titanium alloy with TiN athrombogenic coating), polymer (mostly polyurethanes) and ceramic (i.e. zirconium). Numerous chemical and physical modifications of biomaterials are developed in order to reach better biocompatibility, especially athrombogenicity. There are lack of normative methods of thrombogenicity assessment. The compendium of biomaterials research, ISO 10993 standard, gives only general information about thrombogenicity examination. Therefore some unique methods have been developed.

Methods and results: First problem is to find positive and negative control. As a positive control the glass covered by collagen may be used. Till now negative control has been undeveloped.

The *static thrombogenicity* allows to assess how the biomaterial features (like chemical structure of surface, zeta-potential etc.) affects the platelets.

Specimens are immersed into platelet rich plasma (PRP), next they are washed in phosphate buffer PBS, so only activated and adhered platelets are present on the surface of specimen. The SEM or AFM are used in order to imaging adhered platelets (Fig. 2). In this way it is possible to recognize platelet but only on small part of specimen. However heterogeneous platelet distribution on the surface makes impossible quantitative thrombogenicity determination.

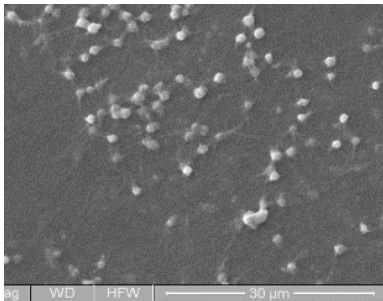


Fig. 2. Platelets adhered to the surface of biomaterial (SEM, magnification 1600x)

Except chemical and electrical manner, platelet may be activated by during blood flow by shear stress. The

dynamic thrombogenicity method allows to assess how the flow morphology affects the platelets activation and its adhesion. Blood is placed between biomaterial and rotating cone, which generates shear stress. After experiment cells are marked by specific antibodies conjugated to fluorochromes. Two aspects of thrombogenicity are assessed: activation of platelets (by means of flow cytometry) and its adhesion to the surface of biomaterial. Activated platelets make aggregates with other cells present in blood (leucocytes, monocytes) which impedes interpretation of flow cytometry data. Cells adhered to the surface of biomaterial are imaging in fluorescence microscope. Unrepeatable conditions of exposition to the UV and fluorochromes degradation in the next expositions significantly limit possibility of quantitative assessment of thrombogenicity (Fig. 3).

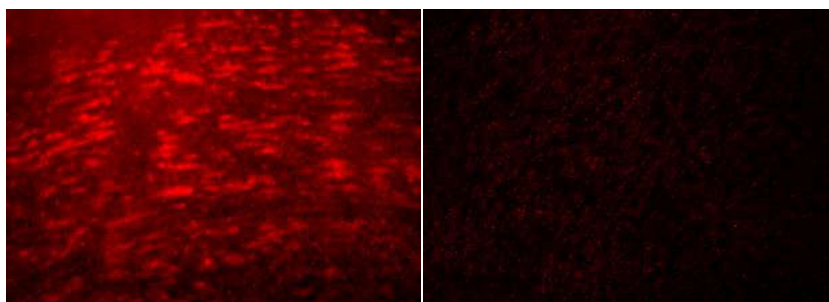


Fig. 3. Fluorescence of the same part of specimen: on the left – overexposed picture due to incorrect set of exposition parameters, on the right site – fluorescent matter degeneration resulting underexposition of picture.

Conclusion: presented methods does not provide a quantitative data essential to make statistical analysis. In turn, the

conclusion based on qualitative analysis is unreliable. It makes significant difficulties during comparison of thrombogenicity of

different biomaterials. It is beneficial to reliable and independent from individual
develop new methods: quantitative, variation of blood.

Determination of gas pressure with use of a camera and neural networks

Leszek GRAD^{*}, Tomasz MALINOWSKI, Krzysztof MURAWSKI

^{*} Military University of Technology, Department of Cybernetics,
2 Gen. Witolda Urbanowicza Str., Warsaw, POLAND

leszek.grad@wat.edu.pl

The paper presents the results of using an artificial neural network to measure gas pressure based on a flat image of a flexible membrane that crowns the chamber. The obtained results were compared with previously developed and presented method based on the analysis

of the image blurring of the marker placed on the surface of the membrane. In the method using neural networks, in order to limit the size of the analyzed data, the transformations of the source signal were used and tested.

Broad-band polymers planar waveguide interferometer

Kazimierz GUT

Department of Optoelectronics, Silesian University of Technology, 2 Krzywoustego Str., 44 100 Gliwice, POLAND
kazimierz.gut@polsl.pl

Recently, broadband interferometers have been developed and realized. In these structures, light from a selected spectral range is simultaneously propagated. Due to a broadband light source used in monochromatic interferometers, phase ambiguity problem which is often encountered in them can be overcome. Description of the broadband Mach-Zehnder interferometer can be found in the literature [1,2].

The analysis of the broadband difference interferometer is presented in [3]. In the broadband interferometers mentioned above, Si₃N₄ is a waveguide layer and SiO₂ is a substrate. These types of structures have a high contrast in the refractive index and, consequently, a high mode sensitivity to changes in the system parameters. This paper presents a model of a broadband difference interferometer based on SU-8. A significant impact of the polymer waveguide layer thickness on the interferometer output signal is shown. Depending on the thickness of the waveguide layer, it is possible to obtain the shift of interference maxima towards short or long waves (so-called blue or red shift). The value of the maximum shift is also dependent on the thickness of the

waveguide layer. In the presented paper, it is shown that the increase in the propagation path in the structure results in the increase in the number of maxima in the output signal. The characteristics presented in the paper allow optimization of the waveguide structure for practical applications. This type of research has not been conducted for polymer waveguides with a relatively low contrast in the refractive index in the visible light range.

-
1. Kitsara M. et al. Integrated optical frequency-resolved Mach-Zehnder interferometers for label-free affinity sensing., OPTICS EXPRESS Vol.18 (8) pp. 8193-8206 (2010).
 2. Misiakos K. et al. Broad-band Mach-Zehnder interferometers as high performance refractive index sensors: Theory and monolithic implementation, OPTICS EXPRESS Vol.22 (8) pp. 8856-8870 (2014).
 3. Gut K. Broad-band difference interferometer as a refractive index sensor, OPTICS EXPRESS Vol.25 (25) pp. 31111-31121 (2017).

Investigation depolarization in variable medium by spatial interferometric system

Aleksandra KALBARCZYK, Leszek R. JAROSZEWICZ, Noureddine BENIS, Idzi MERTA,
Monika CHRUŚCIEL, Paweł MARĆ

* Military University of Technology, 2 Urbanowicza Str., Warsaw, 00-908 POLAND

leszek.jaroszewicz@wat.edu.pl

In depolarizing instrument, such as a broadband imaging spectrometer, the depolarizers are placed on system for stabilization the optical signal. They are also used in order to reduce measurements offsets due to strong polarization dependence, which produce drastic deterioration of the signal to noise ratio. Dynamic depolarizer with controllable degree of polarization is also required for study the effect of noise on

quantum information. Presentation described a new instrument for characterization the variable depolarizer with features which make it different from a polarimetric system. The analysing system based on the simple structure design and has good stability for real time measurement. A practical application of described interferometer system for variable depolarizer characterization are also presented.

Synthesis and propagation of structured light beams in nematic liquid crystals

Urszula A. LAUDYN, Michał KWAŚNY, Jacek PIŁKA, Paweł JUNG, and Mirosław A. KARPIERZ

Faculty of Physics, Warsaw University of Technology, 75 Koszykowa Str., 00-662 Warszawa, POLAND
miroslaw.karpierz@pw.edu.pl

In recent years it has become apparent that the limits of traditional photonics applications could be greatly extended by using the so-called structured light. The concept of structured light initially involved beams with complex structure of phase and/or intensity

distribution and has been subsequently extended to include waves with an inhomogeneous polarization structure, the so-called vector beams i.e. beams and pulses with spatially variant polarization and simultaneous singularity in phase and polarization.

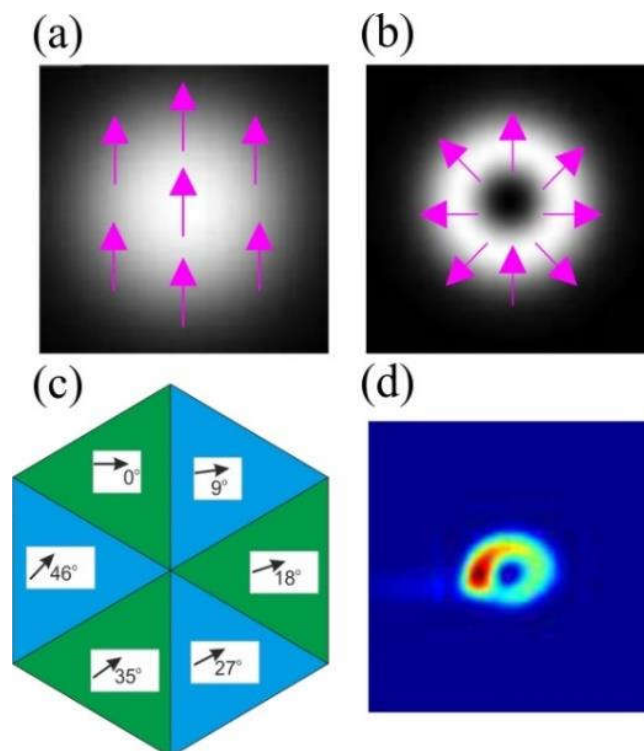


Fig. 1. (a) Conventional uniformly polarized light beam for typical linear state of polarization; (b) vector light beam. For typical state of polarization the direction of the electric vector does not depend on the spatial localization in the beam cross-section; for vector beams the state of polarization is space-variant; (c) scheme of the molecular

orientation (denoted by arrows) in specially design alignment layer and (d) example of generated vector beam in nematic liquid crystal cell with alignment layer as in (c).

In this work we consider a properly engineered dielectric environment with spatially variable orientation of the birefringence axis as a perfect tool for creation such complex beams. As a uniaxial material we choose nematic liquid crystals (NLCs), a prime example of soft matter where, due to the rod-like structure of the organic molecules, both optical and electric anisotropies are present. We employ NLC samples with spatially modulated director orientation forming either isolated domains of specific orientation or periodic structures (Fig.1).

We describe how the propagation of light through such uniaxial birefringent medium can be used as a versatile tool towards the spatial engineering of polarization and phase, thereby providing an all-optical technique for vectorial and scalar singular beam shaping in optics. Besides the prominent role played by the linear change in birefringence axis induced by variable molecular orientation, we also exploit the giant nonlinear response of the NLC molecules which is among others: spatially nonlocal, saturable, having different signs (positive - focusing and negative - defocusing), with different physical mechanism etc. The considered optical nonlinearity causes that the light beam propagation depends on the beam intensity (power density of light), leading to either self-focusing or self-defocusing of light beam (depending

on a type of optical nonlinearity). In particular, the light beam of high enough power can induce optical waveguide, that, in turn, guides itself throughout propagation as if it were confined in an optical fiber. The resulting non-diffracting beam (where the diffraction broadening is counterbalanced by nonlinear self-focusing) is called spatial optical soliton. Interestingly, in such self-induced waveguide, optical solitons can guide another beam, in general with different wavelength and low power, too small to induce nonlinear effects. Thus, we address here the role of the non-trivial nonlinearity of NLCs and demonstrate how the light matter interaction influences the propagation properties of various structured light beams.

The authors gratefully acknowledge support of the Polish National Science Center under the Grant agreement UMOW-2016/22/M/ST2/00261.

-
- [1] Q. Zhan, *Adv. Opt. Photon.* **1**, 1 (2009).
 - [2] T.G. Brown, *Prog. Optics* **56**, 81 (2011).
 - [3] G. A. Swartzlander, *Optical Vortices*, CRC Press, 2014.
 - [4] G. Assanto, M.A. Karpierz, *Liquid Crystals* **36**, 1161 (2009)
 - [5] Y. Isdebskaya, W. Krolikowski, N. Smyth, G. Assanto, *J. Opt.* **18**, 054006 (2016)

[6] U.A. Laudyn, M. Kwaśny, M.A. Karpierz, N.F. Smyth, G. Assanto, Phys. Rev. A **98**, 023810 (2018)

[7] U.A. Laudyna, M. Kwaśny, F.A. Sala, N.F. Smyth, M.A. Karpierz, G. Assanto, Scientific Reports **7**, 12385 (2017).

The problems of the direction finding by air vehicles of the radars working with rotating antenna

Adam RUTKOWSKI, Adam KAWALEC*

* Institute of Radioelectronics, Military University of Technology, 2 Urbanowicza Str., 00-908 Warszawa, POLAND
adam.kawalec@wat.edu.pl

The location of active radars in real environmental terms is a very important and complicated question. The particularly significant difficulties appear in case of observation of radars working with complex signals as well as with impulses having extremely small duration. In these cases the monopulse methods of the direction finding (DF) of microwave sources and devices of instantaneous phase measurement (IPhM) and instantaneous frequency measurement (IFM) of signals emitted by these sources are very useful. The efficiency of the direction finding of ground-based radars by air vehicles is dependent among other things on parameters of applied taking bearings apparatus as well as on

construction and modes of running of observed radar's antenna system, and also on the properties of terrain around this radar. The exemplary shapes of radar antenna directional patterns and their relationships with possibilities of this radar remote detection were described in the work. It was paid attention on multi-path phenomenon, which can make difficult of direction finding of radar, but concurrently it can facilitate undesirable discovery of radar activity. The simulated shapes of signals received by recognition device as well as expected results of the monopulse direction finding accomplishing basing on these signals were presented.

Examination of the bottom of the Gdansk Bay by means of acoustic methods

Eugeniusz KOZACZKA^{*}, Grażyna GRELOWSKA

* Faculty of Ocean Engineering and Ship Technology, Gdansk University of Technology,
Narutowicza 11/12, 80-233 Gdansk, POLAND

kozaczka@pg.edu.pl

The interest in the seabed in various aspects is clearly increasing. This is determined by, among other things, cognitive aspects regarding the mapping of the shape of the bottom and its structure as well as objects lying on the bottom. No less important are practical aspects, such as knowledge of navigational obstacles necessary for sea transport or knowledge about the type of bottom sediments needed in the construction of offshore facilities. The type of bottom sediments also affects the extent of underwater noise spreading, especially in the shallow sea.

The paper presents the main methods and devices currently used in seabed surveys using acoustic waves. The results of own research carried out in the Gulf of Gdansk will be presented. Particular emphasis will be placed on researching the upper layer of bottom sediments using non-linear hydroacoustics. The influence of the selection of parameters of measuring devices and the way of processing data on the obtained images will be shown. Data obtained by acoustic methods will be compared with geological data.

Liquid-crystal diffraction gratings based on azo polymer aligning layers exposed to blue light interference pattern

Anna KOZANECKA-SZMIGIEL¹, Katarzyna RUTKOWSKA¹, Mateusz NIEBOREK¹,
Michał KWAŚNY¹, Dariusz SZMIGIEL²

¹Faculty of Physics, Warsaw University of Technology, 75 Koszykowa Str., 00-662 Warszawa, POLAND

²Institute of Electron Technology, al. Lotnikow 32/46, 02-668 Warszawa, POLAND

annak@if.pw.edu.pl

Switchable liquid-crystal diffraction gratings are of considerable interest as components of functional devices for optical communications. Gratings possessing unique diffraction properties may be fabricated using photosensitive alignment layers exposed to light polarization pattern generated by two coherent laser beams of opposite circular polarization [1,2].

Azobenzene-containing polymers are important group of photoresponsive materials known for the ability to induce a planar alignment of nematic liquid crystals [3]. Irradiation of an azo polymer layer with linearly polarized light of a proper wavelength may orient rod-like azo molecules in directions perpendicular to light polarization direction. Stability of the photoinduced azochromophore order depends on chemical structure of the polymer strongly, and becomes a crucial issue when application in the area of liquid crystal alignment is considered.

In this work we demonstrate the ability of azo polymer to record the interference pattern formed by two 442

nm coherent beams (from a He-Cd laser) crossing at a small angle. We present two configurations of liquid crystal diffraction gratings based either on a pair of photoaligned azo polymer substrates or a photoaligned surface and a rubbed one. A single-step or two-step exposure was employed in order to fabricate one or two dimensional diffraction structures (Fig. 1). A possibility of obtaining a rotating planar alignment of liquid crystal director in the cell assembled from the two substrates exposed to left- and right-handed circularly polarized beams is discussed. Diffraction properties and temporal stability of the fabricated gratings are presented.

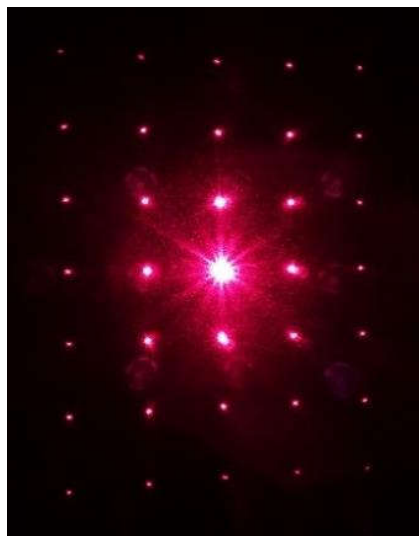


Fig. 1. Photograph of a diffraction pattern produced by two-dimensional liquid crystal grating

Synthesis of the azo polymer was described elsewhere [4], and was financed from the Foundation for Polish Science under grant no. POMOST/2013-7/6 (cofinanced from the European Union under the European Regional Development Fund). This work was also

partially supported by the Polish National Science Centre under the grant no. DEC-2013/11/B/ST7/04330.

-
- [1] H. Sarkissian, B. Park, N. Tabirian, B. Zeldovich, *Mol. Cryst. Liq. Cryst.* **451**, 1 (2006),
- [2] C. Provenzano, P. Pagliusi, G. Cipparrone, *Appl. Phys. Lett.* **89**, 121105 (2006),
- [3] O. Yaroshchuk and Y. Reznikov, *J. Mater. Chem.* **22**, 286 (2012),
- [4] A. Kozanecka-Szmigiel, J. Konieczkowska, D. Szmigiel, K. Switkowski, M. Siwy, P. Kuszewski, E. Schab-Balcerzak, *Dyes Pigm.* **114**, 151 (2015).

Generation of optical vortices in nonlinear photonic crystals

K. SWITKOWSKI,^{1,2} S.LIU,³ Yan SHENG,³ and W.KROLIKOWSKI^{2,3}

¹Faculty of Physics, Warsaw University of Technology, POLAND,

²Science Program, Texas A&M University at Qatar, QATAR;

³Laser Physics Centre, Australian National University, Canberra, ACT 2601, AUSTRALIA

wieslaw.krolikowski@qatar.tamu.edu.au

Second-order nonlinear optical effects, which involve, e.g., second harmonic, sum and difference frequency generation, are of great importance because of their application in laser wavelength extension, ultrafast signal processing, quantum light source, terahertz technology, and more. However, Performance of many optical devices based on frequency conversion critically depends on spatial modulation of the nonlinear optical response of the materials. This modulation ensures, via the quasi phase matching (QPM)¹, an efficient energy exchange between optical waves at different frequencies. In general, the QPM structures, also known as the nonlinear photonic crystals (NPC)²⁻⁴, offer a variety of novel properties and functionalities that cannot be obtained in uniform nonlinear crystals. Common method to modulate spatially $\chi(2)$ nonlinearity is electrical poling which relies on inverting spontaneous polarization of the ferroelectric crystal by applying strong enough electric field (voltage). We have recently introduced a new technique which enables one to achieve spatial modulation of quadratic nonlinearity anywhere inside ferroelectric crystal. It is based on focusing

femtosecond laser beam inside of the ferroelectric.

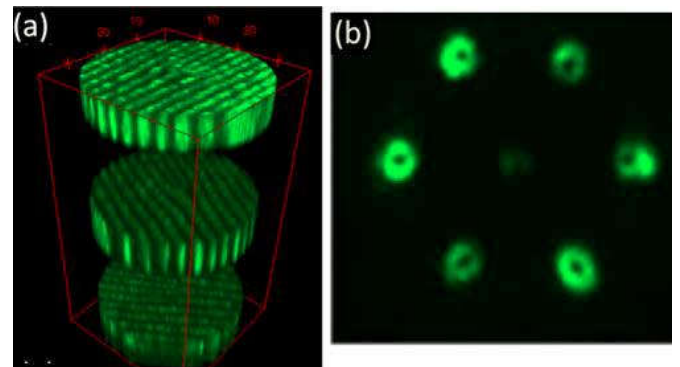


Fig. 1. (a) All-optically engineered $\chi(2)$ multilayer nonlinear structures of three charge-2 fork patterns for second harmonic vortex generation superposed inside the CBN crystal; (b) Six charge 2 optical vortices emitted from the nonlinearity pattern in the second harmonic generation process.

The high light intensity in the focal volume causes strong two photon absorption which drastically increases crystal temperature in the focal volume leading to its high gradient. The resulting thermo-optic electric field inverts locally spontaneous polarization, which amounts to reversal of sign of quadratic $\chi(2)$ nonlinearity. Because of multi-photon absorption takes place in very limited volume, the technique allows one to

invert spontaneous polarization in selected region of the nonlinear medium and hence spatially modulate it as necessary. By using this method we were able to create one, two and three-dimensional nonlinear structures. Furthermore, this light induced nonlinearity engineering can be employed to shape the wave-front of optical beams generated in frequency conversion. We have succeeded in simultaneous generation of vortex second harmonic beams by fabricating three nonlinear structures inside the Calcium Barium Niobate crystal (Fig.1).

In summary, we demonstrated all-optical approach to nonlinearity engineering in ferroelectrics. Our method allows one to realize domain reversal deep below the crystal's surface and for nonstandard crystallographic orientation. We used it to realize various frequency mixing processes, including 3-d nonlinear photonic crystal and wave-front shaping such as generation of vortices in second harmonic generation.

Funding: Qatar National Research Fund (Grant # NPRP 9- 020-1-006); Foundation for Polish Science (Grant HOMING POIR.04.04.00-00-5E4E/18-00).

-
- [1] J.A. Armstrong, N. Bloembergen, J.P. Ducuing, P.S. Pershan, Phys. Rev. **127**, 1918-1939 (1962).
 - [2] V. Berger, Phys. Rev. Lett. **81**, 4136-4139 (1998).
 - [3] A. Arie, and N. Voloch, Laser Photon. Rev. **4**, 355 (2010).
 - [4] X. Chen, P. Karpinski, V. Shvedov, et al., Opt. Lett. **41** (11), 2410 (2016).
 - [5] T. Xu, K. Switkowski, S. Liu et al., Nature Photon. **12**, 591 (2018).

Evaluation of the impact of evolution strategy parameters on the optimization of the markers distribution on the VAD membrane

Tomasz MALINOWSKI^{*}, Leszek GRAD, Krzysztof MURAWSKI

* Military University of Technology, Department of Cybernetics,
2 Gen.W.Urbanowicza Str., Warsaw, 00-908 Poland

tomasz.malinowski@wat.edu.pl

The publication focuses on studying the impact of evolution strategy parameters on the optimization of the distribution of markers on the flaccid membrane surface of an extracorporeal pneumatic heart assist pump. The aim of the research was to select the best combination of selection, mutation and crossover algorithms to select the optimal distribution of markers on the membrane surface. The study was carried out on a

convex membrane with a known mathematical description. The research allowed us to determine the influence of selected options and procedures of the evolutionary strategy on speed of achieving the optimal (sub-optimal) solution and on the error of mapping the obtained shape of the membrane surface in relation to the shape of the reference surface (model), determined on the basis of the formula.

T2SLs InAs/GaSb and T2SLs InAs/InAsSb higher operating temperature detectors – where is the limit?

Piotr MARTYNIUK^{*}, Klaudia HACKIEWICZ

Institute of Applied Physics, Military University of Technology, 2 Urbanowicza Str., 00-908 Warsaw, POLAND
piotr.martyniuk@wat.edu.pl

Up to date many approaches to include materials and structures to improve infrared (IR) photodetector performance for high operating temperature (HOT) conditions have been presented and successfully applied.

Firstly HOT conditions could be met by proper choice of the active layer (absorber) material exhibiting the highest absorption coefficient and thermal generation-recombination (GR) rate ratio (α/GR). GR could be limited by designing the detectors' active layer by materials inherently exhibiting lower GR rates. Here, due to the carrier separation suppressing Auger GR the InAs/GaSb or InAs/InAsSb type-II superlattices (T2SLs) should be enumerated. Both T2SLs InAs/GaSb and "Ga-free" InAs/InAsSb theoretically offer higher performance to HgCdTe at an equivalent cut-off wavelength. On the other hand, T2SLs are reported to be very resisted in attempts to improve its SRH carrier lifetime where Ga is assumed to be responsible for that GR mechanism giving at the same time prospects for "Ga-free" T2SLs InAs/InAsSb.

Secondly, many detectors' structures could be used where improvement in operating temperature without suppression of the detector's performance could be reached. Among them implementation of the non-equilibrium conditions in multilayer detector's structures to suppress an Auger GR process could be listed. Except of the non-equilibrium structures the barrier detectors where suppression of the SRH GR components due to the theoretical lack of depletion layer in comparison to the traditional photodiode must be also taken into account. Unipolar barrier structures operating close to crossover temperature are perspective, however further improvement in HOT conditions could be met by complementary barrier detectors.

Lately, higher than room temperature operation conditions has been reached by interband cascade infrared detectors introduced to increase the absorption efficiency and suppression of the shot noise. The concept of operation is based on serial connection of active regions (shorter than diffusion length) through

interband tunneling with carrier relaxation (transport) region.

In that paper we compare HOT technologies pointing out on utmost performance.

The authors would like to acknowledge the support by The National Centre for Research and Development, Project: TECHMATSTRATEG1/347751/5/NCBR/2017.

[1] P. Klipstein *et al.*, “MWIR InAsSb XBn detector for high operating temperatures”, Proc. SPIE 8012, 80122R (2011).

[2] E. H. Steenbergen *et al.*, “Significantly improved minority carrier lifetime observed in a long-wavelength infrared III-V type-II superlattice comprised of InAs/InAsSb”, Appl. Phys. Lett. 99, 251110 (2011).

[3] B. V. Olson *et al.*, “Time-resolved optical measurements of minority carrier recombination in a mid-wave infrared InAsSb alloy and InAs/InAsSb superlattice”, Appl. Phys. Lett. 101, 092109 (2012).

[4] A. Rogalski, [Infrared Detectors], CRC Press, Boca Raton, (2011).

[5] M. A. Kinch, [State-of-the-Art Infrared Detector Technology], SPIE Press, Bellingham, (2014).

[6] T. Ashley *et al.*, “Non-equilibrium mode of operation for infrared detection”, Electron. Lett. 21, 451–452 (1985).

[7] D. Donetsky *et al.*, “Carrier lifetime measurements in short-period InAs/GaSb strained-layer superlattice structures”, Appl. Phys. Lett. 95, 212104 (2009).

[8] E. Plis, “InAs/GaSb type-II superlattice detectors”, Advances in Electronics, 246769 (2014).

[9] S. Maimon *et al.*, “nBn detector, an infrared detector with reduced dark current and higher operating temperature”, Appl. Phys. Lett. 89, 151109 (2006).

[10] R. T. Hinkey *et al.* “Theory of multiple-stage interband photovoltaic devices and ultimate performance limit comparison of multiple-stage and single-stage interband infrared detectors”, J. Appl. Phys. 114(10), 104506 (2013).

[11] R. T. Hinkey *et al.* “Comparison of ultimate limits of interband cascade infrared photodetectors and single-absorber detectors”, Proc. SPIE 8868, 886804 (2013).

[12] G. J. Brown, “Type-II InAs/GaInSb superlattices for infrared detection: an overview”, Proc. SPIE 5783, 65–77 (2005).

[13] D. Z.-Y. Ting *et al.*, “Type-II superlattice infrared detectors”, in: Semiconductors and Semimetals, Vol. 84, pp. 1–57, edited by S. D. Gunapala, D. R. Rhiger, and C. Jagadish, Elsevier, Amsterdam, (2011).

Sensors characteristics of helically twisted microstructured optical fibers

Paweł MERGO, Mariusz MAKARA, Krzysztof POTURAJ, Lidia CZYZEWSKA,
Grzegorz WÓJCIK, Aleksander WALEWSKI, Jarosław KOPEĆ

Laboratory of Optical Fibers Technology, Maria Curie Skłodowska University in Lublin,
Pl. Marii Curie Skłodowskiej 3, 20-031 Lublin, POLAND

pawel.mergo@umcs.lublin.pl

Research related to twisted optical fibers is currently at an early stage of development and so far only a few works have been published indicating the huge potential of such structures. The combination of microstructural fiber technology and twisted fiber technology seems particularly interesting. The microstructured fibers are used for: supercontinuum generation in a wide spectral range, for propagation in the air core due to the effect of photonic bandgap, which allows the use of such structures in gas spectroscopy, single mode mode of operation in a wide spectral range, to achieve record birefringence, single-polarization working mode and for various sensor applications. Twisted optical fibers have a number of unique properties, including circular birefringence and polarity dependent coupling of basic modes with mantle modes, which is not observed in untwisted optical fibers. It has also already

been shown that in conventional twisted optical fibers, the effect of resonant coupling of the core mode to mantle modes can be observed. In this context, the use of twisted microstructure optical fibers seems particularly interesting in the sensors applications. Technology of twisted microstructured optical fibers is developed in the Laboratory of Optical Fiber Technology UMCS for over two years. During this time, several technologies of various types of twisted microstructured optical fibers have been developed. The work presents the sensor properties of several selected structures. Particular attention was paid to the possibility of twisted microstructured optical fibers use in a distributed sensor systems.

Funding National Science Centre of Poland, grant Maestro 8, DEC-2016/22/A/ST7/00089.

Vision sensor to measure liquid volume

Krzysztof MURAWSKI*, Monika MURAWSKA

* Military University of Technology, 2 Urbanowicza Str., Warsaw, 00-908 POLAND

The paper presents the construction and the use of a video sensor developed to measure liquid volume. A characteristic feature of the device is liquid volume measurement based on digital image processing. The paper presents the results of sensor calibration and measurements taken during the tests. The tests have

been specially prepared to use the sensor to control the value of the VAD stroke volume. It has been shown that the developed sensor that is equipped with a flat, floating diaphragm allows measuring the stroke volume in the range of 0 - 80 ml.

Objects tracking in virtual reality applications using SteamVR tracking system - selected issues

Marcin MACIEJEWSKI, Marek PISZCZEK, Norbert PAŁKA*

* Military University of Technology, 2 Urbanowicza Str., Warsaw, 00-908 POLAND

norbert.palka@wat.edu.pl

Currently, objects tracking issue in immersive Virtual Reality (VR) applications is important for various applications. It is related not only to determination of the position and orientation of the user himself but also as the tool that he exploits in VR environment. Among numerous methods of objects tracking, the "Lighthouse" solution implemented in the SteamVR tracking system deserves

special attention. One of the main reasons is the open concept of the SteamVR tracking system and the availability of simple analytical tools, which allows users to build their own tracker modules. The paper presents the results of work on this type of solutions, including the possibility of developing design tools and methods for testing of original tracker structures for a shooting simulator.

Identification of optical signatures for the augmented reality system

Tomasz PAŁYS^{*}, Artur ARCIUCH

* Military University of Technology, 2 Urbanowicza Str., Warsaw, 00-908 POLAND

tomasz.palys@wat.edu.pl

The article proposes a method that allows simultaneous identification of many optical signatures used for optical control in augmented reality systems. Optical signatures are generated using appropriately coded laser pulse sequences. The developed method of

identifying optical signatures allows to identify individual series of laser pulses and is based on the analysis of video sequence of images. This is an important advance in relation to the systems used to cooperate with objects in the augmented reality environment.

Integrated photonics – technologies and applications

Ryszard PIRAMIDOWICZ, Stanisław STOPIŃSKI,
Andrzej KAŻMIERCZAK, Aleksandra PAŚNIKOWSKA, Mateusz
SŁOWIKOWSKI,
Anna JUSZA, Krzysztof ANDERS, Witold PLESKACZ, Paweł SZCZEPAŃSKI

Warsaw University of Technology, Institute of Microelectronics and Optoelectronics,
75 Koszykowa Str., 00-662 Warsaw, POLAND
r.piramidowicz@elka.pw.edu.pl

The last decades have observed significant progress in the field of integrated photonic technology, which finally resulted in moving photonic integrated circuits (PICs) from the research labs to the market.

Similarly to integrated electronics, the concept of prototyping PICs is based on a generic approach, which assumes that the circuits of any complexity can be designed using a limited number of fundamental building blocks (the same for every foundry), with the use of standardized CAD tools and technological processes.

From the two most promising platforms, based either on silicon or indium phosphide, the latter seems to be the most versatile and attractive as it offers access to all passive and active components, which is the obvious consequence of direct bandgap, inherent to InP-based semiconductors. This feature enables realizing monolithically integrated light sources (coherent and incoherent), optical amplifiers and detectors as well as all passive elements like waveguides, (de)multiplexers, couplers, arrayed

waveguide gratings etc. Furthermore, due to intrinsic electro-optic effect, the InP platform also provides high-speed light modulators.

In this work we discuss the current capabilities and potential of the two above mentioned technological platforms in the context of applications in optical communications and sensing, identified as the main drivers of development of integrated photonics market.

In particular the main features and limitations of major technologies will be discussed, generic approach will be presented using the example of indium phosphide platform and all steps of PIC's manufacturing will be briefly characterized. We will also present and summarize the results of the last few years of R&D works on Application Specific Photonic Integrated Circuits (ASPICs) conducted by the team of Eastern Europe Design Hub (EEDH) of Warsaw University of Technology, IMiO. As a result – two main ASPIC lines have been developed addressing two different fields of applications – multichannel

transmitters for fiber-optic access systems (WDM-PON) and integrated photonic interrogators for fiber Bragg grating (FBG) sensor networks. This lineup of designed devices, presented in Fig. 1 is complemented by a series of proof-of-the-concept devices like integrated OTDR, modules for optical gyroscopes, optical delay lines, multichannel light sources, switches, lossless splitters etc.

All photonic integrated circuits presented on the microscope pictures in Fig. 1 were designed and characterized by

the EEDH team at Warsaw University of Technology and realized in generic processes provided by main European foundries – SMART Photonics and Heinrich Hertz Institute (HHI) [1], offering access to their generic platforms by means of organizing multi-project wafer runs.

In general, all the results have proved the great potential of InP-based integrated photonic platform, showing however also the areas of further development and optimization, which will be discussed in detail.

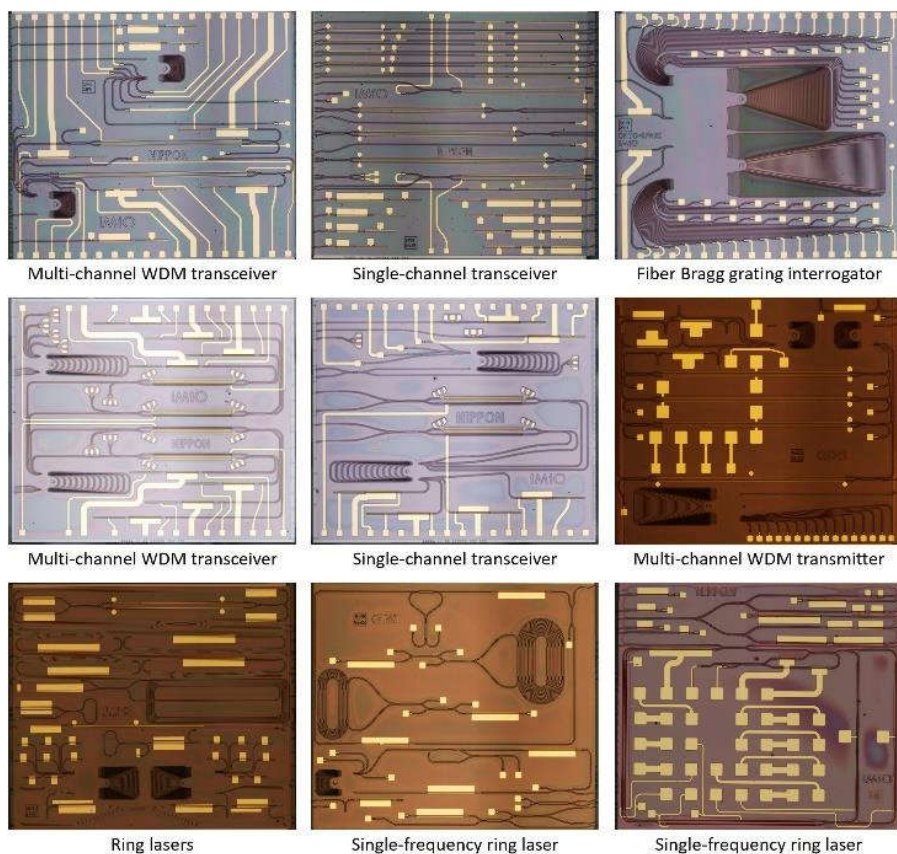


Fig. 1. Microscope pictures of photonic integrated circuits, designed by EEDH team and fabricated in the generic processes of InP foundries.

Acknowledgement: This work has received support from the EU Horizon 2020 research and innovation programme under grant agreement No. 687777

(PICs4All) and by the National Centre for Research and Development through projects NIPPON (PBS3/A3/21/2015) and OPTO-SPARE (PBS3/B9/41/2015).

Optimization of optical properties of photonic crystal fibers infiltrated with chloroform for supercontinuum generation

Chu Van LANH¹, Van Thuy HOANG^{2,3}, Van Cao LONG⁴, Krzysztof BORZYCKI⁵,
 Khoa Dinh XUAN¹, Vu Tran QUOC¹, Marek TRIPPENBACH², Ryszard
 BUCZYŃSKI^{2,3} and Jacek PNIEWSKI²

¹ Department of Physics, Vinh University, 182 Le Duan, Nghe An Province, Vinh City, VIET NAM;

² Faculty of Physics, University of Warsaw, Pasteura 7, 02-093 Warsaw, POLAND;

³ Department of Glass, Institute of Electronic Materials Technology, Wólczyńska 133, 01-919, Warsaw, POLAND;

⁴ Institute of Physics, University of Zielona Góra, Prof. Szafrana 4a, 65-516 Zielona Góra, POLAND;

⁵ National Institute of Telecommunications, Szachowa 1, 04-894 Warsaw, POLAND

j.pniewski@uw.edu.pl

A photonic crystal fiber (PCF) made of fused silica glass, infiltrated with chloroform (CHCl₃), is proposed as a new source of near-infrared supercontinuum (NIR SC) light, pumped with low-energy pulses. Among common non-linear liquids such as CS₂, CCl₄ and CHCl₃, the latter has the lowest material dispersions in the visible region.

The schematic view of the geometrical structure of the modelled CHCl₃-filled PCF is shown in Fig. 1. It consists of 8 rings of air-holes ordered in a hexagonal lattice, surrounding the central liquid-filled hole. The linear filling factor of the cladding is defined as $f = d/\Lambda$, where d is the diameter of a single air-hole, and Λ is the lattice constant. We assume that PCF is made of fused silica glass. The central hole is filled with CHCl₃.

Guiding properties in terms of effective refractive index, attenuation, and dispersion of the fundamental mode

are studied numerically. As a result, two optimized structures are selected and verified against SC generation in detail. The dispersion characteristic of the first structure #F1 is all-normal and equals $-7 \text{ ps}\cdot\text{nm}^{-1}\cdot\text{km}^{-1}$ at $0.92 \text{ }\mu\text{m}$, while the dispersion characteristic of the second structure #F2 has the zero-dispersion wavelength at $1 \text{ }\mu\text{m}$, and SC generation was demonstrated for the wavelength $1.03 \text{ }\mu\text{m}$.

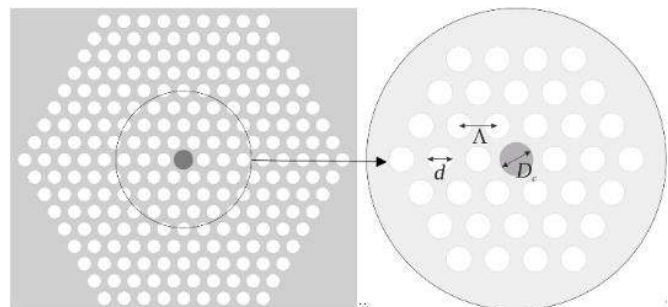


Fig. 1. The schematic of the modelled PCF structure. Coefficient D_c is the diameter of the liquid-filled core.

Both characteristics of dispersion are shown in Fig. 2. The fiber #F1 is intended to generate coherent supercontinuum in the normal dispersion regime while pumped at 1030 nm. The fiber #F2 is expected to generate supercontinuum of low coherence in the anomalous regime at the same pump wavelength as #F1.

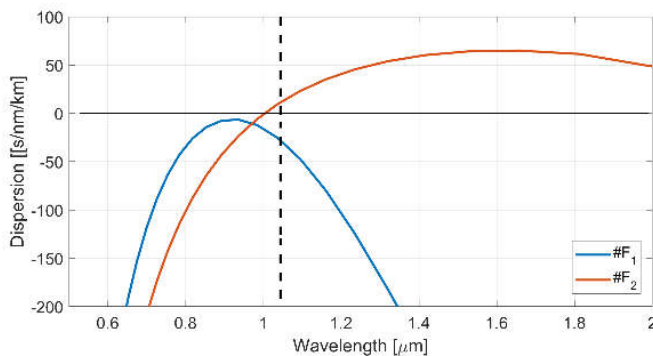


Fig. 2. Characteristics of PCF mode dispersion for the fibers #F1 and #F2. The dotted line indicates the pump wavelength 1030 nm.

The nonlinear properties of the investigated fibers are calculated numerically solving the generalized nonlinear Schrödinger equation (GNLSE) using split-step Fourier method (SSFM).

In Fig. 3 SC spectrum for 10 cm length of the fiber pumped with pulses of 400 fs duration, 1030 nm pump wavelength, various pulse energy and degree of coherence are shown.

The PCF parameters allow for high coupling efficiency with standard femtosecond fibers and high fiber nonlinearity. With the moderate input pulse energy of 1 nJ and the pulse duration 400 fs it is possible to obtain SC with low-cost commercial femtosecond fiber lasers emitting at 1030 nm.

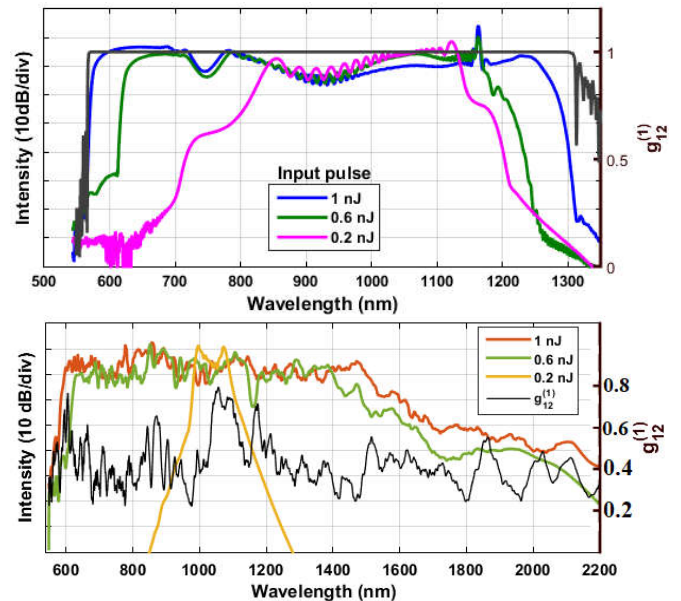


Fig. 3. SC spectrum for various pulse energy and degree of coherence for fibers #F1 and #F2.

-
- [1] J. C. Knight et al., *Opt. Lett.* 21(19), 1547–1549 (1996).
 - [2] J. Pniewski et al., *Applied Optics* 55(19), 5033–5040 (2016).

Silk fibroin thin films - biomaterial for optical humidity sensing

Marcin PROCEK^{1*}, Zbigniew OPILSKI¹, Augusto MÁRQUEZ MAQUEDA²,
Xavier MUÑOZ-BERBEL², Carlos DOMÍNGUEZ HORNA²

¹ Department of Optoelectronics, Silesian University of Technology,
2 Krzywoustego Str. 44-100 Gliwice, POLAND

² Chemical Transducers Group, Institute of Microelectronics of Barcelona IMB-CNM, CISC, C/del Til·lers. Campus Universitat Autònoma de Barcelona (UAB), 08193 Cerdanyola del Vallès (Bellaterra), Barcelona, SPAIN

marcin.procek@polsl.pl

In this work changes of optical parameters of the silk fibroin (SF) thin films caused by changes of relative humidity (RH) was examined. SFs water solutions were obtained from bombyx mori silkworm cocoons via chemical extraction. Water solutions of 5-7 w% silk fibroin was used to obtain thin films on Si substrate, with 100 nm SiO₂ film using spin coating method (Fig. 1) in clean-room conditions. In next step SF films were curried in the vacuum for one night.

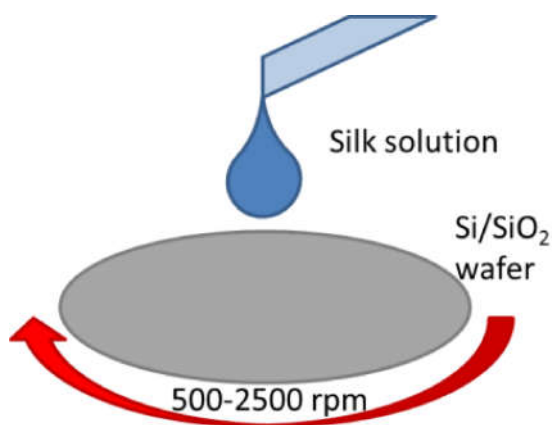


Fig. 1. Silk fibroin thin film fabrication via spin coating method

The potential of application of SF thin films in RH sensors was experimentally proved using spectral ellipsometry. The ellipsometer allowed to determine the thickness of the layers and their complex refractive index in the spectral range from 280 nm to 2500 nm and was equipped by measurement chamber for gas sensing experiments. Experiments were carried out at room temperature in air with different RH values (from 7% up to 90%). In addition, the reaction of the films to the presence of toxic gases: NO₂, NH₃ in ppm range were examined to show their selectivity.

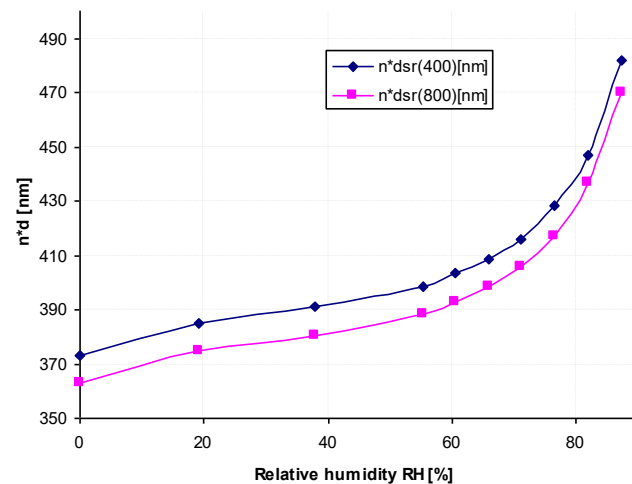


Fig. 2. Optical path ($n \cdot d$) in the function of RH for $\lambda = 400$ nm and 800 nm

The sensor dynamic parameters were tested using interferometry measurement system. This allowed to assess the time of the layer's reaction to rapid changes in

relative humidity and to determine the time of rise and fall of the layer's response.

Obtained results are showing that silk fibroin thin film optical properties strongly depends on RH value (Fig 2.) and these changes are relatively fast.

Distributed optical fiber sensors for high temperature applications

Aleksandra RAFALAK¹, Krzysztof WILCZYŃSKI¹, Tomasz STAŃCZYK¹,
Krzysztof MARKIEWICZ¹, Alejandro Dominguez LOPEZ¹, Jakub
KACZOROWSKI¹, Łukasz SZOSTKIEWICZ², Marek NAPIERAŁA^{1,3}, Tomasz
NASIŁOWSKI¹

InPhoTech Sp. z o.o., Dzika St 15/12, 00-172 Warsaw, POLAND

² Polskie Centrum Fotoniki i Światłowodów, Aleje Raławickie St 8/12, 20-037 Lublin, POLAND

³ IPT Safety Sp. z o.o. Konopnica 133, 21-030 Konopnica, POLAND

arafalak@inphotech.pl

High temperature measurements find applications in many industrial fields like furnaces [1] or power plants [2]. Optical fiber sensors (OFS) have high potential of application in harsh environments, while conventional sensors can not be used.[3], [4] An existing problem for conventional sensors is to measure high temperature in such applications. It is caused by danger of sparking, electromagnetic noise sensitivity (electrical sensors) or relying only on surface measurement (cameras). Those problems can be solved using optical fiber sensors.

OFS possess several unique properties like – durability in high temperatures [3], insensitivity to electromagnetic interference, small size [5] and intrinsic safety. Especially the greatest advantage of fiber optics measurement over other sensors is the possibility of distributed sensing. [2] This makes it possible to measure quantity without blind spots. Combining these

properties we can sensing high temperature using distributed fiber optics sensors (DFOS) in explosive media.

We present distributed fiber optics sensors behavior in high temperatures. The proper selection of the coating and the interrogator are necessary for this task.

DFOS can detect temperature and strain changes. Depending of sensing technique we can choose properties of measurement: define needed length of fiber and resolution. They are still rarely used in commercial applications, while they have potential on such fields as pipelines monitoring, structure health control, intrusion detection, etc. In high temperature environments they can operate as sensors for industrial furnaces and process monitoring.

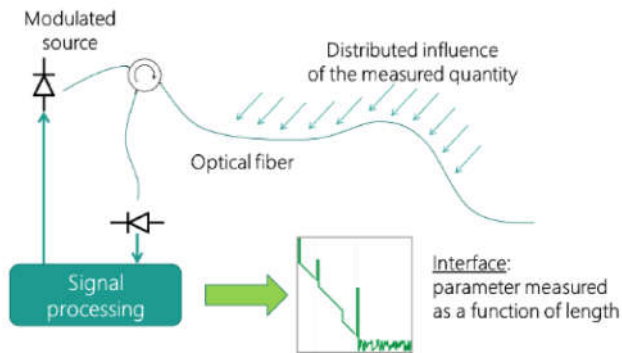


Fig. 1. Distributed fiber optics sensors idea.

The problem with FOS for temperature measurement is that silica optical fibers with conventional coating are degraded at temperatures around 100°C. Therefore they need to be coated to protect silica glass from degradation. At temperatures up to 350°C fibers can be coated with special polyimide. However, because of polyimide degradation in temperatures above 350°C to FOS work at higher temperatures metal coatings should be applied.[6]

To measure temperature using distributed sensing technique we also need to properly choose interrogator. We will talk about important aspects of the selection of the system of optical fiber and interrogator at high temperatures.

Therefore we show the comparison of the quality of data collected using different types of measurement techniques. Summarizing DFOS are strongly promising technology on sensor market. They can be used for distributed measurement at high temperatures and they find applications in wide areas. Used different measurement techniques we can design them for

measurements with high resolutions or over long distances. If we protect them properly they can measure temperatures even around 800°C.

The research was carried out as part of the projects RPMA.01.02.00-14-6224/16 and RPLU.01.02.00-06-0062/16.

-
- [1] E. Zedginidze et al., Temperature measurement in industrial furnances, *Ogneupory i Tekhnicheskaya Keramika*, No. 11, pp. 36-37, 1996
 - [2] F. Jensen et al., Distibuted Raman temperature measurement system for monitoring of nuclear power plant coolant loops, *SPIE*, vol. 2895, npp.132-143, 1996
 - [3] T. Stanczyk et al., Influence of high temperatures on optical fibers coated with multilayer protective coatings, presented at the 16th Conference on Optical Fibers and Their Applications, Lublin and Naleczow, Poland, 2015, p. 98160F,
 - [4] S. J. Mihailov, Fiber Bragg Grating Sensors for Harsh Environments, *Sensors*, vol. 12, no. 2, pp. 1898–1918, Feb. 2012, S. Yin, F. Yu, *Fiber Optic Sensors*, ISBN 9780824744571, CRC Press, 2002
 - [5] K. Wysokiński et al., New Methods of Enhancing the Thermal Durability of Silica Optical Fibers, *Materials*, vol. 7, no. 10, pp. 6947–6964, Oct. 2014,
 - [6] T. Erdogan, V. Mizrahi, P. J. Lemaire, and D. Monroe, Decay of ultraviolet-induced fiber Bragg gratings, *Journal of Applied Physics*, vol. 76, no. 1, pp. 73–80, Jul. 1994.

Structural properties and mid-infrared emission of heavy metal oxide glass and optical fibre co-doped with Ho³⁺/Yb³⁺ ions

Tomasz RAGIŃ^{*}, Agata BARANOWSKA, Marcin KOCHANOWICZ, Jacek ŻMOJDA, Piotr MILUSKI, Dominik DOROSZ

^{*} Białystok University of Technology, Faculty of Mechanical Engineering,
45c Wiejska St. 15-351 Białystok, POLAND

t.ragin@pb.edu.pl

Mid-infrared emission originating from glasses co-doped with rare earth ions has stimulated increasing interest for their potential applications in many areas, both civilian or military field, including eye-safe laser radar, remote sensing, atmosphere pollution monitoring and medical microsurgery [1, 2]. Mid-infrared studies focused on non-oxide glasses, like fluoride and chalcogenide materials, due to their low maximum phonon energy, which reduces the probability of non-radiative transitions and improves the mid-IR luminescence parameters [3, 4]. Simultaneously, research on glassy materials based heavy metal oxides, like germanate [5], tellurite [6] or bismuth [7], are being conducted for application in the mid-infrared spectral range. Special attention has been paid to the bismuth-oxide glasses due to their advantageous properties like high refractive index, high thermal stability, low maximum phonon energy as well as good chemical and mechanical durability [8]. In order to obtain luminescence in the mid-IR region,

the bismuth-oxide glass should be doped with proper lanthanides. Emission in the range 2.85 μm could be realized using Ho³⁺ ions due to radiative transition between high energy levels 5I₆ \rightarrow 5I₇ [9]. However, holmium ions cannot be directly pumped with commercial 980 nm diode. Ytterbium is used as a sensitizer, which effectively transfers energy to Ho³⁺ ions [10], therefore in Ho³⁺/Yb³⁺ co-doped glass, it is possible to obtain broadband mid-infrared luminescence using high power 980 nm semiconductor diode. In this work, bismuth-germanate glasses with low hydroxide content co-doped with Ho³⁺/Yb³⁺ ions have been investigated in terms of structural and spectroscopic properties. Material synthesis has been conducted in low vacuum conditions (50 – 70 mBar) in order to reduce OH⁻ ions content and improve transmittance value at the wavelength of 3.1 μm . The composition of the host glass based on heavy metal oxides affects the maximum phonon energy ($h\nu_{\text{max}} = 724 \text{ cm}^{-1}$), which low value has a positive impact on

the mid-infrared emission parameters. Strong luminescence band at the wavelength of 2.85 μm has been observed in glass co-doped with molar concentration 0.25 Ho_2O_3 / 0.75 Yb_2O_3 under 980 nm laser diode excitation. Measurements of the quantum level $\text{Yb}^{3+}:2F_{5/2}$ lifetime indicates high $\text{Yb}^{3+} \rightarrow \text{Ho}^{3+}$ energy transfer efficiency ($\eta = 61.44\%$). Developed active bismuth-germanate glass has been used as the active core of optical fibre operating in the mid-infrared region.

Acknowledgements

The research activity was supported by the National Science Centre (Poland) granted on the basis of the decisions No. UMO-2016/23/N/ST8/03523.

-
- [1] M. Cai, T. Wei, B. Zhou, Y. Tian, J. Zhou, S. Xu, J. Zhang, Analysis of energy transfer process based emission spectra of erbium doped germanate glasses for mid-infrared laser materials, *Journal of Alloys and Compounds* 626 (2015) 165-172.
- [2] Y. Tian, J. Zhang, X. Jing, Y. Zhu, S. Xu, Intense mid-infrared emissions and energy transfer dynamics in $\text{Ho}^{3+}/\text{Er}^{3+}$ codoped fluoride glass, *Journal of Luminescence* 138 (2013) 94-97.
- [3] F. Huang, X. Li, X. Liu, J. Zhang, L. Hu, D. Chen, Sensitizing effect of Ho^{3+} on the Er^{3+} : 2.7 μm -emission in fluoride glass, *Optical Materials* 36 (5) (2014) 921-925.
- [4] M. Zhang, A. Yang, Y. Peng, B. Zhang, H. Ren, W. Guo, Y. Yang, C. Zhai, Y. Wang, Z. Yang, D. Tang, Dy^{3+} -doped Ga-Sb-S chalcogenide glasses for mid-infrared lasers, *Materials Research Bulletin* 70 (2015) 55-59.
- [5] G. Bai, L. Tao, K. Li, L. Hu, Y.H. Tsang, Enhanced light emission near 2.7 μm from Er-Nd co-doped germanate glass, *Optical Materials* 35 (6) (2013) 1247-1250.
- [6] L. Gomes, D. Rhonehouse, D.T. Nguyen, J. Zong, A. Chavez-Pirson, S.D. Jackson, Energy transfer and energy level decay processes of Er^{3+} in water-free tellurite glass, *Optical Materials* 50 (2015) 268-274.
- [7] Y. Guo, Y. Tian, L. Zhang, L. Hu, J. Zhang, Erbium doped heavy metal oxide glasses for mid-infrared laser materials, *Journal of Non-Crystalline Solids* 377 (2013) 119-123.
- [8] H. Xia, J. Zhang, J. Wang, Y. Zhang, Optical Spectroscopy of Er^{3+} and $\text{Er}^{3+}/\text{Yb}^{3+}$ Co-doped $\text{Bi}_2\text{O}_3\text{-GeO}_2\text{-B}_2\text{O}_3\text{-ZnO}$ Glasses, *Journal of Rare Earths* 24 (4) (2006) 408-412.
- [9] J. He, Z. Zhou, H. Zhan, A. Zhang, A. Lin, 2.85 μm fluorescence of Ho-doped water-free fluorotellurite glasses, *Journal of Luminescence* 145 (2014) 507-511.
- [10] M. Cai, B. Zhou, Y. Tian, J. Zhou, S. Xu, J. Zhang, Broadband mid-infrared 2.8 μm emission in $\text{Ho}^{3+}/\text{Yb}^{3+}$ -codoped germanate glasses, *Journal of Luminescence* 171 (2016) 143-148.

Graphene in infrared and terahertz detector family

A. ROGALSKI

Institute of Applied Physics, Military University of Technology, 2 Urbanowicza Str., 00-908 Warsaw, POLAND
antoni.rogalski@wat.edu.pl

Since the graphene discovery, its applications to electronic and optoelectronic devices have been intensively studied. The extraordinary electronic and optical properties make graphene promising candidates for infrared and terahertz photodetectors to replace traditional ones. Up till now however, their performance is lower in comparison with those detectors existing on global market. This paper reviews the latest achievements in graphene detectors in competition with traditionally commercially dominated ones in different

applications. Also the challenges facing development of focal plane arrays for the future are considered. Special attention is directed toward the main trends in development of arrays in near future - increase in pixel count to above 108 pixels with pixel size decreasing to about 5 μm for both cooled and uncooled long wavelength infrared arrays. Up till now, these questions have been not considered in literature devoted graphene-based infrared and terahertz detectors.

Experimental analysis of the Bragg reflection peaks splitting in gratings fabricated using a multiple order phase mask

Gabriela STATKIEWICZ-BARABACH^{1*}, Karol TARNOWSKI¹, Dominik KOWAL¹, Paweł MERGO²

¹Department of Optics and Photonics, Faculty of Fundamental Problems of Technology, Wrocław University of Science and Technology, Wybrzeże Wyspiańskiego 27, 50-370 Wrocław, POLAND

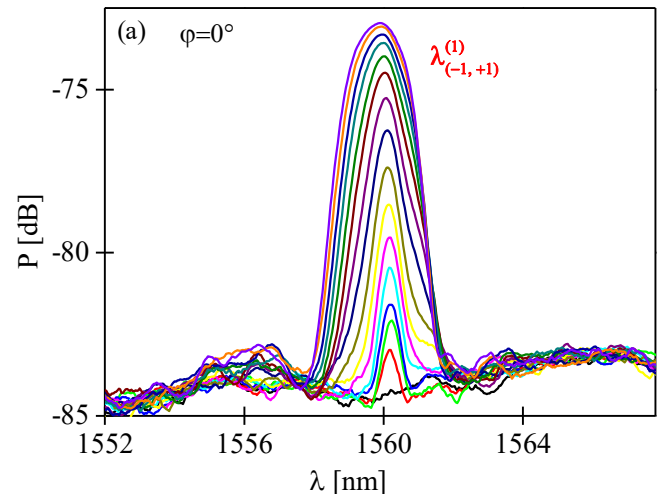
²Laboratory of Optical Fiber Technology, Maria Curie-Skłodowska University, pl. M. Curie-Skłodowskiej 3, 20-031 Lublin, POLAND

gabriela.statkiewicz@pwr.edu.pl

We demonstrate a possibility of fabrication of Bragg gratings in microstructured and step-index polymer fibers with multiple reflection peaks by using He-Cd laser ($\lambda=325$ nm) and a phase mask with higher diffraction orders. We experimentally studied the growth dynamics of the grating with the primary Bragg peak at $\lambda_B=1555$ nm, for which we also observed good quality peaks located at $\lambda_B/2=782$ nm and $2\lambda_B/3=1040$ nm. Detailed numerical simulations of the interference pattern produced by the phase mask suggests that the higher order Bragg peaks originate from interference of UV beams diffracted in $\pm 1^{\text{st}}$, $\pm 2^{\text{nd}}$ and $\pm 3^{\text{rd}}$ orders [1].

In this work, we used a phase mask with the period $\Lambda = 1052$ nm and diffraction orders 0^{th} , $\pm 1^{\text{st}}$, $\pm 2^{\text{nd}}$ and $\pm 3^{\text{rd}}$ to fabricate gratings in a step-index PMMA fiber. We present a detailed experimental study of Bragg gratings reflection spectra around the wavelength of λ_B for different tilt angles set between the fiber and the phase mask, Fig. 1.

We show that with an increasing tilt angle φ , the reflection peak splits into five separate peaks. Among them the side-peaks predicted in [2] were observed which are associated with the interference between 0^{th} and $\pm 2^{\text{nd}}$ diffraction orders.



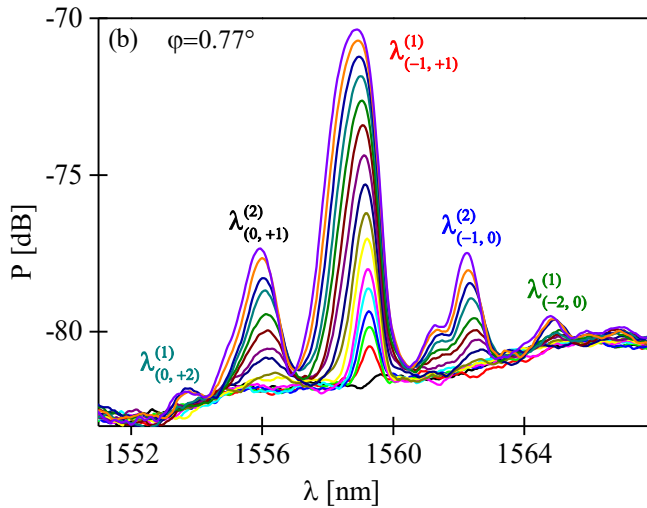


Fig. 1. Evolution of the reflection spectra of the FBG observed for different tilt angles of the POF.

However we also observed an additional pair of side-peaks which, according to our theoretical analysis, can only be second order reflections associated with interference between 0th and $\pm 1^{\text{st}}$ diffraction orders. The fact that the primary Bragg peak is composed of first as well as second order reflections was observed earlier in [3]. The authors of this paper applied theoretical model of reflectivity growth of FBGs presented in [4] to their experimental data and concluded there was a significant influence of second order reflection in the peak at λ_B . Our work goes farther than

that as it reveals directly the composition of the central peak. We analysed the dependence of the peak separation on the tilt angle and we compared the experimental results with the theoretical predictions. We obtained a nearly perfect match for the peaks which are second order reflections from the grating with periodicity close to Λ and a satisfactory match for the first order reflection peaks from grating with periodicity close to $\Lambda/2$.

-
- [1] G. Statkiewicz-Barabach, K. Tarnowski, D. Kowal, P. Mergo, W. Urbanczyk, *Opt. Express* **21**, 8521–8534 (2013).
 - [2] K. Tarnowski, W. Urbanczyk, *Opt. Express* **21**, 21800–21810 (2013).
 - [3] C.M Rollinson, S.A. Wade, B.P. Kouskousis, D.J. Kitcher, G.W. Baxter, S.F. Collins, *J. Opt. Soc. Am. A* **29**, 1259–1268 (2012).
 - [4] W.X. Xie, M. Douay, P. Bernage, P. Niay, J.F. Bayon, T. Georges, *Opt. Commun.* **101**, 85–91 (1993).

Integrated ring lasers for optical gyroscope systems

Stanisław STOPIŃSKI, Marcin SIENNICKI and Ryszard PIRAMIDOWICZ

Warsaw University of Technology, Institute of Microelectronics and Optoelectronics,
Koszykowa 75, 00-662 Warsaw, POLAND
stanislaw.stopinski@pw.edu.pl

Optical gyroscopes based on He-Ne or solid state ring lasers have proven their applicability as rotation sensors in high-performance inertial measurement units [1,2]. However, despite many attempts so far, realizing a fully functional gyro system in integrated optics technology remains a technological and economic challenge, as the ring laser needs to operate on a single frequency, its linewidth cannot exceed 1 MHz and the ring perimeter has to be on the order of a few millimeters. In this work we present and discuss a novel laser source, dedicated for application in optical gyroscope systems, which aims to fulfil all these requirements.

The device is realized in the indium phosphide generic technology provided by SMART Photonics [3,4]. The photonic circuit, schematically depicted in Fig. 1, comprises a semiconductor optical amplifier (SOA) as the gain medium and a cascade of three asymmetric Mach-Zehnder interferometers (MZI) providing wavelength filtering. All these elements are connected using passive waveguides forming a rectangular ring of the length around 14 mm.

The use of three MZI filters, differing by the imbalance of the arm lengths (Δl), provides single frequency

operation as it selects only one of the cavity modes. Electro-optic phase modulators in the interferometer arms allow tuning of the wavelength transmission bands of all MZIs, which enables optimization of the output power.

In the ring cavity there are two additional 2×2 multi-mode interference (MMI) couplers. The first one is introduced to enable characterization of the ring laser. The second coupler is a part of the beating frequency readout circuit. Under rotation of the device the resonant wavelengths of the CW and CCW modes are different, which can be monitored by measuring the beating frequency. Both beams are coupled through another MMI and the resulting signal is detected by two PIN photodiodes. Two SOA sections are used to equalize the power of the CW and CCW modes.

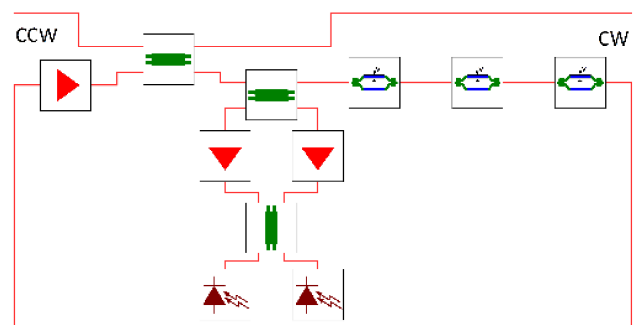


Fig. 1. Circuit scheme of the integrated single-frequency ring laser with the beating frequency readout circuit.

Fig. 2 presents a microscope picture of the fabricated device. The chip layout has been designed to enable flip-chip bonding to a dedicated application specific integrated electronic circuit as the driver.

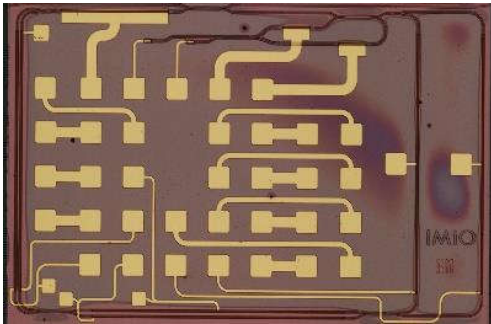


Fig. 2. Microscope picture of the integrated single-frequency ring laser.

The fabricated device has been initially characterized. Fig. 3 presents output spectra, recorded for both CW and CCW modes. The laser operates in the bi-directional regime, the difference of the power is around $\Delta P = 5$ dB, which can be easily compensated by the SOAs implemented in the readout circuit. Side mode suppression ratio for both CW and CCW mode is over 30 dB, which proves single frequency operation. The obtained results are promising with respect to implementation of the integrated ring lasers in novel optical gyroscope systems.

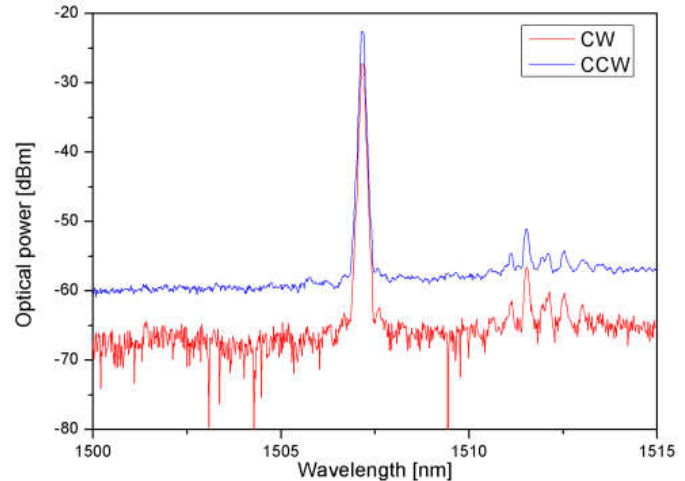


Fig. 3. Recorded single-frequency spectrum of the laser for CW and CCW modes.

Acknowledgement: The research leading to these results has received funding from the National Science Centre (decision DEC-2013/09/N/ST7/04430) and from the EU Horizon 2020 research and innovation programme under grant agreement No. 687777 (PICs4All).

-
- [1] W. M. Macek and D. T. M. Davis, Jr., "Rotation rate sensing with traveling-wave ring lasers," *Appl. Phys. Lett.*, vol. 2, no. 3, pp. 67–68, 1963.
 - [2] M. N. Armenise, *Advances in Gyroscope Technologies*. Berlin, Germany: Springer-Verlag, 2010.
 - [3] M.K. Smit et al., *Semicond. Sci. Technol.* 29, 8, (2014)
 - [4] SMART Photonics website, <http://smartphotonics.nl/>

The SS-OCT endomicroscopy probe based on MOEMS Mirau micro-interferometer and MEMS 2-axis electrothermal microscanner for optical coherence tomography imaging.

Przemysław STRUK^{2,1}, Sylwester BARGIEL¹, Quentin TANGUY^{1,3}, Fernando E. GARCIA RAMIREZ¹, Ravinder CHUTANI¹, Philippe LUTZ¹, Olivier GAIFFE¹, Luc FROEHLI¹, Nicolas PASSILLY¹, Huikai XIE³ and Christophe GORECKI¹

¹ FEMTO-ST Institute (UMR CNRS 6174, Université Bourgogne Franche-Comté), 15B Avenue des Montboucons, 25030 Besançon, FRANCE

² Department of Optoelectronics, Faculty of Electrical Engineering, Silesian University of Technology, 2 Krzywoustego Str., 44-100 Gliwice, POLAND

³ University of Florida, P.O. Box 116200, Gainesville, Florida, USA

Przemyslaw.Struk@polsl.pl

Early diagnosis of the cancers, including stomach cancer in human body is a key issue to increase the chances of survival and improve patient's treatment efficiency. Nowadays, the gold standard for cancer diagnosis is based on: ultrasonography scanning, biopsy of a small part of tissue and histopathological examination. However this method is invasive, painful for the patient and time consuming. From this point of view, development of non-invasive, painless and fast methods for cancer diagnosing is required. Recently, a Swept Source Optical Coherence Tomography imaging method combined with a endomicroscopy device has proven to be promising method of optical biopsy of tissue for non-invasive cancer diagnosis into upper digestive tract.

The Authors present the operation principle, construction, fabrication (MOEMS technology - 4-inch wafer-level vertical stacking and anodic

bonding of Si/glass components) and characterization of a MOEMS integrated probe for endoscopic optical imaging of stomach tissue using Swept Source Optical Coherence Tomography system. Construction of the endoscopic probe is based on monolithically integrated Mirau micro-interferometer, combined with beam-shaping optics (GRIN lens collimator) and hybrid integrated scanning system based on 2-axis electrothermal micro-mirror scanner MEMS in order to perform 3-D side-scanning [1,2]. The presented SS-OCT endomicroscopy probe can operate in two modes:

- forward scanning mode (without the microscanner) the probing beam is focused directly on the sample (solid line the fig. 1).

- transverse scanning mode with the 2-axis electrothermal micro-scanner integrated on top of Mirau interferometer (dashed line in the fig. 1),

The MOEMS based probe is also design and compatible to be attached to a continuum robotic arm, installed at the extremity of the endomicroscope, for 3D positioning of the probe during scanning of stomach tissue.

The single structure of micro-interferometer has external dimensions 4.7x4.7x5mm³ and consist of: assembly port for GRIN lens collimator (I/O circuit for light), plano-convex glass lens - focal length $f_L=9\text{mm}$ (focusing of light beam on sample), reference micro-mirror (reflection of reference signal), Si 4-mm-thick separator, beam splitter plate.

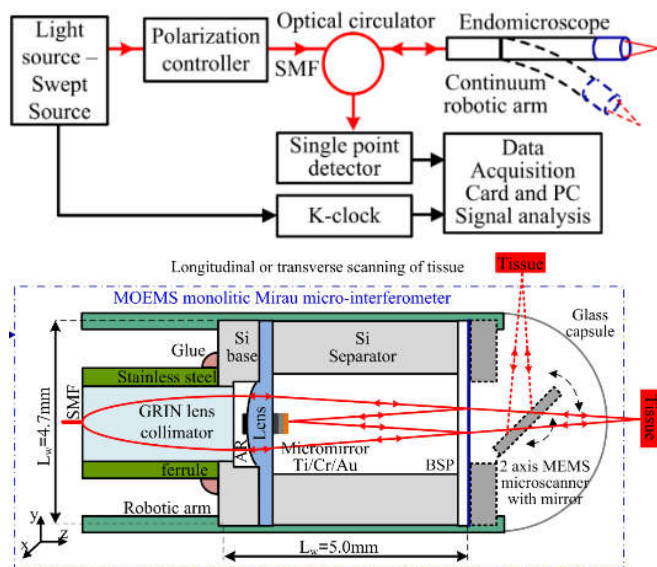


Fig. 1. Scheme of the SS-OCT endoscope probe.

We present endoscope probe based on Mirau micro-interferometer and 2-axis MEMS scanner, the results of characterization of the probe and

obtained 2D and 3D SS-OCT tomogram of the test sample. The SS-OCT images was obtained for central wavelength $\lambda_c=840\text{nm}$, swept range $\Delta\lambda=60\text{nm}$ and A-scan frequency $f_A=110\text{kHz}$. The resolution of the probe are: axial 5.2mm and lateral 9.6mm.

The presented device is a new type of micromachined MOEMS-type endomicroscopy probe. The combination of the Mirau micro-interferometer with 2-axis microscanner MEMS and SS-OCT imaging methods enables the construction of high quality and cost-effective systems, e.g. for in vivo medical diagnostics of cancer in human stomach tissue.

[1] P. Struk, S. Bargiel, Q. A.A. Tanguy, F. E. Garcia Ramirez, N. Passilly, P. Lutz, O. Gaiffe, H. Xie, C. Gorecki, 2018, Swept-source optical coherence tomography microsystem with an integrated Mirau interferometer and electrothermal micro-scanner, *Optics Letters*, Vol. 43, Issue 19, pp. 4847-4850.

[2] Q. A. A. Tanguy, S. Bargiel, H. Xie, N. Passilly, M. Barthès, O. Gaiffe, J. Rutkowski, P. Lutz, C. Gorecki, Design and Fabrication of a 2-Axis Electrothermal MEMS Micro-Scanner for Optical Coherence Tomography, *Micromachines* 2017, 8(5), 146.

0.3 mW MIR output power from multimode chalcogenide glass fiber doped with praseodymium

Slawomir SUJECKI^{1,2}, Lukasz SOJKA¹, Meili SHEN², Dinuka JAYASURIA²,
Zhuoqi TANG²,
Emma BARNEY², David FURNISS², Trevor BENSON², Angela SEDDON²

¹Department of Telecommunications and Teleinformatics, Faculty of Electronics,
Wroclaw University of Science and Technology, Wyb. Wyspianskiego 27, 50-370 Wroclaw, POLAN

²George Green Institute for Electromagnetics Research,
The University of Nottingham, University Park, NG7-2RD, Nottingham, UK

slawomir.sujecki@pwr.edu.pl

The technology of low loss chalcogenide glass optical fibers has been significantly improved in the recent years [1]. One of the important applications of chalcogenide glass fibers is mid infrared (MIR) spectroscopy, which can be used in tissue imaging and gas sensing [2,3]. In

particular chalcogenide glass fibers are used for the construction of MIR light sources, which are essential for the realisation of sensors. Most recently of large interest are supercontinuum sources [2] and spontaneous emission sources [3].

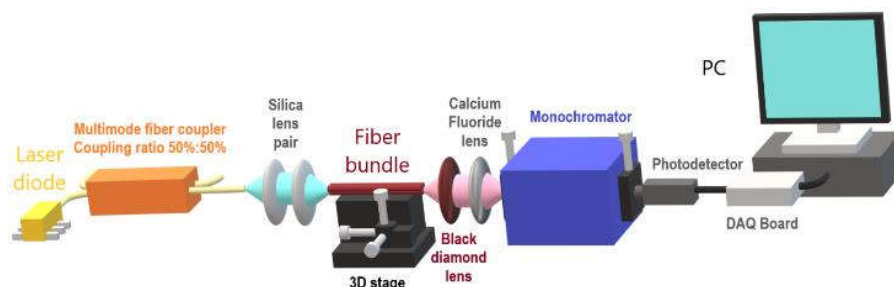


Fig. 1. Experimental setup used for measurements of the output power emitted by lanthanide ion doped multimode chalcogenide glass fibers.

In this contribution a MIR spontaneous emission source made of a praseodymium ion doped chalcogenide glass fiber is used to realise a MIR light source and investigate the dependence of MIR output power on the near infrared pump power. Fig.1 shows an example of the dependence of the output power on

the pump power measured for a chalcogenide glass fiber doped with 1000 ppm of praseodymium ions. The pump laser was a commercially available laser diode (LD) with an operating wavelength of approximately 1500 nm. A combination of a large aperture black diamond lens and a standard calcium fluoride lens were

used to collect the light and deliver it to a photodetector. At high values of pump power the detected power level reached 0.3 mW and was sufficiently high to use low cost thermal photodetectors.

In the realised measurement setup lock-in measurement techniques are used at very low values of the output power in order to improve the signal to noise ratio. Also the monochromator can be replaced by a filter allowing power to be measured for a specified band within the MIR wavelength

range of the total output spectrum. In the realised setup there is a possibility to use a combination of two laser diodes to pump the fiber via a multimode fiber coupler with a coupling ratio of 50 %: 50 %. Furthermore instead of just one fiber a fiber bundle may be placed on a 3D stage and the light emitted can be collected by the lens pair. In the case of a fiber bundle 3D stage can be used to modify the shape of the output spectrum.

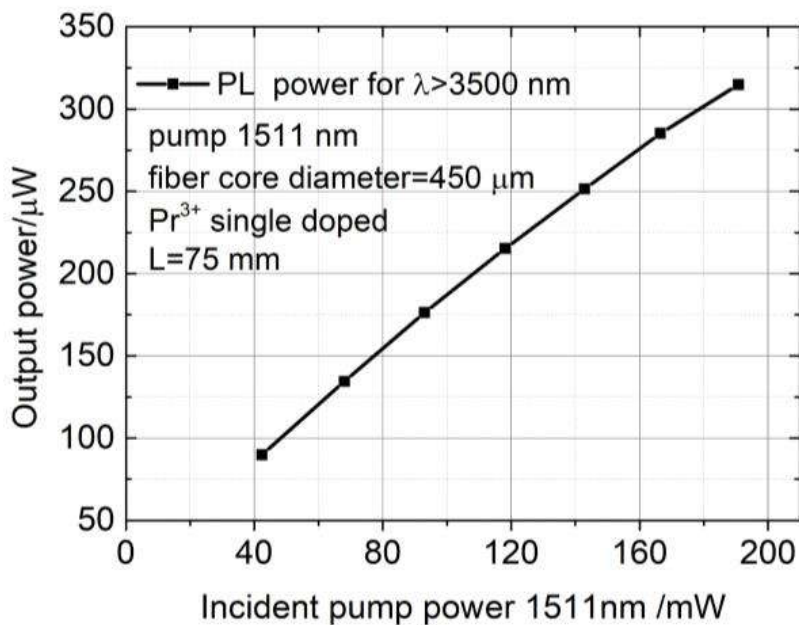


Fig. 2. Measured dependence of output MIR power on pump power.

[1] Z. Tang, V. S. Shiryayev, D. Furniss, L. Sojka, S. Sujecki, T. M. Benson, A. B. Seddon, and M. F. Churbanov, "Low loss Ge-As-Se chalcogenide glass fiber, fabricated using extruded preform, for mid-infrared photonics," *Opt. Mater. Express*. 5(8), 1722-1737 (2015).

[2] C. Petersen, N. Prtljaga, M. Farries, J. Ward, B. Napier, G. Lloyd, J. Nallala, N. Stone, and O. Bang, "Mid-infrared multispectral tissue imaging using

a chalcogenide fiber supercontinuum source," *Opt. Lett.* 43, 999-1002 (2018).

[3] A. L. Pelé, A. Braud, J. L. Doualan, F. Starecki, V. Nazabal, R. Chahal, C. Boussard-Plédel, B. Bureau, R. Moncorgé, and P. Camy, "Dy³⁺ doped GeGaSbS fluorescent fiber at 4.4 μm for optical gas sensing: comparison of simulation and experiment," *Opt. Mater.* 61, 37-44 (2016).

Coupled microresonators

Marek TRIPPENBACH^{*}, Volodya KONOTOP, Nguyen VIET HUNG, Aleksander RAMANIUK,
Krzysztof ZEGADŁO

* University of Warsaw, Faculty of Physics, POLAND

Gain and loss are omnipotent in the physical, chemical and biological systems. Their effects can in a convenient way be modelled by effective non-Hermitian Hamiltonians. Imaginary contributions to the potential introduce source and drain terms for the probability amplitude. A special class of non-Hermitian Hamiltonians are those which possess a parity-time symmetry. In spite of their non-Hermiticity these Hamiltonians allow for real energy eigenvalues, i.e. the existence of stationary states in the presence of balanced gain and loss. This effect has been identified theoretically in a large number of quantum systems. Its existence has also been proved experimentally in coupled optical waveguides. In my talk I will provide concise review of these systems including the aspect of physics of energy conversion in nanostructures.

Effects described above have very broad context. The dynamics can be very interesting and worth studying even if the parity-time symmetry is not conserved. The list of systems that belong to this class include whispering gallery modes in the micro-resonators, coupled wave-guides, unidirectional reflectionless metamaterial

at optical frequencies, polariton condensates and many others. In my talk I consider a nanostructure of two coupled ring waveguides with constant linear gain and nonlinear absorption - the system that can be implemented in various settings including polariton condensates, optical waveguides or atomic Bose-Einstein condensates. It was found that, depending on the parameters, this simple configuration allows for observing several complex nonlinear phenomena, which include spontaneous symmetry breaking, modulational instability leading to generation of stable circular flows with various vorticities, stable inhomogeneous states with interesting structure of currents flowing between rings, as well as dynamical regimes having signatures of chaotic behavior.

-
- V. V. Konotop, Jianke Yang, Dmitry A. Zezyulin, Nonlinear waves in PT - symmetric systems, *Rev. Mod. Phys.* 88, 035002 (2016)
 - Nguyen Viet Hung, Krzysztof Zegadlo, Aliaksandr Ramaniuk, Vladimir V. Konotop, and Marek Trippenbach,

Modulational instability of coupled ring waveguides with linear gain and nonlinear loss, Scientific Reports.

condensation of microcavity polaritons in a trap. Science, 316, 1007 (2007).

- Y. Yamamoto and R. E. Slusher, Optical Processes in microcavities, Phys. Today 46, 66 (1993).
- R. Balili, V. Hartwell, D. Snoke, L. Pfeiffer, L., and K. West, Bose-Einstein

Ultrasensitive detection of selected gases by infrared absorption spectroscopy

J. WOJTAS¹, Z. BIELECKI¹, T. STACEWICZ², J. MIKOŁAJCZYK¹, M. NOWAKOWSKI¹, B. PIETRZYK¹, D. SZABRA¹, A. PROKOPIUK¹, K. ACHTENBERG¹

¹ Institute of Optoelectronics, Military University of Technology, 2 Urbanowicza Str., 00-908 Warsaw, Poland

² Faculty of Physics, University of Warsaw, 5 Pasteura Str., Warsaw 04-093, Poland

jacek.wojtas@wat.edu.pl

The paper presents research related to developments of high-sensitivity optoelectronic sensors to measure trace concentrations of selected gases. The sensors use a phenomenon of infrared radiation absorption by investigated molecules in a special designed optical cavity by Cavity Enhanced Absorption Laser Spectroscopy (CEAS). Using this technique, low detection limit, short response time, high selectivity and resolution have been achieved. The initial motivation for developing sensors to detect nitrous oxide (N₂O) and nitric oxide (NO) was associated with explosive materials detection. NO_x are released by explosives containing nitro groups (NO₂) as products of their thermal decomposition [1,2]. For instance, substances like trinitrotoluene (TNT), dinitrotoluene (DNT), nitroglycerine (NG) or ethylene glycol dinitrate (EGDN) are characterized by a relatively high value of their vapor pressure and they can be detected even at ambient temperature [3]. The CEAS sensors capabilities have also been proved in the analysis of human breath. Many volatile compounds are

identified as biomarkers of human diseases, e.g.: asthma and chronic

obstructive pulmonary disorder (NO), cancers (C₂H₆), liver disease (OCS), etc. The developed sensors enabling detection of different gases using mid infrared spectral range (MWIR) were listed in Tab. 1 [4-7].

There will be also presented preliminary research related to application of long-wavelength infrared (LWIR) technology, i.e.: lasers, detectors and optics designed for selected absorption lines from range of approx. 8-15 μm. This spectral range is much less used for laser absorption spectroscopy due to limited number of absorption bands that could become substances markers and expensive component technology. In the other hand, such systems are promising for many applications due to lower light scattering, less potential interferences, lower requirements for laser parameters, optical systems accuracy and sample filtration. In combination with the advantages of CEAS, LWIR sensors can provide: reduction in size and in weight ensuring high selectivity

and sensitivity even at ppb level [8]; non-invasive and high-resolution real-time measurements; fast detection time for the lowest changes in concentration; no need to replace sensitive components,

automatic self-test with calibration procedure and safety of use. These advantages make these sensors very useful in many applications.

Tab. 1. Example parameters of developed sensors

Type of sensor	Operation wavelength [μm]	Detection limit [ppb]	Detection example
OCS	5.2624	250	Liver disease
NO	5.2630	30	Respiratory diseases, explosives
NH ₃	5.2735	1000	Renal failure
OCS	4.8716	0.9	Transplant rejection
CO	4.7830	6.6	Cardiovascular diseases
CO	4.7875	110	Toxic pollutant
C ₂ H ₆	3.3481	0.3	Diabetes, cancers

ACKNOWLEDGEMENT

The presented works carried out in the laboratory of Institute of Optoelectronics MUT and publication is supported by project „Sense” entitled „Development of technology of single-mode quantum cascade lasers for gas sensing applications”, ID: 347510.

[1] J.C. Oxley. A survey of the thermal stability of energetic materials. In P. Politzer, J. S. Murray eds., Elsevier, Amsterdam, (2003).

[2] P.Z. Jankowski, A.G. Mercado, S.F. Hallowell, Proc. SPIE, vol. **1824**, pp. 13-20, (1993), doi: 10.1117/12.142901.

[3] J. Wojtas, T. Stacewicz, Z. Bielecki, et al., Opto-Elektron. Rev. **21**, 210–219, (2013), doi: 10.2478/s11772-013-0082-x.

[4] T. Stacewicz, Z. Bielecki, J. Wojtas, et al., Opto-Elektron. Rev. **24**, 82–94, (2016), doi: 10.1515/oere-2016-0011

[5] J. Wojtas, Sensors **15**, 14356-14369; (2015), doi:10.3390/s150614356.

[6] D. Szabra, et. al., Rev. Sci. Instrum., **88**, 115006-1 - 115006-6 (2017), doi: 10.1063/1.4995502.

[7] Z. Bielecki, et. al., Opto-Electronics Review **26**, 2, 122–133 (2018), doi: 10.1016/j.opelre.2018.02.007.

[8] J. Wojtas, et. al., Int. J. 10.1007/s10765-014-1586-4.
Thermophysics **35**, 2215–2225 (2014), doi:

Optimization of silica glass capillary and rods drawing process.

Grzegorz WÓJCIK, Krzysztof POTURAJ, Marusz MAKARA, Paweł MERGO

Laboratory of Optical Fibers Technology, Maria Curie Skłodowska University in Lublin,
Pl. Marii Curie Skłodowskiej 2, 20-031 Lublin, POLAND
grzegorzwojcik@poczta.umcs.lublin.pl

In our research we investigated partial processes in a microstructured optical fiber fabrication process. To fabricate a microstructured fiber it is necessary to conduct several following steps. One of them is a preparation of basic elements – capillary and rods, which are used to stack the first stage preform. In the investigation we set a goal to decrease diameter fluctuations revealing themselves in the drawing process. Increasing the quality of capillary and rods will allow to produce more stable microstructured fibers with better optical properties.

We planned to fabricate series of capillary and rods, drew in different conditions. In processes we used commercially available pure silica tubes (HX-S) and rods (F300). In each process we drew material with three different velocities. At the same time we registered diameter fluctuations on the digital recorder. Next we classified capillary and rods and divide elements into two groups. In the first on we selected rods and capillary with the lowest fluctuation of diameter, in the second with the highest.

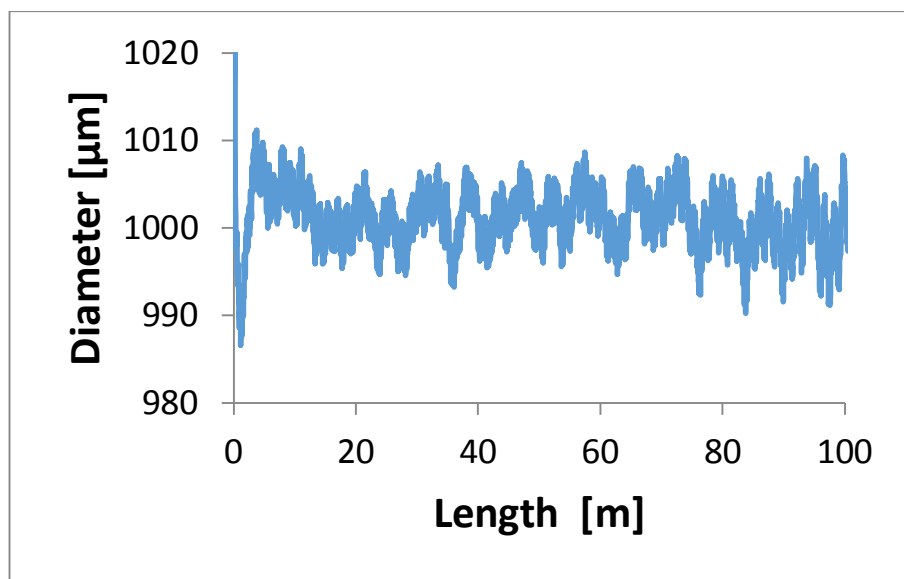


Fig.1 Fluctuations of diameter during drawing.

In the next stage of research we compared how significant is the influence of capillary and rods quality on fibers properties. We fabricated two preforms and drew microstructural fibers. The first one was made of elements characterized by the lowest diameter fluctuations, the second with the highest. Both preforms possessed identical cross-section, central

core, two rings of capillary and outer section of rods.

In the drawing processes we drew two $l=1\text{km}$ length sections of fibers. Both fibers possessed outer diameter $\phi=125\mu\text{m}$, core diameter $\phi=6\mu\text{m}$ and fill factor of the hole section $w=0,9$. Fibers were measured with a reflectometer in order to determinate longitudinal losses.

Stability of information coding in the phase difference of radiation pulses in a fibre optic pulse interferometer

Marek ŻYCZKOWSKI

Institute of Optoelectronics, Military University of Technology, 2 Urbanowicza Str., 00-908 Warsaw, POLAND
marek.zyczkowski@wat.edu.pl

The era of globalisation enabled tremendous access to information, which has become common, accessible, but also valuable and requiring safe, fast and high capacity transferring. This is extremely important in the critical areas of life, i.e. military, banking or personal data protection, thus, it is necessary to implement the method of data security during its transmission. Modern data exchange systems are based mainly on optical fibre technology. Therefore, various types of optical fibres cable protection were developed to avoid eavesdropping, which includes fibre-optic track monitoring using fibre-optic sensors [1-3]. Newer methods of optical protection of data exchange are based on the distribution of the quantum key [4-7]. Bearing in mind the above state of technology, the authors have attempted to develop a system that will more effectively protect data transmitted in a fibre-optic transmission channel. As the start position, the use of the data exchange scheme was adopted as in the quantum key distribution (QKD) systems but with crucial changes. The use of single-photon transmission for the pulsed laser source was abandoned in order to

suppress the technological limitations of single-photon detection. Therefore, the idea of data exchange security based on the uncertainty principle of the photon was abandoned. The basis of the system presented in the article is the technical optoelectronic designing of the system's operation in order to save bit information in the phase difference between two pulses of light propagating in the optical fibre path from the transmitter to the receivers. By assumption, every disturbance of the optical fibre path results in the desynchronization of the mentioned phase relations and as a result, the eavesdropper automatically disturbs this information.

The particular number of errors in a given unit of measurement duration for a given length of the optical fibre has made it possible to determine the BER coefficient for each case of the PM modulation frequency. Table 1 summarizes the test results of the system.

Tab. 1 indicates that the system allows encoding information in the optical physical layer of the telecommunication channel with working parameters consistent with telecommunication STM-1 regulatory requirements. Bearing in mind

that the system uses phase coding of light, it should be stated that it is possible to develop a new type of a secure information transmission system. This type of system may have much better parameters (bit rate in the range of 100 Mbit/s) in the transmission of the code

key than the current QKD systems. The safety of the setup is guaranteed by the need to restore the generation-detection system. The authors assume that in order to read the information, it is necessary to obtain 90% certainty of the correct reading of the eavesdropped information.

Tab. 1. BER values of the tested system

Measurement time [s]	Bit rate [Mbit/s]	BER (Bit Error Rate)			
		Length of the measuring fiber			
		1k	2 km	4 km	9 km
2303	10	1.1 10 ⁻¹¹	1.6 10 ⁻¹¹	2.1 10 ⁻¹¹	7.8 10 ⁻¹¹
921	25	1.2 10 ⁻¹¹	1.5 10 ⁻¹¹	2.2 10 ⁻¹¹	8 10 ⁻¹¹
460	50	1.1 10 ⁻¹¹	1.4 10 ⁻¹¹	2.3 10 ⁻¹¹	8.2 10 ⁻¹¹
360	64	1.2 10 ⁻¹¹	1.6 10 ⁻¹¹	2.1 10 ⁻¹¹	9.1 10 ⁻¹¹
230	100	1.2 10 ⁻¹¹	1.5 10 ⁻¹¹	2.1 10 ⁻¹¹	8 10 ⁻¹¹
184	125	1.3 10 ⁻¹¹	1.5 10 ⁻¹¹	2.2 10 ⁻¹¹	7.9 10 ⁻¹¹

Measured: at 25°C - laboratory, at 18°C - fiber optic test field.

- [1] G. Allwood, G. Wild, and S. Hinckley, *Optical fibre sensors in physical intrusion detection systems: A review*, IEEE Sensors Journal, vol. 16, no. 14, pp. 5497-5509, July 2016.
- [2] M. P. Fok, Z. Wang, Y. Deng, and P. R. Prucnal, *Optical layer security in fibre-optic networks*, IEEE Trans. Inf. Forensics Security, vol. 6, no. 3, pp. 725-736, 2011.
- [3] B. Javidi, et al., *Roadmap on optical security*, J. Opt., vol. 18, no. 8, p. 083001, 2016.
- [4] D. Rosenberg, J.W. Harrington, P.R. Rice, P.A. Hiskett, C.G. Peterson, R.J. Hughes, et al., *Long-distance decoy-state quantum key distribution in optical fibre*,

Phys. Rev. Lett., vol. 98, pp. 010503-1-010503-4, 2007.

[5] R.H. Hadfield, J.L. Habif, J. Schlafer, R.E. Schwall, and S.W. Nam, *Quantum key distribution at 1550 nm with twin superconducting single-photon detectors*, Appl. Phys. Lett., vol. 89, pp. 241129-1-241129-3, 2006.

[6] J. Scheuer, and A. Yariv, *Giant fibre lasers: a new paradigm for secure key distribution*, Phys. Rev. Lett., vol. 97, pp. 140502-1-140502-4, 2006.

[7] M. Ben-Or, M. Horodecki, D.W. Leung, D. Mayers, and J. Oppenheim, *The universal composable security of quantum key distribution*, Theory of Cryptography: Second Theory of Cryptography

IOS'2019, Szczyrk 25.02-01.03.2019

Conference, Lecture Notes in Computer Science, ed. J. Kilian, (Springer Verlag, 2005), vol. 3378, pp. 386-406, 2005.

ABSTRACTS

OF

POSTERS

Analysis of optical magnetic field sensor in wide range of wavelengths

Kamil BARCZAK

Silesian University of Technology, Department of Optoelectronics, ul. Krzywoustego 2, 44-100 Gliwice, POLAND
Silesian University of Technology, Institute of Power System and Control, ul. Krzywoustego 2,
44-100 Gliwice, POLAND

kamil.barczak@polsl.pl

Optical sensors are usually equivalent to existing classical sensors, which are the result of many years of experience, research and improvement. Optical sensors are often characterized by high resolution, reliability and stability. The main reason for the introduction of optical waveguide sensors (optical sensors in general) are their insulating properties, which allow for safe operation in high current and voltage environment. Another advantage is their immunity to electromagnetic disturbances. In the world of metrology so strongly dependent on electricity, the quality of optical waveguide sensors consisting in their insulating properties is their most important advantage [1].

Optical waveguide sensors based on the Faraday effect are such sensors. They are applied for measurements of magnetic field under the severe electromagnetic disturbance conditions as well as for the measurements of electric currents in power systems. These sensors

always directly convert magnetic field changes into changes of optical wave parameters.

This work presents results of analysis of optical waveguide magnetic field sensor with external conversion fabricated in the Department of Optoelectronics of the Silesian University of Technology [2]. This study is focused on possibility of using a wide range of optical wavelengths in order to extend the measuring range of this sensor.

[1] H. Mościcka-Grzesiak, *Inżynieria wysokich napięć w elektroenergetyce*, Wyd. Politech. Poznańskiej, Poznań, (1999).

[2] Barczak K., *Optical fibre current sensor for electrical power engineering*, Bulletin Of The Polish Academy Of Sciences-Technical Sciences, 59(4), pp. 409-414 (2011).

Luminescence properties in SGB glass fibers co-doped with Eu^{3+}/Ag ions

Karol CZAJKOWSKI, Jacek ŻMOJDA*, Piotr MILUSKI, Marcin KOCHANOWICZ

Department of Power Engineering, Photonics and Lighting Technology, Białystok University of Technology
Wiejska 45D Street, 15-351 Białystok, POLAND

j.zmojda@pb.edu.pl

Nanocomposite optical glasses and fibers give a novel way to manage luminescent properties of RE ions, mainly due to their unique properties, obtained as a result of the interaction of nanoparticles with photons [1-3]. The most advanced systems are found in the currently used waveguide structures, characterized by sophisticated optical properties and an excellent thermal

stability parameter required in modern optical fiber technology. State-of-art is a combination of noble metals properties, ie. silver (Ag^+), gold (Au^+) and technology of rare earth (RE) ions doped glassy materials. Modification of emission properties of glassy materials doped with lanthanide ions, which is obtained by co-doping with nano-sized metal particles, is an innovative research area.

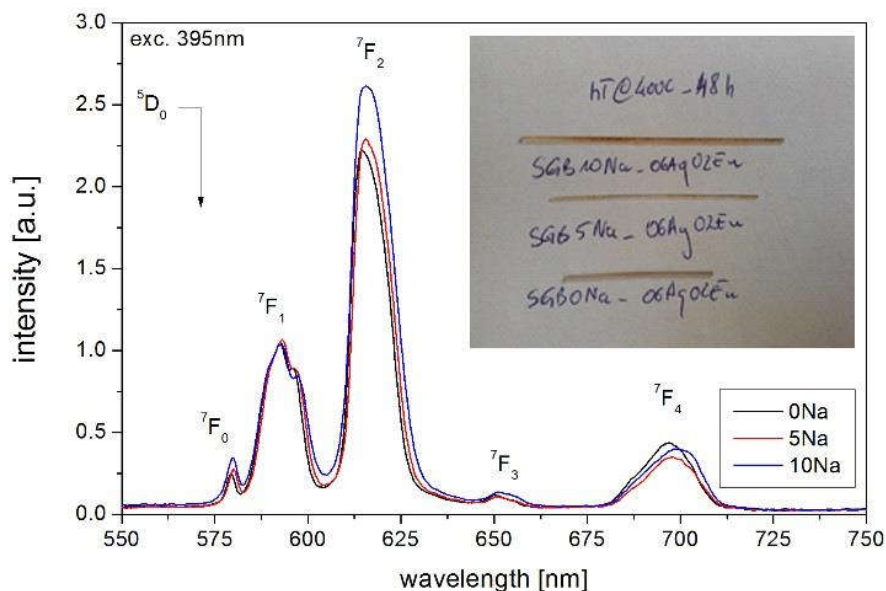


Fig. 1. Luminescent spectra of nanocomposite SGB glass-fibers doped with 0.2 mol% Eu_2O_3 with different Na_2O content. (inset) Photograph of SGB glass fibers after heat-treatment process under 400C by 48h. Brownish color is an effect of silver reduction.

In this article, we have focused on the effect that silver might have on the luminescent properties of Eu^{3+} ions embedded in antimony-germanate-borate SGB glass fibers. The luminescent analysis of the Eu^{3+} doped glass fiber as a function of Ag ions and annealing time has been performed.

Also, we have shown non-conventional methodology of silver thin film fabrication over glass fiber by self-assembled AgO nanoparticles, using thermal reduction of AgO in a bottom-up process

Antimony-germanate-borate SGB glass characterized by highest emission intensity at the wavelength of 616 nm (SGB_06Ag02Eu) was selected to analyze the influence of annealing and alkali content on luminescence properties of europium ions. The observed changes in the luminescence spectra of Eu^{3+} doped SGB glasses as a function of different heating time is shown in Figure 1. The second approach showed the non-conventional technology for the creation of silver nanoparticles on to glass fibers surface by a bottom-up process (inset Fig 1). This process was activated thermally without a reduction atmosphere, and strongly depends on Ag ion concentration. Ag^0 nanoparticles were obtained only in SGB glass fibers doped with 0.6 mol.% AgNO_3 . Moreover, the nanoparticles were

observed even before the additional heat-treatment. Thus, the optimization of the silver content allows the production of nanocomposite SGB glass fiber covered by a thin film of AgO NPs directly, in a one-step method. It can be concluded that the proposed methodology for nanoparticle synthesis has potential applications in SERS substrates and biophotonic devices.

ACKNOWLEDGMENTS

The research activities were performed by the National Science Centre (Poland) granted on the basis of the decision No. DEC-2016/21/D/ST7/03453.

-
- [1] H. A. Atwater, and A. Polman, *Plasmonics for improved photovoltaic devices*, *Nature Materials* **9**, 205 (2010).
 - [2] P. Candeloro, E. Luele, G. Perozziello *et al.*, *Plasmonic nanoholes as SERS devices for biosensing applications: An easy route for nanostructures fabrication on glass substrates*, *Microelectronic Engineering* **175**, 30-33 (2017).
 - [3] W. Q. Lim, and Z. Gao, *Plasmonic nanoparticles in biomedicine*, *Nano Today* **11**, 168-188 (2016).

Spectral characteristics of anion derivatives of the benzoic acid

Lidia CZYZEWSKA, Malgorzata GIL, Pawel MERGO

Laboratory of Optical Fibers Technology, Maria Curie Skłodowska University in Lublin, Pl. Marii Curie Skłodowskiej 3, 20-031 Lublin, POLAND

pawel.mergo@umcs.lublin.pl

Recently, one can notice a clear trend related to the use of optically active compounds. In particular, this applies to compounds containing rare earth elements commonly called lanthanides. As active compounds, inorganic lanthanide compounds are usually used which, at high temperatures, decompose into an oxide form in which the lanthanide atoms occur as three-positive cationic groups characterized by the greatest optical activity. In recent years, complex metal-organic lanthanide compounds have become very popular, which optical properties far outweigh inorganic compounds. The great advantage of using organic ligands in these compounds is the observed antenna effect, which results in much higher optical performance of the metal-organic complexes compared to

inorganic compounds. It is obvious that not every structure of the organic ligand allows to obtain an antenna effect. It is necessary here to match the electronic structures of the ligand and lanthanide. Therefore, the ability to theoretically predict the optical properties of organic ligands becomes extremely important. The paper presents theoretically determined relationships between UV-VIS spectra of chloride and fluoride derivatives of benzoic acid. The UV-VIS spectra were also shown in relation to the number of chlorine and fluorine atoms in the ligand molecule.

Funding National Science Centre of Poland, grant Maestro 8, DEC-2016/22/A/ST7/00089.

Sensitivity of the graphene oxide under the influence of hydrogen

Sabina DREWNIAK, Marcin PROCEK

Silesian University of Technology, Department of Optoelectronics, 2 Krzywoustego Str., 44-100 Gliwice, POLAND
Sabina.Drewniak@polsl.pl

Graphene oxide is a material whose properties depend on graphite precursor and a method of preparation [1]. We decided to use the graphene oxide prepared from natural, flake graphite, oxidized by modified Tour's method and reduced using thermally reduction. The ready material we dropped (after previous preparation to the appropriate form) on to resistive structure and tested in various atmospheres. We analysed the resistance of the structure in mixtures of hydrogen and nitrogen or synthetic air (with different concentrations of hydrogen). We made the measurements in various temperatures. Fig. 1 shows the results obtained for nitrogen as a carrier gas. The temperature of such measurements was equal 175°C.

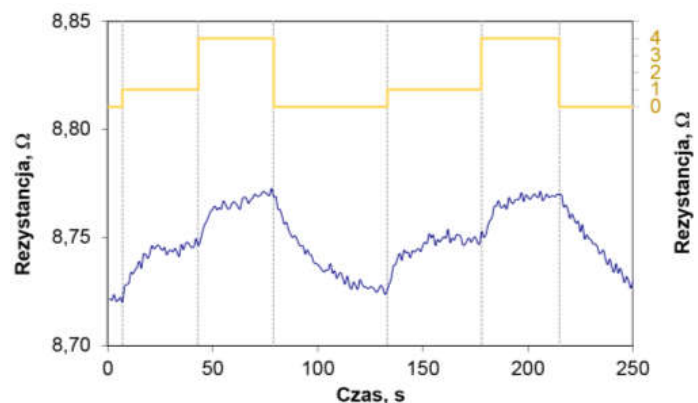


Fig. 1. Resistance of the structure with graphene oxide in mixture of hydrogen and nitrogen, temperature: 175°C

[1] R. Muzyka, S. Drewniak, T. Pustelny, M. Chrubasik, G. Gryglewicz, *Materials*, **11**, (2018)

Determination the optimal extrusion temperature PMMA optical fibers

Malwina NIEDŹWIEDŹ, Małgorzata GIL, Mateusz GARGOL, Wiesław PODKOŚCIELNY, Paweł MERGO

Laboratory of Optical Fiber Technology, Maria Curie-Skłodowska University, Pl. Skłodowskiej 3, 20-031 Lublin, Poland University

The aim of this work was to determine optimal extrusion temperature for polymer optical fibers. The granulate used was poly(methyl methacrylate). PMMA is cheap and widely used material therefore is perfect for a preliminary tests.

Samples of commercially available PMMA were subjected to 90⁰C for 2h, towards dispose of physically adsorbed water. The next step was a heat treatment. The samples were subjected to four different temperature: 180⁰C, 210⁰C, 240⁰C, 270⁰C, in which were kept in three different

period of time: 20 min., 40min., 60 min. The change in chemical structure of tested samples was evaluated by using ATR-FT-IR(attenuation total reflaction Fourier transform infrared spectroscopy).

Based on obtained results it was found that the bands ranging from 1000 to 1300 cm⁻¹ which coresponds to the C-O stretching vibration are changing. Taking this into account we have concluded that sample which was expose to temperature 240 for 1 hour was thermally changed.

[1] Bo-SungKangaSang GukKimbJoo-SikKima *Thermal degradation of poly(methyl methacrylate) polymers: Kinetics and recovery of monomers using a fluidized bed reactor* , Journal of Analytical and Applied Pyrolysis Volume 81, Issue 1, January 2008, Pages 7-13.

[2] Colom, X., García, T., Suñol, J. ., Saurina, J., & Carrasco, F. (2001). *Properties of PMMA artificially aged. Journal of Non-Crystalline Solids*, 287(1-3), 308–312.

[3] Lu, G., Yazdan Mehr, M., van Driel, W. D., Fan, X., Fan, J., Jansen, K. M. B.,

& Zhang, G. Q. (2015). *Color Shift Investigations for LED Secondary Optical Designs: Comparison between BPA-PC and PMMA. Optical Materials*, 45, 37–41.

[4] Zidan, H. M., & Abu-Elnader, M. (2005). *Structural and optical properties of pure PMMA and metal chloride-doped PMMA films. Physica B: Condensed Matter*, 355(1-4), 308–317.

[5] Kuo, S.-W., Kao, H.-C., & Chang, F.-C. (2003). *Thermal behavior and specific interaction in high glass transition temperature PMMA copolymer. Polymer*, 44(22), 6873–6882.

Organic Thin Film Transistor based on conductive graft copolymer thin films as a gas sensor

P. KAŁUŻYŃSKI^{1*}, M. PROCEK¹, E. MACIAK¹, A. STOLARCZYK²

¹ Department of Optoelectronics, Silesian University of Technology, Krzywoustego 2 Str, Gliwice, Poland

² Department of Physical Chemistry and Technology of Polymers, Silesian University of Technology, 9 Strzody St., 44-100 Gliwice, POLAND

piotr.kaluzynski@polsl.pl

Nowadays, much attention is focused on the detection of compounds harmful to human health and world environment. One of such compounds is nitrogen oxides (NO_x) and nitrogen dioxide (NO_2) gases, which are produced and released into environment as a fuel combustion product, especially from diesel engines. Recent research show that nitrogen oxides are carcinogenic and are associated with increased mortality. Air pollution is still one of main environmental hazard and is and is also, for example, regulated by European law and normative acts.

Moreover modern diesel cars (Euro 3-5) have increased nitrogen oxides emission than older ones, which can be correlated to increasing power and use of turbo-charging equipment in engines. Even petrol cars (Euro 1-2) shown increased emission of harmful NO_x/CO_2 gases over the years. For these reasons, monitoring air pollution in terms of nitrogen oxide contamination is very important and very much effort is put on it in recent research. Novel sensing materials, like inorganic semiconductor oxides, organic conducting polymers, graphene and graphite oxides

as well as various sensor types, like surface acoustic wave (SAW), quartz crystal microbalance (QCM) and organic thin film transistors (OTFT) are currently being studied. As a sensing materials, polymers like: poly-3-hexylthiophene, polystyrene, polyaniline are widely used. But due their poor processability, scientist are looking for novel easy processable, available and cheap materials, so by grafting P3HT we can change it parameters.

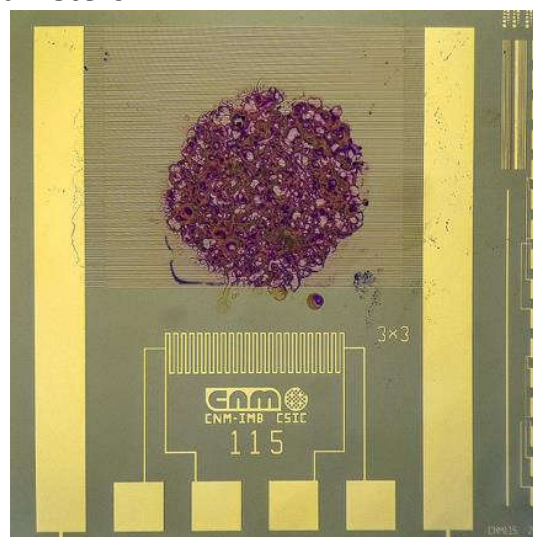


Fig. 1. OTFT sensor structure with rr-P3HT layer

This work presents an investigation on conductive graft comb copolymer polymethylsiloxane (PMS) with poly(3-hexylthiophene) (P3HT) and poly(ethylene glycol) as functional side groups and its mixtures with different nanomaterials like zinc oxide or titanium dioxide, which were used as a sensing layer for organic thin film transistor (Fig. 1) or chemoresistor for gas sensing.

Acknowledgements: Syntheses of graft combcopolymer materials were performed with the support from the Foundation for Polish Science grant POMOST 2011-3/8. The work was partially sponsored by the Faculty of Electrical Engineering of Silesian University of Technology within the grant BKM/563/RE4/2016.

Light-driven bending of the azo poly(amide imide) cantilevers

Anna KOZANECKA-SZMIGIEL¹, Dariusz SZMIGIEL², Jolanta KONIECZKOWSKA³, Ewa SCHAB-BALCERZAK³

¹Faculty of Physics, Warsaw University of Technology, 75 Koszykowa Str., 00-662 Warszawa, POLAND

²Institute of Electron Technology, al. Lotnikow 32/46, 02-668 Warszawa, POLAND

³Centre of Polymer and Carbon Materials Polish Academy of Sciences, 34 M. Curie-Sklodowska Str., 41-819 Zabrze, POLAND

annak@if.pw.edu.pl

Light-induced deflection of cantilevers prepared from photoresponsive azo materials has been widely studied for liquid crystalline polymer networks and elastomers [1]. The deflection is a consequence of strong attenuation of passing light and nonuniform strain generation across the cantilever thickness.

It is known that the magnitude of cantilever deformation depends on irradiation conditions, thermomechanical properties of a polymer or cantilever dimensions [2]. Azo polymers exhibiting the photomechanical effect are of great interest from the viewpoint of light-driven actuators.

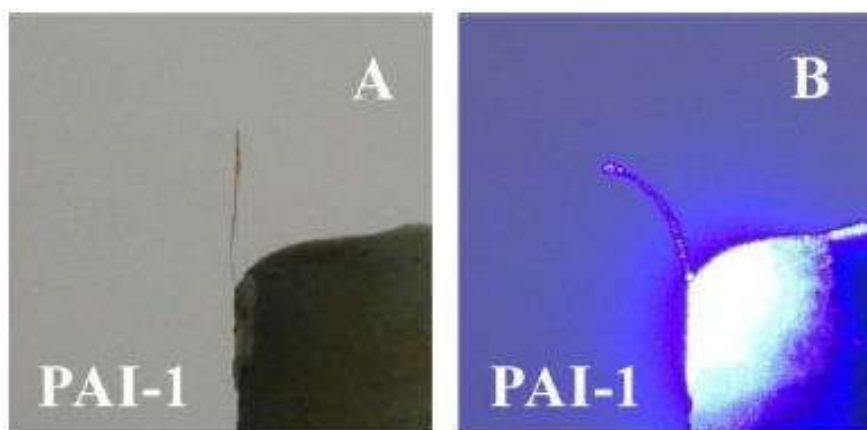


Fig. 1. Photoinduced deformation of a cantilever prepared from one of the studied materials (A) before irradiation, (B) upon exposure to 445 nm linearly polarized light

In this work we demonstrate a photomechanical response of a series of glassy “T-type” azobenzene poly(amide imide)s together with their selected physicochemical properties. To our knowledge, it is the first report on light-induced bending of cantilevers for this

class of azo polymers. We present the sample preparation steps and explain the adopted irradiation procedure focused on observation of a bidirectional movement of the cantilevers. The magnitude of the observed photomechanical response (Fig. 1) is related to the results of

photoinduced birefringence measurements. Moreover, we indicate a possible reason for asymmetric forward and reverse bending of the cantilevers. Stability of the bent samples after switching off the 445 nm beam is presented as well.

-
- [1] T. J. White, *J. Polym. Sci. Part B: Polym Phys.* **56**, 695 (2018),
- [2] D. H. Wang, K. M. Lee, Z. Yu, H. Koerner, R. A. Vaia, T. J. White, and L-S. Tan, *Macromolecules* **44**, 3840 (2011).

Set of the fiber optic rotational seismographs for mining activity monitoring

Anna KURZYCH, Leszek R. JAROSZEWICZ, Zbigniew KRAJEWSKI, Jerzy K. KOWALSKI,
Michał DUDEK

Institute of Technical Physics, Military University of Technology, Gen. W. Urbanowicza St.2, 00-908 Warsaw, POLAND

anna.kurzych@wat.edu.pl

Until recently, there have been only three translational components of soil movement measured in the seismology and seismic engineering (along two horizontal x, y and z-axis). Three rotational components have been underestimated due to lack of accurate and appropriate devices. However, it turned out that additional three degrees of freedom during measurements of ground vibrations can provide new information which can be valuable for seismological society for better understanding Earth's inner structure, seismic sources as well as engineering purposes.

The FOSREM[®] – Fiber-Optic Rotational Seismograph presented in this paper have been constructed to meet all technical requirements for rotational seismology. Rotational Seismology caused highly interest in the investigation of rotational movements generated by earthquakes, explosions, and ambient vibrations. FOSREM[®] uses autonomous and mobile fiber-optic rotational seismometers which enable to detect

rotational movements in wide signal amplitude ($5 \cdot 10^{-8}$ rad/s – 10 rad/s) as well as frequency range (DC - 328.12 Hz).

It works by measuring Sagnac effect and generally consists of two basic elements: optical sensor and electronic part. The optical sensor is based on so-called the minimum configuration of FOG. The main advantage and attribute of such kind of sensor is its complete insensitivity to linear motions and a direct measurement of rotational speed. It may work even when tilted, and moreover, it may recording the tilt if is used in continuous mode.

The electronic part calculates and records rotational events by realizing synchronous detection in a digital form by using 32 bit DSP. FOSREM[®] is fully remotely controlled as well as it is suited for a continuous, autonomous work in very long period of time, thus it is useful for a systematic seismological investigation at any place. Laboratory investigation has indicated that FOSREM[®] possesses high sensitivity ($3.07 \cdot 10^{-8}$ rad/s/√Hz), wide frequency range (DC -

328.12 Hz), thermal stability (0.06 %/°C) as well as wide measured amplitude of signal ($5 \cdot 10^{-8}$ rad/s – 10 rad/s). The carried out Allan variance noise analysis (ARW - Angle Random Walk equals $4.9 \cdot 10^{-8}$ rad/Vs, BI - Bias Instability of the order of $1.20 \cdot 10^{-8}$ rad/s) confirmed the extremely advanced technical solutions.

In this paper we present observations of the one-direction rotational component around a vertical

axis caused by crumps as well as a rotational component or strain around a vertical axis generated by artificial detonation and mining activity. Data clearly shows the completely different nature of these events, especially in shape of the plot as well as energy of the signal. Data has been recorded by two FOSREMs[®] as well as Twin Antiparallel Pendulum Seismometers (TAPS).

Tab. 1. Rotational events recorded by the FOSREMs in the geophysical observatory in Książ, Poland in period 8/01/2017 – 1/25/2018.

FOSREM -1 / FOSREM -2	Date	Max. amplitude [rad/s]	Signal energy [rad]	Correlation coefficient
FOS 1 FOS 2	1/08/2018	$3.89 \cdot 10^{-6}$ $1.81 \cdot 10^{-6}$	$3.94 \cdot 10^{-6}$ $2.13 \cdot 10^{-6}$	0.82
FOS 1 FOS 2	12/01/2017	$8.25 \cdot 10^{-6}$ $4.17 \cdot 10^{-6}$	$4.56 \cdot 10^{-6}$ $2.48 \cdot 10^{-6}$	0.95
FOS 1 FOS 2	12/01/2017	$1.67 \cdot 10^{-5}$ $1.03 \cdot 10^{-5}$	$5.78 \cdot 10^{-5}$ $2.97 \cdot 10^{-5}$	0.94
FOS 1 FOS 2	11/28/2017	$1.86 \cdot 10^{-6}$ $1.61 \cdot 10^{-6}$	$6.17 \cdot 10^{-7}$ $5.31 \cdot 10^{-7}$	0.84
FOS 1 FOS 2	11/28/2017	$1.58 \cdot 10^{-6}$ $1.01 \cdot 10^{-6}$	$1.93 \cdot 10^{-6}$ $1.11 \cdot 10^{-6}$	0.79
FOS 1 FOS 2	10/05/2017	$2.00 \cdot 10^{-5}$ $1.00 \cdot 10^{-5}$	$1.31 \cdot 10^{-5}$ $6.66 \cdot 10^{-6}$	0.98
FOS 1 FOS 2	12/13/2017	$1.65 \cdot 10^{-6}$ $1.32 \cdot 10^{-6}$	$6.86 \cdot 10^{-7}$ $5.95 \cdot 10^{-7}$	0.86
FOS 1 FOS 2	12/13/2017	$1.77 \cdot 10^{-6}$ $1.09 \cdot 10^{-6}$	$1.04 \cdot 10^{-6}$ $6.73 \cdot 10^{-7}$	0.88
Mean value		$5.5226 \cdot 10^{-6} \pm$ $0.0005 \cdot 10^{-6}$	$8.6772 \cdot 10^{-6} \pm$ $0.0003 \cdot 10^{-6}$	0.88 ± 0.03

Growth and preliminary characterization of InAsSb photodiodes for mid-wave infrared range

Kordian LIPSKI¹, Łukasz KUBISZYN^{1,2}, Krystian MICHALCZEWSKI²
Krzysztof MURAWSKI¹, Piotr MARTYNIUK¹

¹Institute of Applied Physics, Military University of Technology, Gen. Witolda Urbanowicza 2 Str., 00-908 Warsaw, POLAND

²Vigo System S.A., 129/133 Poznańska Str., 05-850 Ożarów Mazowiecki, POLAND

kordian.lipski@wat.edu.pl

HgCdTe infrared (IR) detectors have a wide range of applications in significant fields, like medicine, defense and security. However, in spite of many advantages there are still some difficulties, for example: thermal instability. InAsSb ternary alloy is one of alternative compound to HgCdTe covering wide range of detection in both 3 – 5 and 8 – 12 μm IR atmospheric windows [1]. There is high interest in developing new materials for HgCdTe replacement.

In our research, InAsSb heterostructures have been grown on InAs buffer on semi-insulating GaAs substrates (001) with 2° offcut using RIBER Compact 21-DZ solid-state molecular beam epitaxy (MBE). This paper reports on growth details and preliminary characterization of mid-wave InAsSb simple barrier structures (Fig. 1). Main device parameters were measured for photodetector with 3 different InAsSb absorber thicknesses 1 μm (sample no. 1);

1.70 μm (sample no. 2); 2.56 μm (sample no. 3) and one undoped 1.70 μm (sample no. 4).

The characterization was performed for crystallographic structure, bandgap energy, responsivity, I-V characteristic and detectivity.

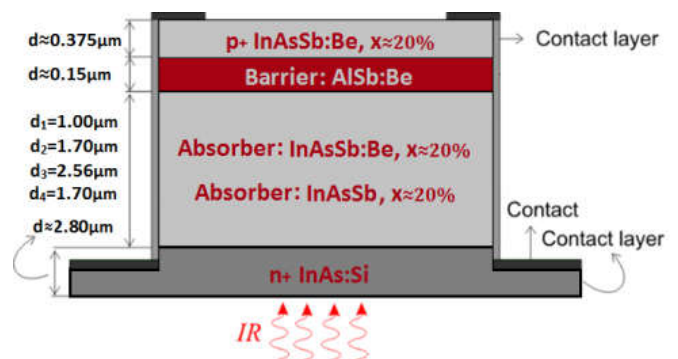


Fig. 1. Schematic cross-section of mid-wave IR barrier photodetector

1. A. Rogalski, InAs_{1-x}Sb_x infrared detectors, Prog. Quantum Electron. 13, 191–231, 1989

Investigation of room temperature optical gas sensing properties of chitosan/AuNPs blend nanostructures

Erwin MACIAK

Department of Optoelectronics, Silesian University of Technology, 2 Krzywoustego Str. 44-100 Gliwice, POLAND
erwin.maciak@polsl.pl

Chitosan, the primary derivative of chitin, is obtained at a relatively low cost from the shells of shellfish (mainly crabs, lobsters and shrimps), the wastes of the seafood processing industry. Insoluble in water, chitosan readily dissolves in weak acidic solutions, which is due to the presence of amino groups in its molecules [1-3]. The ability to detect and monitor acetone and other VOCs is highly important, however to achieve this at room temperature and allow for remote sensing applications is a significant challenge. Here, it is tackle this issue and investigate optoelectronic gas sensors that operate at room temperature using a chitosan containing gold nanoparticles (AuNPs) sensing structures formed via simply immersing fiber optic substrate. These films were characterized by scanning electron microscopy and surface plasmon resonance technique. The sensors show a response to acetone and good recovery at 25°C.

Funding: This work was supported in part by the Rector of the Silesian University of Technology within grant agreement no. 05/040/RGH17/0019 and no. 05/040/RGJ18/0021.

-
- [1] N.V. Majeti, R.Kumar, A review of chitin and chitosan applications, *Reactive and Functional Polymers* 46 (2000) 1–27.
 - [2] K.V.H. Prashanth, R.N. Tharanathan, Chitin/chitosan: modifications and their unlimited application potential-an overview, *Trends Food Science and Technology* 18 (2007) 117–131.
 - [3] C.K.S. Pillai, W. Paul, C.P. Sharma, Chitin and chitosan polymers: chemistry, solubility and fiber formation, *Progress in Polymer Science* 34 (2009) 641–678.

Singular-value decomposition model for partial polarizing optical fiber elements

Paweł MARC, Karol STASIEWICZ, Joanna KOREC, Leszek R. JAROSZEWICZ

Military University of Technology, 2 Urbanowicza Str., Warsaw, POLAND

pawel.marc@wat.edu.pl

Polarization properties of optical fiber elements are limited to a polarization dependent loss (PDL) measurement. Their extensive study is possible by using the Mueller matrix measurement. Such measurement allows to extract full information about optical parameters of the tested elements such as losses, dichroism, depolarization and birefringence. In order to calculate these parameters, it is necessary to use dedicated matrix manipulation methods. A common one is a polar decomposition, but its significant disadvantage is its non-

symmetry. Any optical fiber element has a symmetric configuration because it consists of an input and output fiber. Therefore, in this work a symmetric model based on a singular-value decomposition was proposed. This model is applicable to polarizing optical fiber elements and any optical fiber element is a partial polarizer with retardance placed between a pair of linear birefringent elements. Measurements of a partial polarizer and a liquid crystal cell with a tapered optical fiber and calculation of their optical parameters were presented.

Hybrid connection of functional materials and tapered optical fiber

Joanna E. MOŚ, Karol A. STASIEWICZ, Leszek R. JAROSZEWICZ

Institute of Technical Physics, Military University of Technology, gen. Witolda Urbanowicza 2, 00-908 Warsaw, POLAND

joanna.mos@wat.edu.pl

In the classic optical fiber, the propagation of the light is described by the principle of total internal reflection. The light is propagated in the core of the fiber structure, and the cladding keep the light beam inside [1, 2]. This is due to material properties - core has a higher refractive index than cladding. Applying the technologic process of heating a certain section of the fiber, as a result a tapered optical fiber can be obtain [3]. As a result, we can get a very thin structure in which it is able to influence the propagating beam with external factors in main taper area. In extreme cases, the beam of light completely fulfills the area of new structure - the propagation conditions change, the light beam propagates at the border of structure / surroundings. When we apply additional material, which will be the environment of structure tapered optical fiber will detect changes reflection index this extra material. Liquid crystals which have anisotropic properties were selected as an additional material. The refractive index of this material can be controlled by the electric field and temperature [4].

A cell filled with a 1550 * mixture was built. The tests show that with the increase of voltage in the range of 0-200V, the beam power increases and it is possible using a variable electrical signal (shape change, frequencies in the 1-10Hz range) to selectively amplify a certain range of wavelengths – which can be used as bandpass filter.

This work was supported by project of National Science Centre (NCN) PRELUDIUM 2018/29/N/ST7/02347 and RMN 08/689 of Military University of Technology.

-
- [1] M. Sumetsky i L. Tong, *Subwavelength and Nanometer Diameter Optical Fibers*, Jointly published with Zhejiang University Press, 2010,
 - [2] L.Tong, J.Lou, E.Mazur, *Optics Express*, 12, 6, (2004),
 - [3] K. Stasiewicz, R. Krajewski, L. Jaroszewicz, M. Kujawińska, R. Świłło, *Opto-Electronics Review*, 18, 1,(2010),
 - [4] C.Veilleux, J. Lapierre, J. Bures, *Optics Letters*, 11, 11, (1986).

Temperature dependence of Raman scattering in nanometric films of GaS and SnS₂

Katarzyna OLKOWSKA^{1,3}, Cezariusz JASTRZEBSKI¹, Daniel J. JASTRZEBSKI²,
Sławomir PODSIADŁO²

¹Faculty of Physics, Warsaw University of Technology, Koszykowa 75, 00-662 Warsaw, POLAND

²Faculty of Chemistry, Warsaw University of Technology; Noakowskiego 3, 00-664 Warsaw, POLAND

³Institute of Physics, Polish Academy of Sciences, Al. Lotników 32/46, 02-668 Warszawa, POLAND

olkowska@ifpan.edu.pl

This work concerns the study of Raman scattering processes in thin films chalcogenide materials of metals group III and IV. These materials have been intensively studied in the last decade due to their application potential in the field of photodetectors.[1]

Gallium sulfide and tin(IV) sulfide are a semiconducting materials with a layered structure (fig.1) and a characteristic low interlayer interaction.

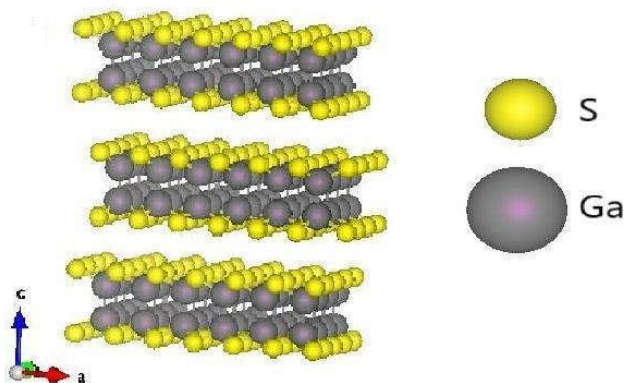


Fig.1. Stacking order (side view) of layers in β -type structure of GaS. Atoms of Ga and S are represented by grey and yellow spheres, respectively

Because of weak van der Waals forces, GaS and SnS₂ crystals are relatively easy to exfoliate to nanometric-size layers. The purpose of this work is to investigate the temperature properties of phonons in two two-dimensional materials. Bulk materials of chalcogenides were prepared in cooperation with the Faculty of Chemistry of the Warsaw University of Technology. In this work nanometric-GaS and SnS₂ layers were obtained by a micro-mechanical exfoliation process and were transferred to Si/SiO₂ substrate. The layers thicknesses of the materials have been examined using topographic measurements of Atomic Force Microscope (AFM).

Temperature dependencies for bulk materials and two-dimensional materials have been compared (fig.2). Raman spectra were collected for different layer thickness: 4nm, 7nm and bulk. Measurements were conducted in the range of temperature from 80 to 470 K. An analytical function fitted to experimental data is proposed (fig.3). The

first order temperature coefficients have been determined as well as for bulk materials and thin films of GaS and SnS₂.

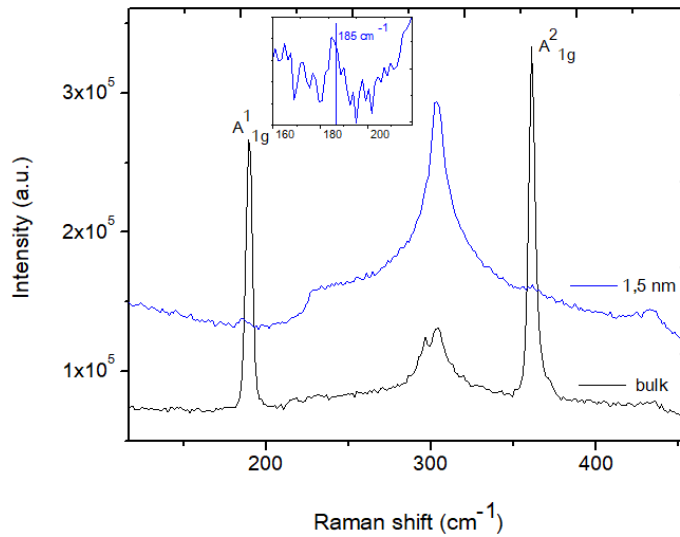


Fig. 2 The Raman spectrum for very thin sample (blue line) in comparison to the spectrum obtained for a thick GaS sample (black line)

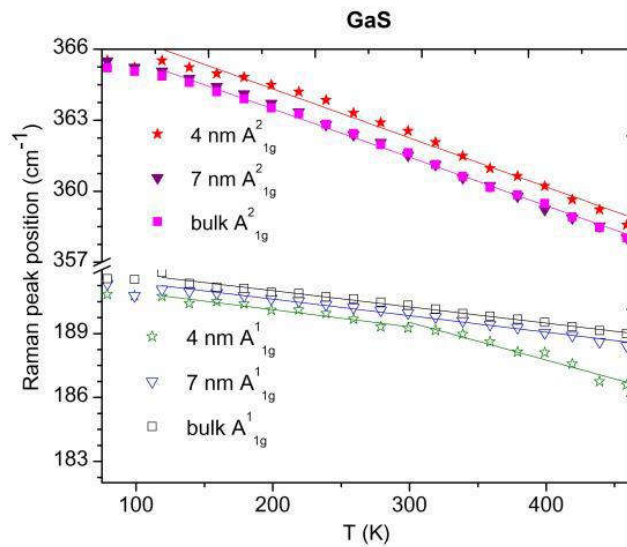


Fig.3. Temperature dependence of Raman frequency A_{1g} and A_{2g} modes in GaS for different thickness of the sample layers

Raman peak position in bulk and in nanometric thickness samples were temperature dependent. The Full Width at Half Maximum (FWHM) of Raman peaks was increasing with increase of temperature. Further work connected to

minimalization of Raman spectrometer are necessary to develop a compact device which will utilize the advantages of GaS and SnS₂.

- [1] Hu P., Wang L., Yoon M., Zhang J., Feng W., Wang X. et al, Nano Lett., 2013, 13, 1649-1654

Sensor-based perimeter protection of hard-to-reach wetlands and rivers - conception of the system

Norbert PAŁKA^{*}, Jarosław MŁYŃCZAK, Marek ŻYCZKOWSKI, Marek PISZCZEK, Mateusz KAROL, Marcin MACIEJEWSKI, Wiesław CIURAPIŃSKI, Marcin KOWALSKI, Artur GRUDZIENI, Michał WALCZAKOWSKI, Elżbieta CZERWIŃSKA, Piotr MARKOWSKI, Konrad BREWCZYŃSKI
and Mieczysław SZUSTAKOWSKI

^{*} Military University of Technology, 2 Urbanowicza Str., Warsaw, 00-908 POLAND

npalka@wat.edu.pl

We propose a modern system for detecting and visualizing people, means of transportation and smuggled goods to solve the problem of detection of events related to illegal crossing of the state border in wetlands, coastal areas and rivers. The system will be based on the fusion of data from a variety of sensors for perimeter protection (acoustic, hydroacoustic, magnetic, microwave, pyroelectric and other) and optoelectronic observation systems (thermal imaging

cameras and visible radiation cameras). The developed system will be characterized by autonomy, the ability to adapt to the ambient conditions and will be resistant to possible attempts to emulate the sensors as well as the interference of unauthorized persons. We plan to develop a concept of the system with scenarios and a research program, as well as to develop a prototype, conduct tests in real conditions, and organize training for end-users.

A simulation tool to check correctness of optical signatures detection

Artur ARCIUCH, Tomasz PAŁYS*

* Military University of Technology, Department of Computer Science,
2 Gen. W. Urbanowicza Str., Warsaw, 00-908 Poland

tomasz.palys@wat.edu.pl

The article presents a tool for generating and detecting optical signatures. The tool has been implemented in the Matlab environment using the Matlab Simulink package. The publication contains a proposal to use the developed tool to study the impact of laser activation time, camera image resolution, frame rate as a

result of optical signature detection. The obtained results proved that the developed tool successfully allows to research various methods of generating and detecting optical signatures. It also allows a quantitative assessment of the correctness of the detection process.

Zero- and ultra- low-field nuclear magnetic resonance with atomic magnetometer

Kacper POPIOŁEK, Piotr PUT, Szymon PUSTELNY

Marian Smoluchowski Institute of Physics, Jagiellonian University, Łojasiewicza 11, 30-348 Krakow, POLAND
kacper.popiolek@doctoral.uj.edu.pl

Nuclear magnetic resonance (NMR) is mainly used in the apparatus for non-invasive medical imaging and chemical analysis [1]. Conventionally, NMR requires a high (>1 T) magnetic field for the polarization of the samples and the detection of magnetization. The need for an ultra-strong homogenous field is probably the largest disadvantage of the standard NMR, leading to a high cost and low mobility of NMR scanners and spectrometers. Since 1980s scientists have been attempting to perform NMR experiments at ultra-low magnetic fields or even entirely without the field [2]. In the ZULF NMR experiments, the detection of magnetization that is coming from the samples takes place through the application of one of the most sensitive magnetic-field sensors: the atomic magnetometer [3]. This method seems especially promising, as atomic magnetometers can operate in near room temperature, can be miniaturized and reach the near-DC field sensitivity better than $10 \text{ fT Hz}^{-1/2}$..

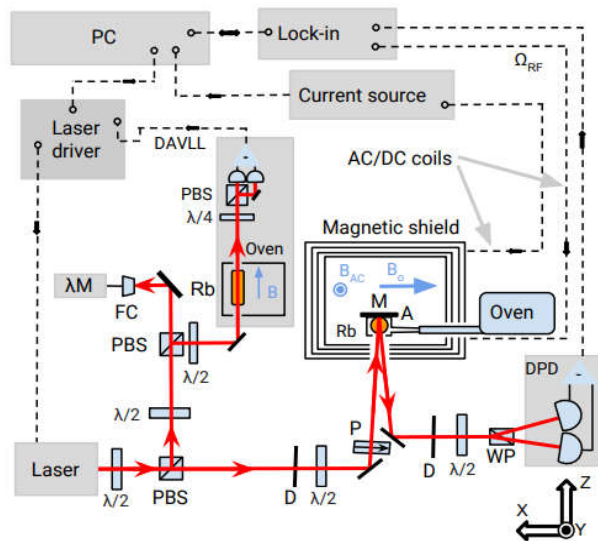


Fig. 1. Diagram of the experimental apparatus used for magnetic-field detection. B is a static field for the DAVLL system, B_{AC} is an oscillating field and B_0 is a static field used for magnetometric purposes. Directions of magnetic fields are marked by bright blue arrows.

We describe an experimental setup (Fig. 1.) used to perform preliminary NMR experiments at ultra-low magnetic field using a high sensitivity atomic magnetometer. To eliminate environmental noise, a gradiometer scheme, employing differential signal from two sensors is used. This enables the measurement of magnetization of a sample (a vessel of a distilled water),

which is shuttled pneumatically from a high field region produced by the pseudo-Halbach magnet, to a volume inside of an ultra-low magnetic field, where detection is performed.

[1] Levitt, Malcolm H. "Spin dynamics." Jon Wiley and Sons 196 (2001).

[2] Ledbetter, Micah P., Budker, D. "Zero-field nuclear magnetic resonance." *Physics Today* 66(4) (2013).

[3] Budker, D., Romalis, M. "Optical magnetometry." *Nature Physics* 3.4 (2007): 227

Theoretical studies on refractive index profile of nanostructured fibre

Piotr PUCKO^{1,2*}, Marcin FRANCZYK¹, Adam FILIPKOWSKI¹, Ryszard BUCZYŃSKI^{1,3}

¹Institute of Electronic Material Technology, 133 Wólczyńska Str., 01-919 Warsaw, POLAND

² Faculty of Physics, Warsaw University of Technology, 75 Koszykowa Str., 00-662 Warsaw, POLAND

³Faculty of Physics, University of Warsaw, 5 Pasteura Str., 02-093 Warsaw, POLAND

261698@pw.edu.pl

Nanostructurization [1] is novel technology for manufacturing optical fibres which could overcome capabilities of standard methods.

The difference between nanostructured fibre and standard telecommunication optical fibre is the structure of the core. In fabrication process two or more kinds of glass rods are stacked to form a mosaic (Fig. 1).

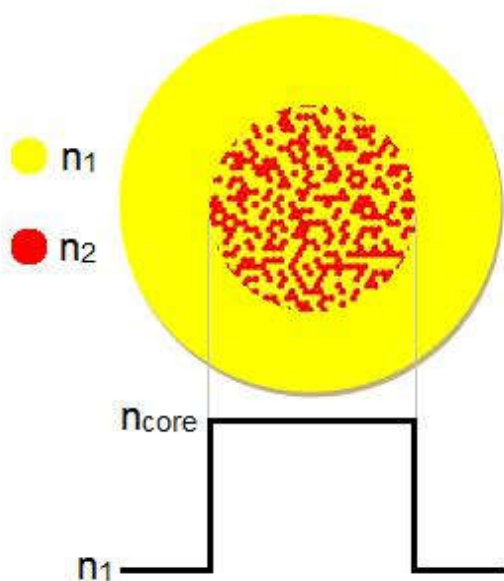


Fig. 1. Exemplary design of fibre core structure for perfect step index profile. Red and yellow elements indicate higher and lower refractive index glass respectively

Because single element in a core structure is much lower than the wavelength of propagating light the refractive index of the medium is “seen” by light as averaged refractive index profile [2]. Controlling the distribution of glass elements within the core, we can create any gradient refractive index profile. That technology opens new possibilities for development of passive or active fibres which could lead to new generation fibres [3].

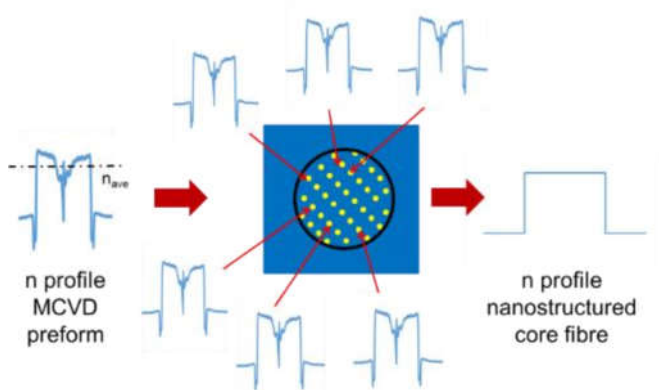


Fig. 2. Schematic process of obtaining ideal step-index profile in nanostructured core fibre with the use of several glass rods made with MCVD technology

In this publication we present theoretical studies on imperfections of refractive index profiles made with MCVD technology. We parallel them with step-index profile achieved with nanostructurization (Fig.2).

In our numerical simulations we compare the refractive index profile with peripheral and central dips versus perfect step-index profile attainable with nanostructurization technology and we

present their influence on performance of single-mode fibre. We particularly studied the impact of the central inequalities in standard fibre profile on intensity shape of fundamental mode. It is important issue in fibres for laser applications due to the overlapping of the mode area with dopants distribution within the fibre core and gain properties of the laser medium.

-
- [1] A. Anuszkiewicz, R. Kasztelan, A. Filipkowski, G. Stepniewski, T. Stefaniuk, B. Siwicki, D. Pysz, M. Klimczak, R. Buczynski, *Scientific Reports*, **8**, 12329 (2018).
- [2] F. Hudelist, R. Buczynski, A.J. Waddie, M.R. Taghizadeh, *Opt. Express* **17**, 3255–3263 (2009).
- [3] M. Franczyk, K. Stawicki, J. Lisowska, D. Michalik, A. Filipkowski, R. Buczynski, *J. Lightwave Technol.* **36**, 5334-5343 (2018).

The hypothesis about the electrical non-neutrality of the Universe

Tadeusz PUSTELNY

Department of Optoelectronics, Silesian University of Technology, 2 Krzywoustego Str, 44-100 Gliwice, POLAND
tadeusz.pustelny@polsl.pl

Consideration of the Universe's electrical non-neutrality and existence in It to a greater extent than it is considered today, atomic nuclei of heavier elements, as remnants after the early Universe, allows a better understanding of the Universe and explanations of many of his states and many of Its behaviors. The theory of the Universe must take into account, alongside gravitational interactions, also the electrically non-neutral character of the Universe.

Dark Matter and Dark Energy form a major part of the mass-energy of the Universe - totally of about 95%.

The author believes that Dark Energy and Dark Matter can not have their sources of origin in abstract, unknown and undiscovered elementary particles.

At very high level of scientific researches both in the field of elementary particles and in the field of astrophysical observations, the components of the Universe, which this Universe practically form (representing 95% of its mass-energy) if they existed, would have been detected.

The author raises his own hypotheses about the origin of Dark Energy and Dark Matter.

Light guiding channels in polymer-supported liquid crystalline materials and structures

Katarzyna RUTKOWSKA, Anna KOZANECKA-SZMIGIEL, Miłosz CHYCHŁOWSKI

Faculty of Physics, Warsaw University of Technology, 75 Koszykowa Str., 00-662 Warsaw, POLAND
kasia@if.pw.edu.pl

Liquid crystals (LCs) are unique materials, combining properties of liquids and solids and thus finding many practical applications in modern optics and photonics [1]. Special class of such substances are those mixed, combined and co-organized with monomers/polymers.

Polymer-dispersed and stabilized liquid crystals are promising candidates for new elements and devices in photonic systems, while offering often wider functionality and tunability than achieved in pure liquid crystalline materials.

On the other hand, polymer surfaces are typically applied for liquid crystal alignment for different molecular orientation. For this purpose various types of polymer materials and surface treatments are applied. One of the well-known technique of molecular orientation in liquid crystal cell is mechanical rubbing performed on polyimide layer, another one is a photo-orientation process performed via UV-illumination of specific polymer surface.

Possibility of waveguiding channels formation in liquid crystalline materials are of particular attention in this communication. Specifically, formation of specific spatial distribution within liquid crystal layer by means of independently applied photo-polymerization and photo-orientation processes are described.

In the first option LC-monomer mixture of specific composition has been prepared to be illuminated with UV light of specific parameters to fabricate waveguiding channels of satisfactory quality.

In the second proposed process, an orienting polymer material in a form of specifically adopted azo-polymer has been exposed to linearly polarized UV light to create sections of planar and twisted alignment in nematic liquid crystal cell with varying angular orientation with respect to propagation direction in created waveguiding channels.

Proposed methods can be potentially applied to obtain light guiding structures with accessible spatial resolution of single micrometers, as well

as periodic waveguiding structures. High tunability of polymer-assisted liquid crystalline waveguiding structures are of particular importance especially when compared to waveguiding structures manufactured in other materials (e.g. semiconductors). They may find potential applications as functional elements and devices for LC-based integrated optics.

Author would like to acknowledge support by the Polish National Science Center (NCN) under the grant no. DEC-2013/11/B/ST7/04330.

[1] D. Yang, Fundamentals of Liquid Crystal Devices, John Wiley & Sons 2014.

Tuning optical properties of fluorescent nanodiamonds: influence of solvent polarity and pH

Mateusz FICEK^{1,*}, Michał RYCEWICZ¹, Maciek GŁOWACKI¹, Marcin MARZEJON¹, Katarzyna KARPIENKO¹, Mirosław SAWCZAK² and Robert BOGDANOWICZ¹

¹ Faculty of Electronics, Telecommunications and Informatics, Gdańsk University of Technology, 11/12 Narutowicza St., 80-233 Gdansk, POLAND

² Centre for Plasma and Laser Engineering, The Szewalski Institute of Fluid-Flow Machinery, Polish Academy of Sciences, 14 Fiszerza St., 80-231 Gdansk, POLAND

mateuszficek@gmail.com

The development and applications of quantum technologies and nonlinear spectroscopy for studies of color centers in diamonds are very fast. Thanks to the stable crystallographic and electron structure of diamond, NV-color centers exhibit very stable electronic spectra, resistant to various perturbations. Their excellent optical and spin properties allow one to use different resonance and spintronic methods of and enable precision metrology.

In this study, fluorescent suspensions of diamond particles have been produced by microbead assisted ultrasonic disintegration of commercially obtained diamond powder containing NV color centers¹. The suspensions characterization was based on optical (absorption, emission, Raman) and microwave spectroscopy with high spatial resolution². The treatment allows for decrease of grain size and surface modification of nanodiamonds to achieve stable deionized water-based suspensions.

Furthermore, fluorescent suspensions were deposited onto tapered fiber structures by dip-coating procedure. Photonic tapered structures were fabricated by using a fiber-optic splicer (Ericsson FSU 975) and a telecom, multi-mode optical fibers. The tapered section was performed in three phases characterized by duration time and current value. The desired shapes of the structures were obtained by adjusting the splicing parameters. The tapered optical fibers covered with fluorescent nanodiamond nanoparticles are used as optical fiber probes of organic matter, providing a waveguide delivery of optical fields for the initialization, polarization, and readout of the electron spin in NV centers with proteins (e.g. albumin).

Acknowledgments

The authors gratefully acknowledge financial support from the Polish National Science Centre (NCN)

under Grant No. 2016/21/B/ST7/01430, 2016/22/E/ST7/00102 and National Centre for Science and Development Grant Techmatstrateg No. 347324. This work was partially supported by the Science for Peace Programme of NATO (Grant no. G5147). The DS funds of the Faculty of Electronics, Telecommunications and Informatics of the Gdansk University of Technology are also acknowledged.

[1] M. J. Głowacki, M. Ficek, M. Sawczak, R. Bogdanowicz, *proc. SPIE* 104550E (2017).

[2] M. Mrozek, A. Wojciechowski, D.S. Rudnicki, J. Zachorowski, P. Kehayias, D. Budker, W. Gawlik, *ArXiv151203996 Phys* (2015).

Design of an integrated optics sensor structure for haemoglobin property detection.

Przemysław STRUK

Department of Optoelectronics, Faculty of Electrical Engineering,
Silesian University of Technology, 2 Krzywoustego Str., 44-100 Gliwice, POLAND

Przemyslaw.Struk@polsl.pl

This manuscript presents a theoretical analysis of a diamond-based integrated optics structure for applications in biosensor for hemoglobin properties detection (oxidation and concentration). The geometrical, optical, and sensitivity properties of an integrated optical sensor structure were theoretically analyzed and optimized for research of hemoglobin properties [1].

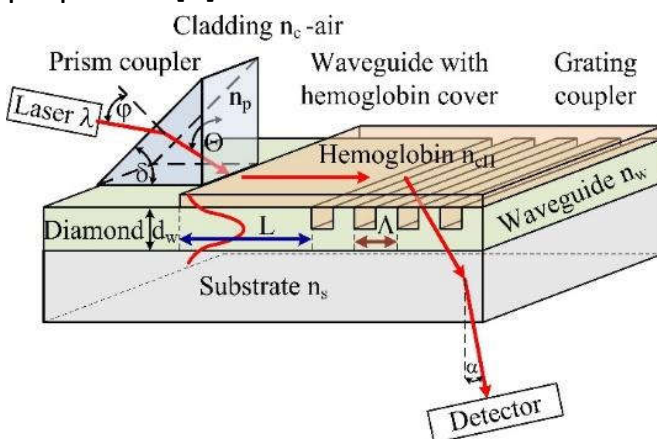


Fig. 1. Scheme of the hemoglobin sensor structure.

The analysis focused on determining the waveguide properties, including the effective refractive index N_{eff} as a function of refractive index n_w and thickness d_w of waveguide layer, refractive index of the

hemoglobin cover layer n_{CH} and substrate layer n_s , homogeneous sensitivity $d_{N_{eff}}/d_{n_{CH}}$, and modal field distribution of guided waveguide modes [1]. The analysis was completed for waveguide layer based on diamond materials with or without the hemoglobin cover layer.

The concept and idea of the hemoglobin sensor structure is presented in Figure 1. The sensor is composed of three sections: prism coupler, planar waveguide with length L and grating coupler with spatial period Λ . In the case of hemoglobin, two parameters are most interesting for the determination of patient health: hemoglobin concentration and hemoglobin oxidation. In presented structure the prism coupler is responsible for introduction of light into waveguide structure, The planar waveguide with length L is responsible for the determination of absorption coefficient (imaginary part of refractive index k) of hemoglobin cover layer corresponding to oxidation level by evanescent field of guided mode. The evanescent field of guided mode penetrates the hemoglobin cover layer and hence is attenuated, the

output power of light is detected by detector. The grating coupler have two functions: is responsible for uncoupling the light from waveguide to cladding. Second function the grating coupler acts as a sensor for the determination of the real part of refractive index of the cover layer and hence, the refractive index of hemoglobin which correspond the concentration of hemoglobin. Changes of refractive index in the cover layer n_H and hence, causing changes in effective refractive index N_{eff} have influence of the uncoupling angle α (measured by detector) [1,2,3]. The presented experimental results form a base for developing biosensor structures based on integrated optics for determining the properties of hemoglobin.

- [1] Przemysław Struk, *Design of an Integrated Optics Sensor Structure Based on Diamond Waveguide for Hemoglobin Property Detection*, Materials, Vol. 12(1), 175, 1-12, 2019
- [2] Jedrzejewska-Szczerska, M.; Majchrowicz, D.; Hirsch, M.; Struk, P.; Bogdanowicz, R.; Bechelany, M.; Tuchin, V.V. Chapter 14—Nanolayers in Fiber-Optic Biosensing. In *Nanotechnology and Biosensors A volume in Advanced Nanomaterials*; Nikolelis, D., Nikoleli, G.P., Eds.; Elsevier: Amsterdam, The Netherlands, 2018; pp. 395–426, doi:10.1016/B978-0-12-813855-7.00014-3
- [3] Lukosz, W.; Tiefenthaler, K. Sensitivity of integrated optical grating and prism couplers as (bio)chemical sensors. *Sens. Actuators* 1988, 15, 273–284, doi:10.1016/0250-6874(88)87016-1.

An application of thulium doped fiber laser in wood cutting

Slawomir SUJECKI^{1,2}, Monika ANISZEWSKA³, Adam MACIAK³, Witold ZYCHOWICZ³, Samir LAMRINI⁴, Karsten SCHOLLE⁴, Peter FUHRBERG⁴

¹Department of Telecommunications and Teleinformatics, Faculty of Electronics, Wroclaw University of Science and Technology, Wyb. Wyspianskiego 27, 50-370 Wroclaw, POLAND

²George Green Institute for Electromagnetics Research, The University of Nottingham, University Park, NG7-2RD, Nottingham, UK

³Faculty of Production Engineering, Warsaw University of Life Sciences, Nowoursynowska 164, 02-787 Warsaw, POLAND

⁴Futonics laser GmbH, Albert-Einstein-Str. 3, Katlenburg-Lindau 37191, GERMANY

slawomir.sujecki@pwr.edu.pl

Fiber lasers doped with thulium ions emit light at the operating wavelength of 2000 nm. This wavelength is intensely absorbed by water. Therefore one of the potential applications of thulium ion doped fiber lasers is tree branch and tree cutting. Currently the main laser used in relation to wood processing is the carbon dioxide gas laser [1]. However, it has not found a widespread application in tree cutting and tree trimming. In this contribution an application of thulium doped fiber laser to tree trimming is studied. When compared with gas lasers fiber thulium ion lasers are more compact and have lower value of the M^2 parameter.

The main aim of the research is the analysis of the wood cutting speed for four kinds of wood along and across wood fiber. This included in particular the measurement of the cutting speed and an analysis of the wood surface resulting from the cutting process. The analysis included the study of the fiber laser

output beam total power and M^2 parameter on the cutting speed. A selection of wooden logs with varying diameter and water content were considered. Fig.1 shows an example dependence of the cutting speed for oak wood, along the wood fibers when applying a thulium doped fiber laser with CW operation and maximum output power of 210 W.

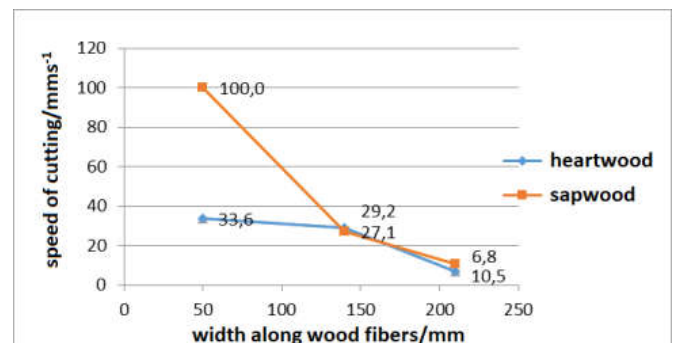


Fig. 1. Dependence of wood cutting speed on the wood section width.

Fig.2 shows the measurement setup consisting of the pump laser operating at 788 nm, thulium doped fiber section, optical beam handling bulk optics and a

wood sample. The setup was used throughout all experiments. The results obtained show the cutting speed depends on the laser beam orientation with respect to the wood fibers, the content of water and the type of wood.

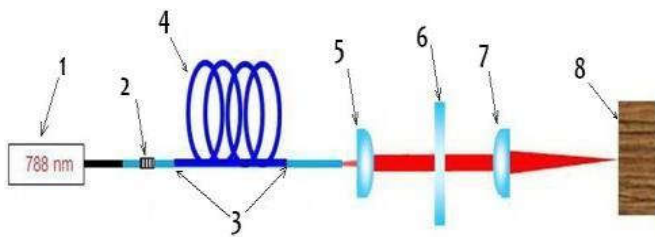


Fig. 2. The experimental setup: pumping laser diode operating at 788 nm 1, fiber

Bragg grating 2, end couplers 3, thulium doped fiber 4, collimator 6, filter (HR 788 nm / AR 2 μ m) 6, focusing lens 7 and wood sample 8.

[1] I. Swaczyna, P. Beera, „Charakterystyka drewna ciętego laserem CO₂ o ciągłej pracy i przerywanej”. *Przemysł Drzewny* 11, 9-14 (1995)

Application of Evolutionary Algorithm to Optimization of DWDM networks

Kacper WNUK¹, Slawomir SUJECKI², Stanislaw KOZDROWSKI¹

¹ Institute of Computer Science, Warsaw University of Technology, Nowowiejska 15/19, 00-665 Warsaw, POLAND

² Department of Telecommunications and Teleinformatics, Faculty of Electronics, Wroclaw University of Science and Technology, Wyb. Wyspianskiego 27, 50-370 Wroclaw, POLAND

s.kozdrowski@elka.pw.edu.pl

The subject of the study is an application of Integer Programming (IP) method and metaheuristic i.e. evolutionary algorithm to optical DWDM network optimization. The wider context of the presented research results is a problem faced by network operators, which in essence reduces to an improvement of service flexibility and achieving savings in capital expenditures. Thus the main objective of the optimization is to minimize capital expenditure, which includes the costs of optical node resources, such as transponders and filters used in new generation of reconfigurable optical add drop multiplexers (NG-ROADMs) [1],[2]. For this purpose a model based on IP is proposed. The efficiency of the IP based software is compared with that of evolutionary algorithms (EAs). The results obtained show that there is a large advantage in using EAs for optimizing large optical networks when compared with IP. The IP fails to find the optimal solution within reasonable computational time. Finally it is noted that the numerical

experiments were carried out for realistic networks of different dimensions and traffic demand sets.

Figures 1 and 2 show the calculated time for Polish DWDM national network for both methods: Integer Programming (Figure 1) and Evolutionary Algorithm (Figure 2).

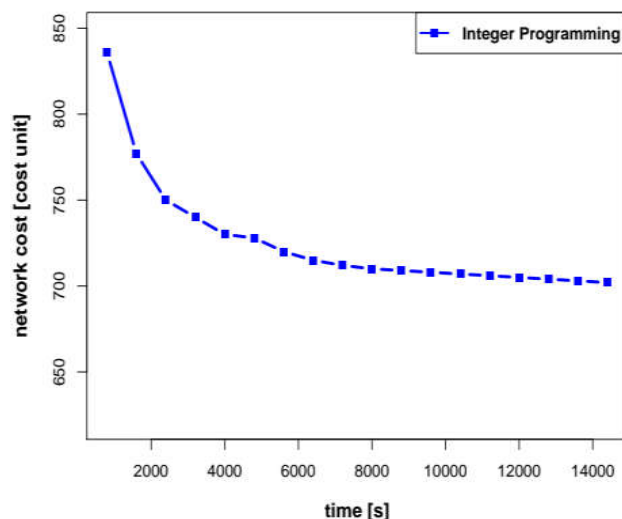


Fig. 1. Convergence curve (network cost vs. computational time) for Polish DWDM network calculated by Integer Programming method.

The Evolutionary Algorithm finds the optimal solution 10 times faster than

the Integer Programming method. This leads to the conclusion that the Evolutionary Algorithm method may be better suited for an optimization of large practical networks when compared with IP.

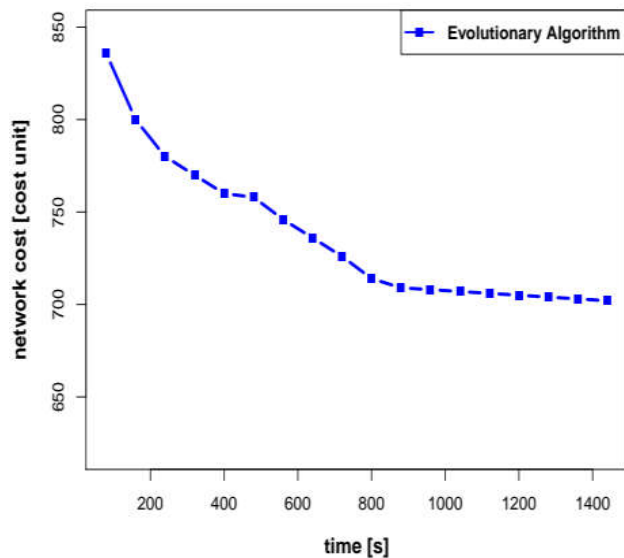


Fig. 2. Convergence curve (network cost vs. computational time) for Polish DWDM network calculated by Evolutionary Algorithm method.

-
- [1] Dallaglio, M.; Giorgetti, A.; Sambo, N.; Velasco, L.; Castoldi, P. Routing, Spectrum, and Transponder Assignment in Elastic Optical Networks. *Journal of Lightwave Technology*, 2015, 33, 4648–4658.
- [2] Kozdrowski, S.; Żotkiewicz, M.; Sujecki, S. Resource optimization in fully flexible optical node architectures. In *Proceedings of the 20th International Conference on Transparent Optical Networks (ICTON)*, 2018, 1291-1295, Bucharest, Romania, 1–5 July 2018.

Application of Machine Learning Methods in provisioning of DWDM channels

Piotr PAZIEWSKI¹, Sławomir SUJECKI², Stanisław KOZDROWSKI¹

¹Institute of Computer Science, Warsaw University of Technology,
Nowowiejska 15/19, 00-665 Warsaw, POLAND

²Department of Telecommunications and Teleinformatics, Faculty of Electronics, Wrocław University of Science and Technology, Wyb. Wyspińskiego 27, 50-370 Wrocław, POLAND

s.kozdrowski@elka.pw.edu.pl

Complexity and sizes of modern optic-fiber networks that support Internet of Things (IoT) and sensor networks start to challenge the traditional methods of managing them and yet majority of telecommunication companies still report rapid growth of their optic networks. One of essential problems in managing optic-fiber networks is calculating the Quality of Transmission (QoT) of given path in network. The unit responsible of this task is Optical Performance Unit (OPU) which sends its calculation to Network Management System (NMS) when asked to do it. NMS needs only information whether it's possible to transmit through path or not. Modern OPU's are still operating based on traditional algorithms e.g. take into consideration known physics rules and information about the network parameters, calculating transmission losses for each path. Such approach will not be sufficiently efficient in future networks. The obvious solution is the usage of Artificial Intelligence (AI) and Machine Learning (ML) algorithms.

In this contribution the performance of two methods in calculating QoT is compared:

- calculating QoT based on ML algorithm using Artificial Neural Networks (ANN).
- calculating QoT based on ML algorithm using Support Vector Machines (SVM).

ANN was selected since it proved its efficacy in numerous ML problems. The result of ANN algorithm is based on parameters of a set of neurons that change while neural network is trained. In the second method (SVM) one needs to separate paths into 2 groups. An SVM algorithm then constructs a hyperplane that separates two groups of data based on provided training data.

[1] Rui Manuel Morais, and João Pedro: Evaluating Machine Learning Models for QoT Estimation; In Proceedings of the 20th International Conference on Transparent Optical Networks (ICTON), 2018, 1-4, Bucharest, Romania, 1–5 July 2018.

[2] Aurelien Geron: Hands-On Machine Learning with Scikit-Learn and TensorFlow, O'Reilly Media; March 2017, ISBN 9781491962268

[3] Paweł Wawrzyński, Podstawy Sztucznej inteligencji, Oficyna Wydawnicza Politechniki Warszawskiej 2015.

Integrated transceiver of free space optics

Janusz MIKOŁAJCZYK, Dariusz SZABRA, Artur PROKOPIUK, Krzysztof ACHTENBERG, Jacek WOJTAS, Zbigniew BIELECKI

Institute of Optoelectronics, Military University of Technology, 2 Urbanowicza Str., 00-908 Warsaw, POLAND
janusz.mikolajczyk@wat.edu.pl

The paper presents a project of the Free Space Optics (FSO) transceiver operating at the wavelength of $9.35 \mu\text{m}$ [1]. This range is determined by a spectral emission of optical source (quantum cascade laser) and a photodetector responsivity (MCT heterostructures) [2,3]. In comparison with the FSO systems operating in the NIR or SWIR spectra, it provides better free-space light transmission in the case of bad weather conditions (low visibility caused by fog, mist) and of turbulence (scintillation) [4].

The FSO construction uses many optomechanical solutions to provide unique functionalities to ensure extra-operational performances of the data link system. There is applied a monitoring system to determine power of pulses emitted from the transmitter. This system consists of a small mirror mounted on the edge of the output beam profile, photodetector with preamp, and a two-channel peak detector. The second channel of peak detector is connected to the output of receiver detection module. In this way, it is possible to monitor the power level of the beam emitted by the FSO transmitter and registered by the FSO receiver. These data are saved to the status register of the FSO system

operation. Using this information, it is possible to implement special procedures:

- adjusting and stabilizing the output power of the transmitter and power level registered by receiver,
- identification of the cause of the beam interruption.

The control of transmitter power pulses is important to ensure the safety operation, to save the energy power and to increase the radiation source reliability. In the case of interruption in data transmission, it may be due to:

- disturbance in the field of view of FSO system caused by atmospheric phenomena or external objects,
- failure of some components of the transmitter or the receiver.

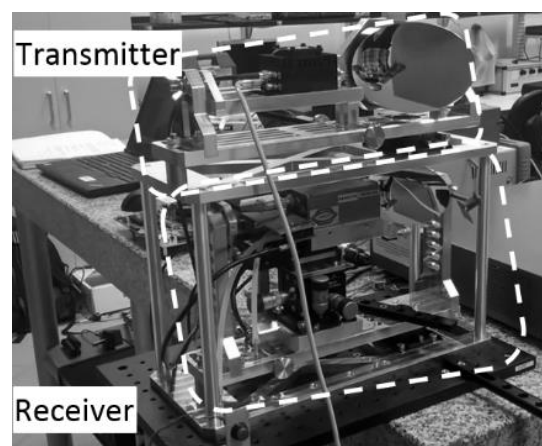


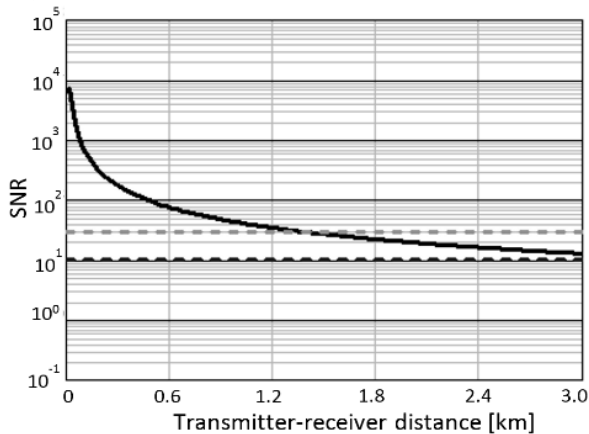
Fig. 1. View of the FSO transceiver**Fig. 2.** SNR values vs. datalink range for favorable weather conditions (good visibility: 5 km, low scintillations $C_n^2=10^{-16} \text{ m}^{-2/3}$)

Figure 1 shows a view of the constructed transceiver. Preliminary tests of the FSO system consists of two transceivers were carried out in lab conditions. The performed tests have proved correct of operation of the FSO components. The test procedure of the data link performed with the *netcat* utility with a 256 MB-size file showed the data rate of 1.37 MB/s. Basing on the tests results and parameters of the FSO transceiver components, changes in the signal-to-noise power ratio

versus transmitter-receiver distance were also calculated (Fig.2).

In further work, the designed FSO system tests will be carried out in outdoor conditions. They will ensure the determination of the maximum data rate and link range in real conditions.

This research was supported by The Polish National Centre for Research and Development grant DOB-BIO8/01/01/2016 and research work No 877/2018/PBS

-
- [1] J. Mikołajczyk, et, al., *Metrol. & Meas. Syst*, **24** (4) (2017).
 - [2] K. Pierscinski, et al., *Proc.SPIE*, **10437** (2017).
 - [3] J. Mikołajczyk, et al., *Proc. SPIE*, **10437** (2017).
 - [4] T. Plank, et. al., *Wavelength-selection for high data rate Free Space Optics (FSO) in next generation wireless communications,* in NOC, 2012, 1–5.

Optical anisotropy of phosphorene flakes

Aleksandra WIELOSZYŃSKA, Łukasz MACEWICZ, Paweł JAKOBCZYK, Robert BOGDANOWICZ

Department of Metrology and Optoelectronics, Faculty of Electronics, Telecommunications and Informatics, Gdańsk University of Technology, Gabriela Narutowicza 11/12, 80-233 Gdańsk, POLAND

owieloszynska@gmail.com

2D materials, because of their very attractive mechanical, electrical and optical parameter, have been used in many applications, e.g. photodetectors, sensors, modulators. [1]

Recently, the scientist discovered new 2D material – phosphorene. It has very interesting parameter which have filled the gap between the graphene and the transition metal dichalcogenide (TMD). The phosphorene is characterized by direct bandgap tuned by number of layers in 2D structure, high carrier mobility, large on/off ratio, and size-dependent thermal conductivity. The differences in the absorption of polarized light in the armchair and the zigzag direction was reported. [2] Moreover, we

present detailed polarization studies of the phosphorene flakes versus etching and aging processes. They have changed in time.

Hence, such an approach allows for non-contact diagnostics of exfoliated phosphorene for various application e.g. polarizers and polarization sensitive photodetectors.

[1] Guo, Z., Zhang, H., Lu, S., et al., *Advanced Functional Materials* 25(45), 6996–7002 (2015),

[2] Lan, S., Rodrigues, S., Kang, L. and Cai, W., *ACS Photonics* 3(7), 1176–1181 (2016).

Laser detection and tracking system for low-flying objects

Marek ŻYCKOWSKI, Piotr MARKOWSKI, Konrad BREWCZYŃSKI, Norbert PAŁKA, Jarosław MŁYŃCZAK, Marek PISZCZEK, Mateusz KAROL, Marcin MACIEJEWSKI, Wiesław CIURAPIŃSKI, Marcin KOWALSKI, Artur GRUDZIENIĆ, Michał WALCZAKOWSKI, Elżbieta CZERWIŃSKA
and Mieczysław SZUSTAKOWSKI

Institute of Optoelectronics, Military University of Technology, Urbanowicza 2, 00-908 Warsaw, POLAND

marek.zyckowski@wat.edu.pl

The article contains a description of the assumptions for the construction of an optoelectronic system designed to detect and track low-flying objects (drones). The key component of the System will be a laser scanner - fig.1, which will continuously monitor the observed sector and locate objects in this area.

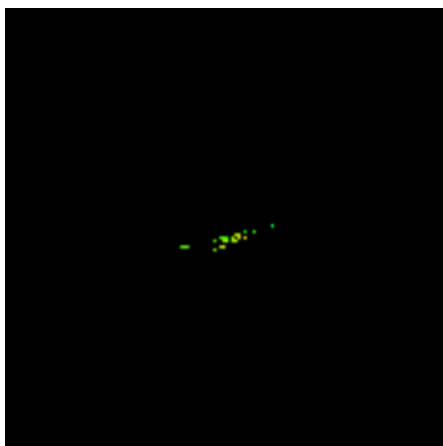


Fig. 1. A optical signature of a low-flying object with small dimensions.

Based on the specific optical signatures of the received echo signals, the initial classification of objects will also be made. In addition, precise coordinates of every detected object will be

transmitted automatically to the digital camera control module.

This module will instantly set the right direction of observation and the optimal magnification (electronically adjustable zoom) so that the suspicious object could easily be verified. Information about location of the detected objects will be refreshed several dozen times a second, which will allow real-time tracking of fast-moving drones.

The laser sensor prototype will be developed on the basis of optoelectronic elements that will allow a minimum distance detection of low-flying objects from a distance of at least 3 km – fig. 2 and a dead zone limited by the method of installation in a container. At the stage of laser scanner construction, it is assumed to purchase commercial sources of laser radiation in the form of fiber lasers with pulse repetition with a frequency of several hundred kHz and a peak power of several dozen kW. The prototype will be based on laser radiation safe for the human eye. Dedicated one-time scanning of the assumed area,

enabling compliance with the conditions of early detection of flying objects weighing less than 5 kg in less than 1 second. The detection range in the development of the prototype will be

calculated for normal conditions of light propagation in the atmosphere with the assumed reflection of a given radiation range from the object at the level of 20%.

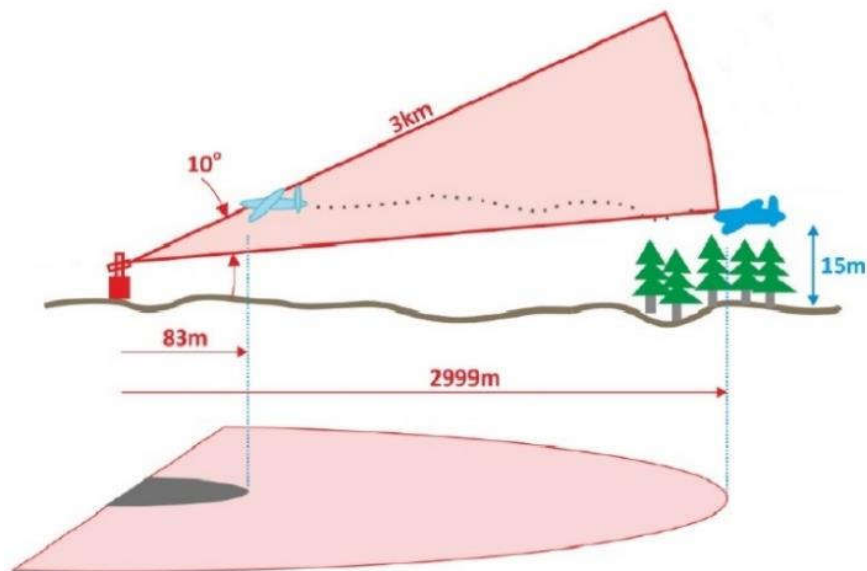


Fig. 2. Parameters of the drone detection system using a laser scanner.

[1] J. Wojtanowski, *Efficient numerical method of freeform lens design for arbitrary irradiance shaping*, J. Mod. Opt. **65(9)**, pp. 1019-1032, 2018.,

[2] J. Wojtanowski, M. Traczyk, *Optical design of transmitter lens for asymmetric distributed free space optical networks*, Opt. Laser Technol. **101**, pp.319-327, 2018.

[3] M. Kaszczuk, Z. Mierczyk, M. Zygmunt, J. Wojtanowski, *Wielospektralny skaner laserowy w ochronie i monitoringu środowiska*, Elektronika 2016, **57**, 26-27.,

P. Knysak, Z. Mierczyk, M. Zygmunt, J. Wojtanowski, M. Traczyk, *Laser data transmission with the application of reflectance modulator*, Proc. SPIE 2016, 10159, 1015910,

[4] M. Traczyk, J. Wojtanowski, Z. Mierczyk, M. Zygmunt, P. Knysak, T. Drozd, M. Muzal, *Theoretical analysis and optimization of 3D laser beam shaping*, Bull. Pol. Acad. Sci., Tech. Sci. 2015, 63(2), 555-560.,

Table of contents

25.02.2019 Monday.....	3
26.02.2019 Tuesday.....	5
27.02.2019 Wednesday.....	7
28.02.2019 Thursday.....	9

ABSTRACTS OF ORAL PRESENTATIONS..... 15

High-resolution optical fiber bundles based on high-contrast soft glasses for fluorescence imaging

Ryszard BUCZYNSKI, Berna MOROVA, Rafal KASZTELANIC, Nima BAVILI, Ömer YAMAN, Adam FILIPKOWSKI, Dariusz PYSZ, Buket YIĞIT, Mujdat ZEYBEL, Musa AYDIN, Buket DOGAN and Alper KIRAZ

Bend sensor based on microstructured multicore optical fiber

Dawid BUDNICKI, Piotr DEBOWSKI, Zbigniew HOLDYNSKI, Lukasz SZOSTKIEWICZ, Krzysztof MARKIEWICZ, Krzysztof WILCZYNSKI, Michal MURAWSKI, Grzegorz WOJCIK, Mariusz MAKARA, Krzysztof POTURAJ, Pawel MERGO, Oskar KARCZEWSKI, Marek NAPIERALA, Tomasz NASIŁOWSKI

Study on feature detection analysis used for designing hand-held retina vessels detection sensor

Piotr Adam BULER, Krzysztof MURAWSKI..... 20

Research of advanced signal detection methods for optical fiber methane sensor

Sylwester CHOJNOWSKI, Karol WYSOKIŃSKI, Zbigniew HOŁDYŃSKI, Jan ZAJIC, Krzysztof MARKIEWICZ, Oskar KARCZEWSKI, Tadeusz TENDERENDA, Marek NAPIERAŁA, Tomasz NASIŁOWSKI..... 22

Ellipsometric studies of antibody-functionalized sensors: estimation of surface coverage of diamond and gold electrodes

Bartłomiej DEC, Michał RYCEWICZ , Robert BOGDANOWICZ..... 24

Near-infrared emission in fluoroindate glasses co-doped with rare-earth

Marcin KOCHANOWICZ, Jacek ŻMOJDA, Piotr MILUSKI, Agata BARANOWSKA,
Tomasz RAGIN, Jan DOROSZ, Marta KUWIK, Wojciech A. PISARSKI,
Joanna PISARSKA, Magdalena LEŚNIAK, Bartłomiej STARZYK,
Maurizio FERRARI, Dominik DOROSZ..... 26

Thrombogenicity assessment of biomaterials – do we need new methods?

Maciej
GAWLIKOWSKI..... 28

Determination of gas pressure with use of a camera and neural networks

Leszek GRAD*, Tomasz MALINOWSKI, Krzysztof MURAWSKI..... 30

Broad-band polymers planar waveguide interferometer

Kazimierz GUT..... 31

Investigation depolarization in variable medium by spatial interferometric system

Aleksandra KALBARCZYK, Leszek R. JAROSZEWICZ, Nouredine BENIS, Idzi
MERTA, Monika CHRUŚCIEL, Paweł MARĆ..... 32

Synthesis and propagation of structured light beams in nematic liquid crystals

Urszula A. LAUDYN, Michał KWAŚNY, Jacek PIŁKA, Paweł JUNG,
and Mirosław A. KARPIERZ..... 33

The problems of the direction finding by air vehicles of the radars working with rotating antenna	
Adam RUTKOWSKI, Adam KAWALEC.....	35
Examination of the bottom of the Gdansk Bay by means of acoustic methods	
Eugeniusz KOZACZKA, Grażyna GRELOWSKA.....	36
Liquid-crystal diffraction gratings based on azo polymer aligning layers exposed to blue light interference pattern	
Anna KOZANECKA-SZMIGIEL, Katarzyna RUTKOWSKA, Mateusz NIEBOREK, Michał KWAŚNY, Dariusz SZMIGIEL.....	37
Generation of optical vortices in nonlinear photonic crystals	
K. SWITKOWSKI, S.LIU, Yan SHENG, and W.KROLIKOWSKI.....	39
Evaluation of the impact of evolution strategy parameters on the optimization of the markers distribution on the VAD membrane	
Tomasz MALINOWSKI, Leszek GRAD, Krzysztof MURAWSKI.....	41
T2SLs InAs/GaSb and T2SLs InAs/InAsSb higher operating temperature detectors – where is the limit?	
Piotr MARTYNIUK, Klaudia HACKIEWICZ.....	42
Sensors characteristics of helically twisted microstructured optical fibers	
Paweł MERGO, Mariusz MAKARA, Krzysztof POTURAJ, Lidia CZYZEWSKA, Grzegorz WÓJCIK, Aleksander WALEWSKI, Jarosław KOPEĆ.....	44
Vision sensor to measure liquid volume	
Krzysztof MURAWSKI, Monika MURAWSKA.....	45

Objects tracking in virtual reality applications using SteamVR tracking system - selected issues

Marcin MACIEJEWSKI, Marek PISZCZEK, Norbert PAŁKA..... 46

Identification of optical signatures for the augmented reality system

Tomasz PAŁYS, Artur ARCIUCH..... 47

Integrated photonics – technologies and applications

Ryszard PIRAMIDOWICZ, Stanisław STOPIŃSKI, Andrzej KAŻMIERCZAK, Aleksandra PAŚNIKOWSKA, Mateusz SŁOWIKOWSKI, Anna JUSZA, Krzysztof ANDERS, Witold PLESKACZ, Paweł SZCZEPAŃSKI..... 48

Optimization of optical properties of photonic crystal fibers infiltrated with chloroform for supercontinuum generation

Chu Van LANH, Van Thuy HOANG, Van Cao LONG, Krzysztof BORZYCKI, Khoa Dinh XUAN, Vu Tran QUOC, Marek TRIPPENBACH, Ryszard BUCZYŃSKI and Jacek PNIEWSKI..... 50

Silk fibroin thin films - biomaterial for optical humidity sensing

Marcin PROCEK, Zbigniew OPILSKI, Augusto MÁRQUEZ MAQUEDA, Xavier MUÑOZ-BERBEL, Carlos DOMÍNGUEZ HORNA..... 52

Distributed optical fiber sensors for high temperature applications

Aleksandra RAFALAK, Krzysztof WILCZYŃSKI, Tomasz STAŃCZYK, Krzysztof MARKIEWICZ, Alejandro Dominguez LOPEZ, Jakub KACZOROWSKI, Łukasz SZOSTKIEWICZ, Marek NAPIERAŁA, Tomasz NASIŁOWSKI..... 54

Structural properties and mid-infrared emission of heavy metal oxide glass and optical fibre co-doped with Ho³⁺/Yb³⁺ ions

Tomasz RAGIŃ, Agata BARANOWSKA, Marcin KOCHANOWICZ, Jacek ŻMOJDA, Piotr MILUSKI, Dominik DOROSZ..... 56

Graphene in infrared and terahertz detector family	
A. ROGALSKI.....	58
Experimental analysis of the Bragg reflection peaks splitting in gratings fabricated using a multiple order phase mask	
Gabriela STATKIEWICZ-BARABACH, Karol TARNOWSKI, Dominik KOWAL, Paweł MERGO.....	59
Integrated ring lasers for optical gyroscope systems	
Stanisław STOPIŃSKI, Marcin SIENNICKI and Ryszard PIRAMIDOWICZ.....	61
The SS-OCT endomicroscopy probe based on MOEMS Mirau micro-interferometer and MEMS 2-axis electrothermal microscanner for optical coherence tomography imaging	
Przemysław STRUK, Sylwester BARGIEL, Quentin TANGUY, Fernando E. GARCIA RAMIREZ, Ravinder CHUTANI, Philippe LUTZ, Olivier GAIFFE, Luc FROEHLI, Nicolas PASSILLY, Huikai XIE and Christophe GORECKI.....	63
0.3 mW MIR output power from multimode chalcogenide glass fiber doped with praseodymium	
Sławomir SUJECKI, Lukasz SOJKA, Meili SHEN, Dinuka JAYASURIA, Zhuoqi TANG, Emma BARNEY, David FURNISS, Trevor BENSON, Angela SEDDON.....	65
Coupled microresonators	
Marek TRIPPENBACH, Volodya KONOTOP, Nguyen VIET HUNG, Aleksander RAMANIUK, Krzysztof ZEGADŁO.....	67
Ultrasensitive detection of selected gases by infrared absorption spectroscopy	
J. WOJTAS, Z. BIELECKI, T. STACEWICZ, J. MIKOŁAJCZYK, M. NOWAKOWSKI, B. PIETRZYK, D. SZABRA, A. PROKOPIUK, K. ACHTENBERG.....	69

Optimization of silica glass capillary and rods drawing process

Grzegorz WÓJCIK, Krzysztof POTURAJ, Marusz MAKARA, Paweł MERGO..... 71

Stability of information coding in the phase difference of radiation pulses in a fibre optic pulse interferometer

Marek ŻYCKOWSKI..... 73

ABSTRACTS OF POSTERS..... 75

Analysis of optical magnetic field sensor in wide range of wavelengths

Kamil BARCZAK..... 77

Luminescence properties in SGB glass fibers co-doped with Eu³⁺/Ag ions

Karol CZAJKOWSKI, Jacek ŻMOJDA, Piotr MILUSKI,
Marcin KOCHANOWICZ..... 78

Spectral characteristics of anion derivatives of the benzoic acid

Lidia CZYZEWSKA, Małgorzata GIL, Paweł MERGO..... 80

Sensitivity of the graphene oxide under the influence of hydrogen

Sabina DREWNIAK, Marcin PROCEK..... 81

Determination the optimal extrusion temperature PMMA optical fibers

Malwina NIEDŹWIEDŹ, Małgorzata GIL, Mateusz GARGOL, Wiesław
PODKOŚCIELNY, Paweł MERGO..... 82

Organic Thin Film Transistor based on conductive graft copolymer thin films as a gas sensor

P. KAŁUŻYŃSKI, M. PROCEK, E. MACIAK, A. STOLARCZYK..... 83

Light-driven bending of the azo poly(amide imide) cantilevers Anna KOZANECKA-SZMIGIEL, Dariusz SZMIGIEL, Jolanta KONIECZKOWSKA, Ewa SCHAB-BALCERZAK.....	85
Set of the fiber optic rotational seismographs for mining activity monitoring Anna KURZYCH, Leszek R. JAROSZEWICZ, Zbigniew KRAJEWSKI, Jerzy K. KOWALSKI, Michał DUDEK.....	87
Growth and preliminary characterization of InAsSb photodiodes for mid-wave infrared range Kordian LIPSKI, Łukasz KUBISZYN, Krystian MICHALCZEWSKI, Krzysztof MURAWSKI, Piotr MARTYNIUK.....	89
Investigation of room temperature optical gas sensing properties of chitosan/AuNPs blend nanostructures Erwin MACIAK.....	90
Singular-value decomposition model for partial polarizing optical fiber elements Paweł MARĆ, Karol STASIEWICZ, Joanna KOREC, Leszek R. JAROSZEWICZ.....	91
Hybrid connection of functional materials and tapered optical fiber Joanna E. MOŚ, Karol A. STASIEWICZ, Leszek R. JAROSZEWICZ.....	92
Temperature dependence of Raman scattering in nanometric films of GaS and SnS₂ Katarzyna OLKOWSKA, Cezariusz JASTRZEBSKI, Daniel J. JASTRZEBSKI, Sławomir PODSIADLO.....	93

**Sensor-based perimeter protection of hard-to-reach wetlands and rivers -
conception of the system**

Norbert PAŁKA, Jarosław MŁYŃCZAK, Marek ŻYCKOWSKI, Marek PISZCZEK,
Mateusz KAROL, Marcin MACIEJEWSKI, Wiesław CIURAPIŃSKI, Marcin KOWALSKI,
Artur GRUDZIEN, Michał WALCZAKOWSKI, Elżbieta CZERWIŃSKA,
Piotr MARKOWSKI, Konrad BREWCZYŃSKI
and Mieczysław SZUSTAKOWSKI..... 95

A simulation tool to check correctness of optical signatures detection

Artur ARCIUCH, Tomasz PAŁYS..... 96

**Zero- and ultra- low-field nuclear magnetic resonance with atomic
magnetometer**

Kacper POPIOŁEK, Piotr PUT, Szymon PUSTELNY..... 97

Theoretical studies on refractive index profile of nanostructured fibre

Piotr PUCKO, Marcin FRANCZYK, Adam FILIPKOWSKI,
Ryszard BUCZYŃSKI..... 99

The hypothesis about the electrical non-neutrality of the Universe

Tadeusz PUSTELNY..... 101

**Light guiding channels in polymer-supported liquid crystalline materials and
structures**

Katarzyna RUTKOWSKA, Anna KOZANECKA-SZMIGIEL,
Miłosz CHYCHŁOWSKI..... 102

**Tuning optical properties of fluorescent nanodiamonds: influence of solvent
polarity and pH**

Mateusz FICEK, Michał RYCEWICZ, Maciek GŁOWACKI, Marcin MARZEJON,
Katarzyna KARPIENKO, Mirosław SAWCZAK
and Robert BOGDANOWICZ..... 104

Design of an integrated optics sensor structure for haemoglobin property detection

Przemysław STRUK..... 106

An application of thulium doped fiber laser in wood cutting

Sławomir SUJECKI, Monika ANISZEWSKA, Adam MACIAK, Witold ZYCHOWICZ, Samir LAMRINI, Karsten SCHOLLE, Peter FUHRBERG..... 108

Application of Evolutionary Algorithm to Optimization of DWDM networks

Kacper WNUK, Sławomir SUJECKI, Stanisław KOZDROWSKI..... 110

Application of Machine Learning Methods in provisioning of DWDM channels

Piotr PAZIEWSKI, Sławomir SUJECKI, Stanisław KOZDROWSKI..... 112

Integrated transceiver of free space optics

Janusz MIKOŁAJCZYK, Dariusz SZABRA, Artur PROKOPIUK, Krzysztof ACHTENBERG, Jacek WOJTAS, Zbigniew BIELECKI..... 114

Optical anisotropy of phosphorene flakes

Aleksandra WIELOSZYŃSKA, Łukasz MACEWICZ, Paweł JAKOBCZYK, Robert BOGDANOWICZ..... 116

Laser detection and tracking system for low-flying objects

Marek ŻYCZKOWSKI, Piotr MARKOWSKI, Konrad BREWCZYŃSKI, Norbert PAŁKA, Jarosław MŁYŃCZAK, Marek PISZCZEK, Mateusz KAROL, Marcin MACIEJEWSKI, Wiesław CIURAPIŃSKI, Marcin KOWALSKI, Artur GRUDZIENI, Michał WALCZAKOWSKI, Elżbieta CZERWIŃSKA and Mieczysław SZUSTAKOWSKI..... 117